

MELT POLYESTERIFICATIONS: KINETICS IN
WHOLLY AROMATIC SYSTEMS

A THESIS
SUBMITTED TO THE
UNIVERSITY OF PUNE
FOR THE DEGREE OF
DOCTOR OF PHILOSOPHY
(IN CHEMISTRY)

TH-1054

By
ANJALI LODHA

POLYMER SCIENCE AND ENGINEERING GROUP
CHEMICAL ENGINEERING DIVISION
NATIONAL CHEMICAL LABORATORY
PUNE - 411 008 (INDIA)

SEPTEMBER 1996

FORM - A

Certified that the work incorporated in this thesis " Melt Polyesterifications: Kinetics in Wholly Aromatic Systems " submitted by Ms. Anjali Lodha was carried out by the candidate under my supervision. Such material as has been obtained from other sources has been duly acknowledged in this thesis.



Dr. S. Ponrathnam

[Research Guide]

TH-1054

ACKNOWLEDGEMENT

I sincerely thank Dr.S. Ponrathnam, my research guide for his invaluable guidance and fruitful discussions in the course of this investigation.

I deeply appreciate Dr. Ramesh Ghadge who has evinced keen interest in my work and has been the greatest asset through out the progress of this work.

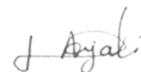
I thank Dr. Prasad very much for his expertise in the field of kinetics has been very beneficial to me.

I take this opportunity to acknowledge Dr. Rajan for the co-operation extended during the tenure of this work.

I am also thankful to my colleagues, Arika, Smita, Sunita, Varsha, Rethi, Sunny, Yemul, Suresh, Raju and Gopakumar for their help and encouragement.

I am particularly grateful to my family members whose inspiration and blessings helped me to complete this successfully.

I thank Dr.R. A. Mashelkar (D.G. CSIR), Ex-Director National Chemical Laboratory for his approval to submit this work in the form of a thesis. Lastly, I thank the Council of Scientific and Industrial Research for the award of the fellowship during the tenure of this work.



Ms Anjali Lodha

C O N T E N T S

	ABSTRACT	1
	CHAPTER-1 INTRODUCTION	
1.1	HISTORY	5
1.2	CAUSE OF LIQUID CRYSTALLINITY	6
1.3	CLASSIFICATION	7
1.3.1	Lyotropic Liquid Crystal Polymers	7
1.3.2	Thermotropic Liquid Crystal Polymers	7
1.3.2.1	Main Chain Liquid Crystal Polymers	7
1.3.2.2	Side Chain Liquid Crystal Polymers	10
1.3.3	Classification Based on Molecular Order	10
1.4	POLYMORPHISM IN THERMOTROPIC MATERIALS	12
1.5	THEORY	12
1.5.1	Virial Model	12
1.5.2	Lattice Model	12
1.6	STRUCTURE PROPERTY RELATIONSHIP	13
1.7	MESOPHASE STABILITY	16
1.7.1	Effect of mesogenic links on mesophase stability	16
1.7.1.1	Azo and azoxy links	17
1.7.1.2	Trans vinylene links	17
1.7.2	Effect of Central Group	18
1.7.3	Effect of Substitution on The Mesogen	19
1.7.4	Effect of Flexible Spacer	20

1.8	DEPRESSING MELTING TEMPERATURE (T_m)	20
L9	SYNTHESIS	25
1.9.1	Low Temperature Methods	25
1.9.1.1	Schautten-Baumann Reaction	25
1.9.1.2	Interfacial Polymerisation	25
1.9.1.3	Solution Polymerisation	26
1.9.2	High Temperature Melt Method	26
1.10	CHEMICAL KINETICS AND KINETIC ANALYSIS	26
1.10.1	Basic Concepts of Kinetics	26
1.10.2	Rate Equation	29
1.10.3	Order and Molecularity of a Reaction	31
1.10.3.1	Van't Hoff Method	31
1.10.3.2	Reaction Half Life Method	32
1.10.3.3	Experimental Method	32
1.10.3.4	From Initial Rates	32
1.10.3.5	Ostwald's Isolation Method	32
1.10.4	Complex Reactions	34
1.10.5	Steady State Approximation	34
1.10.6	Temperature Dependence of Rate Constants	35
1.11	KINETICS OF STEP POLYMERISATION	35
1.11.1	Analysis of Polymerisation Kinetics	36
1.11.2	Kinetic Expressions	37
1.12	THERMODYNAMIC FORMULATION OF RATE EQUATIONS	39
1.12.1	Collision Theory	39

1.12.2	Theory of Absolute Reaction Rates	43
1.13	CHARACTERISATION	46
1.13.1	Differential Scanning Calorimetry	46
1.13.2	Optical Microscopy	47
1.13.3	X-Ray Analysis	47
	REFERENCES	49

CHAPTER-2 EXPERIMENTATION

2.1	MATERIALS	56
2.1.1	1,4-Benzene diol (Hydroquinone)	56
2.1.2	1,3-Benzene diol (Resorcinol)	57
2.1.3	1,4-Benzene dicarboxylic acid (Terephthalic acid)	57
2.1.4	1,3-Benzene dicarboxylic acid (Isophthalic acid)	57
2.2	Catalysts	58
2.2.1	Zinc acetate	58
2.2.2	Sodium acetate	58
2.2.3	Dibutyl tin oxide	58
2.2.4	Dibutyl tin dilaurate	58
2.3	ACETYLATION OF DIOLS	59
2.3.1	Acetic anhydride	59
2.3.2	Hydroquinone diacetate	59
2.3.3	Resorcinol Diacetate	60
2.4	POLYESTERIFICATION	60
2.5	OPTIMISATION OF REACTION PARAMETERS	62

2.6	CHARACTERISATION	62
2.6.1	Differential Scanning Calorimeter (DSC)	62
2.6.2	Polarising Microscopy	63
2.6.3	X-Ray Diffraction	63
2.6.4	Kinetic Analysis	63
2.6.5	Thermodynamic Analysis	64

CHAPTER-3 HOMOPOLYESTERIFICATION KINETICS

3.1	INTRODUCTION	65
3.2	EXPERIMENTAL	68
3.2.1	Materials	68
3.2.2	Preparation of polymers	68
3.2.3	Measurements	69
3.3	RESULTS AND DISCUSSION	69
3.3.1	Thermodynamic treatment of rate constant	74
3.3.2	Hydroquinonediacetate-terephthalic acid (HT) system	75
3.3.3	Hydroquinone diacetate-isophthalic acid (HI) system	83
3.3.4	Resorcinol diacetate-terephthalic acid (RT) system	90
3.4	CHARACTERISATION	108
	REFERENCES	129

CHAPTER-4 COPOLYESTERIFICATION KINETICS

4.1	INTRODUCTION	132
4.2	HRT copolyesterification	134
4.3	HIT copolyesterification	153
4.4	CHARACTERISATION	171
	REFERENCES	182
	CHAPTER - 5 CONCLUSION	184

LIST OF FIGURES

FIGURE NO.	CAPTION	PAGE NO.
FIGURE 1.1	Classification of liquid crystalline polymers	8
FIGURE 1.2	Thermotropic polymers with either main chain or side chain mesogenic units	9
FIGURE 1.3	Major liquid crystalline topologies	11
FIGURE 1.4	Variation of volume fraction of isotropic and anisotropic phases with the axial ratio	14
FIGURE 1.5	Structure - property relationship observable in liquid crystal polymers.	15
FIGURE 1.6	Dependence of transition temperature on spacer length	21
FIGURE 1.7	Blundell's schematic diagram of the morphologies above and below the crystal melting point for (a) Rigid chain nematic polymer, and (b) Conventional polymer with chain folded lamellar crystals	23
FIGURE 1.8	Strategies for lowering T_m in main chain liquid crystal polymers	24
FIGURE 1.9	Schemes for the synthesis of polyesters	27
FIGURE 1.10	Van't Hoff plot of $\log(-d[A]/dt)$ versus $\log[A]$ for various reaction orders	33
FIGURE 1.11	Enthalpy diagram for a chemical reaction	40
FIGURE 2.1	Experimental setup for melt acidolytic transesterification reactions	61

FIGURE 3.1	Reaction scheme for the synthesis of HT polyester	76
FIGURE 3.2	First order rate law plot illustrating the effect of temperature for HQDA/TPA uncatalysed reactions	77
FIGURE 3.3	Second order rate law plot illustrating the effect of temperature for HQDA/TPA uncatalysed reactions	78
FIGURE 3.4	2.5th order rate law plot illustrating the effect of temperature for HQDA/TPA uncatalysed reactions	79
FIGURE 3.5	Third order rate law plot illustrating the effect of temperature for HQDA/TPA uncatalysed reactions	80
FIGURE 3.6	Second order rate law plot illustrating the effect of temperature for HQDA/TPA catalysed reactions	81
FIGURE 3.7	Arrhenius plot for HQDA/TPA uncatalysed reactions prior to the break	85
FIGURE 3.8	Arrhenius plot for HQDA/TPA uncatalysed reactions after the break	86
FIGURE 3.9	Arrhenius plot for HQDA/TPA catalysed reactions prior to the break	87
FIGURE 3.10	Arrhenius plot for HQDA/TPA catalysed reactions after the break	88
FIGURE 3.11	Reaction scheme for the synthesis of HI polyester	89
FIGURE 3.12	Second order rate law plot illustrating effect of temperature for HQDA/IPA catalysed reactions	91

FIGURE 3.13	Second order rate law plot illustrating effect of temperature for HQDA/IPA uncatalysed reactions	92
FIGURE 3.14	Arrhenius plot for HQDA/IPA uncatalysed reactions prior to the break	94
FIGURE 3.15	Reaction scheme for the synthesis of RT polyester	95
FIGURE 3.16	Second order rate law plot illustrating effect of temperature for RDA/TPA catalysed reactions	97
FIGURE 3.17	Second order rate law plot illustrating effect of temperature for RDA/TPA uncatalysed reactions	98
FIGURE 3.18	Arrhenius plot for RDA/TPA uncatalysed reactions prior to the break	101
FIGURE 3.19	Arrhenius plot for RDA/TPA uncatalysed reactions after the break	102
FIGURE 3.20	Arrhenius plot for RDA/TPA catalysed reactions prior to the break	103
FIGURE 3.21	Arrhenius plot for RDA/TPA catalysed reactions after the break	104
FIGURE 3.22	Comparison of Arrhenius plots of first stage uncatalysed reactions of HT, HI and RT systems	105
FIGURE 3.23	Comparison of Arrhenius plots of second stage uncatalysed reactions of HT, HI and RT systems	106

FIGURE 3.24	IR spectrum of HQDA (solid line) and HT polyester (dotted line)	109
FIGURE 3.25	First heating DSC traces of uncatalysed reactions of HT polyesters	111
FIGURE 3.26	First heating DSC traces of catalysed reactions of HI polyesters	112
FIGURE 3.27	DSC traces of sample - A (a) Second heating; (c) First heating; (b) Cooling and (d) First heating DSC trace of sample - B	113
FIGURE 3.28	First heating DSC traces of uncatalysed reactions of RT polyesters	115
FIGURE 3.29	Optical micrographs of sample - A, (a) At 222° C and (b) At 225° C	117
FIGURE 3.30	Optical micrographs of sample - A (a) At 229° C and (b) At 243° C	118
FIGURE 3.31	Optical micrographs of sample - A (a) At 234° C and (b) At 224° C	119
FIGURE 3.32	Optical micrographs of sample - A (a) At 233° C and (b) At 230° C	121
FIGURE 3.33	X-ray diffraction pattern of as made polyesters: (a) RT; (b) HT; (c) HI	122
FIGURE 3.34	X-ray diffraction pattern of: (a) sample - A; (b) HT	123

FIGURE 3.35	High temperature X-ray diffraction film of sample - A recorded at : (a) Room temperature; (b) 186° C	124
FIGURE 3.36	High temperature X-ray diffraction film of sample - A recorded at :(a) 198° C; (b) 220° C	125
FIGURE 3.37	High temperature X-ray diffraction film of sample - A recorded at (a) 236° C (b) sample - B recorded at 186° C.	128
FIGURE 4.1	Reaction scheme for the synthesis of HRT copolyester	138
FIGURE 4.2	First order rate law plot illustrating the effect of temperature for HRT/50:50:100 reaction	142
FIGURE 4.3	Second order rate law plot illustrating the effect of temperature for HRT/50:50:100 reaction	143
FIGURE 4.4	2.5th order rate law plot illustrating the effect of temperature for HRT/50:50:100 reaction	144
FIGURE 4.5	Third order rate law plot illustrating the effect of temperature for HRT/50:50:100 reaction	145
FIGURE 4.6	Second order rate law plot illustrating the effect of temperature for HRT/80:20:100 reaction	148
FIGURE 4.7	Second order rate law plot illustrating the effect of temperature for HRT/20:80:100 reaction	149
FIGURE 4.8	Second order rate law plot illustrating the effect of temperature for HRT/75:25:100 reaction	150

FIGURE 4.9	Second order rate law plot illustrating the effect of temperature for HRT/60:40:100 reaction	151
FIGURE 4.10	Second order rate law plot illustrating the effect of temperature for HRT/40:60:100 reaction	152
FIGURE 4.11	Arrhenius plot for HRT/50:50:100 reactions prior to the break	154
FIGURE 4.12	Arrhenius plot for HRT/50:50:100 reactions after the break	155
FIGURE 4.13	Effect of copolyesterification on reaction kinetics	157
FIGURE 4.14	Reaction scheme for the synthesis of HIT copolyester	161
FIGURE 4.15	Second order rate law plot illustrating the effect of temperature for HIT/100:50:50 reaction	164
FIGURE 4.16	Second order rate law plot illustrating the effect of temperature for HIT/100:45:55 reaction	165
FIGURE 4.17	Second order rate law plot illustrating the effect of temperature for HIT/100:10:90 reaction	166
FIGURE 4.18	Arrhenius plot for HIT/100:50:50 reactions.	168
FIGURE 4.19	Effect of copolyesterification on reaction kinetics	170
FIGURE 4.20	First heating DSC traces illustrating the effect of reaction temperature on HRT/50:50:100 copolyester	172
FIGURE 4.21	First heating DSC traces illustrating the effect of composition on the HRT copolyesters synthesised at 320° C	172

FIGURE 4.22	Comparison of DSC traces of (a) - HT; (b)-RT and HRT/50:50:100 [(c)-First Heating; (d)-Second Heating] polyesters synthesised at 320° C	174
FIGURE 4.23	First heating DSC traces illustrating the effect of composition on the HRT copolyesters synthesised at 320° C	174
FIGURE 4.24	First heating DSC traces illustrating the effect of reaction temperature on HIT/100:50:50 copolyester	175
FIGURE 4.25	First heating DSC traces illustrating the effect of composition on HIT copolyesters synthesised at 320° C	175
FIGURE 4.26	A plot of composition versus melting temperature of HRT copolyesters synthesised at 320° C	177
FIGURE 4.27	A plot of composition versus melting temperature of HRT copolyesters synthesised at 300° C	177
FIGURE 4.28	X-ray diffraction pattern of as made HRT polyesters:(a) HRT/70:30:100; (b) HRT/50:50:100; (c) HRT/30:70:100	179
FIGURE 4.29	Comparison of X-ray diffraction patterns of as made HIT polyesters with HI polyester	181

LIST OF TABLES

TABLE NO.	TITLE	PAGE NO.
TABLE 3.1	High temperature Poly-transesterification of Hydroquinone diacetate [HQDA] and Terephthalic acid [TPA] without catalyst at 320.0°C	70
TABLE 3.2	High temperature Poly-transesterification of Hydroquinone diacetate [HQDA] and Isophthalic acid [IPA] without catalyst at 280.0°C	71
TABLE 3.3	High temperature Poly-transesterification of Resorcinol diacetate [RDA] and Terephthalic acid [TPA] without catalyst at 320.0°C	72
TABLE 3.4	High temperature Poly-transesterification of Resorcinol diacetate [RDA] and Terephthalic acid [TPA] with Dibutyl tin oxide [DBTO] catalyst at 320.0°C	73
TABLE 3.5	Results of Kinetics of Uncatalysed and Catalysed Acidolysis between Hydroquinone diacetate and Terephthalic acid	84
TABLE 3.6	Results of Kinetics of Uncatalysed and Catalysed Acidolysis between Hydroquinone diacetate and Isophthalic acid	93
TABLE 3.7	Results of Kinetics of Uncatalysed and Catalysed Acidolysis between Resorcinol diacetate and Terephthalic acid	99
TABLE 3.8	Results of Kinetics and thermodynamics analysis of acidolysis reactions of HT, HI and RT polyesters	100

TABLE 3.9	DSC Results of mesomorphic transitions of HT polyesters prepared by uncatalysed reaction at differing polymerisation reaction temperatures.	114
TABLE 3.10	Results of room temperature X-ray diffraction analysis	126
TABLE 3.11	Results of High Temperature X-ray diffraction analysis.	126
TABLE 4.1	High temperature Poly-transesterification of Hydroquinone diacetate [HQDA], Resorcinol diacetate [RDA] and Terephthalic acid [TPA] without catalyst at 320.0°C.	139
TABLE 4.2	Variation of Reactivity ratio (k_D/k_O) with concentration of RDA	141
TABLE 4.3	Results of Kinetics of HRT copolyesterification	146
TABLE 4.4	Activation Energies (AE) For HRT Copolyesterification Prior to (AE_D) and After the Break (AE_O)	156
TABLE 4.5	High temperature Poly-transesterification of Hydroquinone diacetate [HQDA], Isophthalic acid [IPA] and Terephthalic acid [TPA] without catalyst at 320.0°C.	163
TABLE 4.6	Results of Kinetics of HIT copolyesterification	167
TABLE 4.7	Activation Energies (AE) For HIT Copolyesterification	169
TABLE 4.8	Results of room temperature X-ray diffraction analysis	180

ABSTRACT

IMPORTANCE, INTRODUCTION AND OBJECTIVES:

Today's innovation of technology demands high performance new materials and spurs its R & D race. Especially, in the plastics field numerous new engineering plastics have been developed. Liquid crystal polymers are a new class of engineering plastics which attract significant interest.

Thermotropic liquid crystalline polymers, often referred to as second generation high performance liquid crystalline systems, are a quantum jump from the first generation aramid fibers of which KEVLAR is well known. The first generation lyotropic liquid crystalline polymers, which display liquid crystallinity in solution, are nonmelting. Polymers were developed by wet spinning from expensive, corrosive solvents. Thermotropic systems display liquid crystalline melts in a specific temperature range. On processing from the melt, these polymers have outstanding features/properties till now not realized in any other high performance engineering polymer. Some salient features are: (i) Very high crystallisation rate, (ii) Spontaneous alignment in flow direction, (iii) Composite type (bone-flesh) morphology, (iv) Extremely low coefficient of thermal expansion, (v) Excessive shear thinning of melts, (vi) Enhanced mechanical properties and (vii) High thermal and chemical stabilities.

First commercialised in late 1984 all currently available LCPs are random copolymers of aromatic copolyesters produced from a select group of monomers. Unlike most resins, LCPs have the ability to form highly oriented, fibrous crystalline chains under shear in the melt phase. Despite their impressive thermal and physical properties, commercial utilisation reportedly amounts to only 1-2.5 million kg/yr. Primarily in small electrical surface mount connectors and encapsulated devices, along with some chemical processing applications and microwave cookware. Wider utilisation would help to bring down the cost of LCPs typically

15-22\$/kg. But since high prices have been identified as one of the barriers to wider utilisation, LCP suppliers are taking the initiative on seeking the ways to reduce LCP cost and increase their value in use.

The unusual combination of high performance and processing ease of these polymers originate from the presence of rigid anisotropic structural elements known as mesogens. They do not conform to a specific exact chemical structure but comprise of 1,4-disubstituted aromatics coupled to rigid groups such as ester, azoxy, azomethine etc. and having an axial ratio not exceeding three. Structural probabilities are innumerable. Polyesters prepared by coupling wholly aromatic mesogens together are found to be very high melting. Different strategies have been adopted to decrease the phase transition without compromising the mechanical properties. These are: 1) decreasing axial ratio by attaching pendent groups to the mesogen; 2) disrupting the co-linearity of the molecular axis by non-para 1,3-disubstituted aromatics; 3) attaching monomer moieties resembling crank-shaft; 4) altering the directional vectors of the rigid linking groups and 5) decoupling the mesogens by attaching to aliphatic moieties.

The most widely used reactions for the preparation of polyesters are direct esterification and alcoholysis, usually performed at high temperatures in the melt. Also reactions of acyl chlorides with hydroxyl compounds or phenolates are used and generally carried out at medium/low temperatures in solution or by interfacial synthesis. For the preparation of liquid crystalline polyesters, the exchange reaction between aromatic esters and aromatic carboxylic acids, acidolysis is commonly used and yields wholly aromatic polyesters.

The mechanism of acidolysis has been studied for low molecular weight compounds in a temperature range well below that commonly used for polyesterifications. Two

mechanisms have been proposed for polyesterification by acidolysis route. But only minor contributions pertaining to their kinetic data are available in the open literature especially for polyesterification of all aromatic systems.

It is generally accepted that the reactivities of the functional groups are independent of chain length as first stated by Flory. But when reactions are carried out in the molten state the complexity of reaction medium contributes to the over all kinetic behaviour. Further complications arise from the high reaction temperatures needed to maintain the polyesters in the molten state. Side reactions at such high temperatures may affect the reaction kinetics. Another difficulty arises from the low solubility of reactants in the reaction medium. Consequently very few studies have been devoted to establish certain kinetic behaviour to all aromatic thermotropic systems.

The present study is carried out with the objective of investigating the kinetics of homo and copolyesterification reactions forming wholly aromatic thermotropic polyesters. This includes:

1. Synthesis of homopolyesters : hydroquinone terephthalate (HT), hydroquinone isophthalate (HI) and resorcinol terephthalate (RT) by acidolysis type of polycondensation at various temperatures with and without the catalyst.
2. Studying the effect of temperature, catalyst and the type of monomer on the reaction kinetics by monitoring volume of side product collected with time.
3. Synthesis of copolyester systems namely HIT and HRT and study the effect of comonomer type and composition on the reaction kinetics.
4. Kinetic and thermodynamic analysis: Fitting the experimental kinetic data to suitable rate model in order to determine the order of reaction and calculating related kinetic parameters

like rate constants, energy of activation etc. The relation between kinetic and thermodynamic parameters was made use of to evaluate thermodynamic parameters like free energy of activation, frequency factors etc.

5. Instrumental methods of analysis: Polyesters were characterised by various thermal, optical, I.R. and X-ray methods of analysis to explain the role of kinetics on structure and property of the final polymer.

CHAPTER - 1

CHAPTER - 1

INTRODUCTION

Today's innovation in technology demands high performance new materials and spurs its research and development race. Especially in the plastics field, numerous new engineering plastics have been developed. *Liquid Crystal Polyesters* (LCPs) are a new class of engineering plastics which has attracted significant interest.

1.1 HISTORY

The liquid crystal phase (mesomorphism) occurs on the phase diagram between the crystal and the liquid phase. It is an unusually fascinating state because it combines properties of both the above phases. Liquid crystals behave mechanically as liquids yet exhibit many of the optical properties of crystals. The molecular organisation pattern is such that orientational ordering is dominant while long range positional ordering characteristic of a crystal is absent.

Lehmann¹ confirmed Reinitzer's² observation of liquid crystal phase in cholesteryl benzoate by polarising microscope and coined the term "*liquid crystal*" to denote the partially ordered fluid phase that forms upon melting the crystalline state. Much credit for the early work that extended the number of known liquid crystal systems belongs to Gattermann,^{3,4} Lehmann and Vorlander.⁵

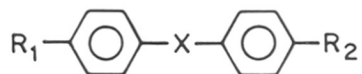
Coming to macromolecules, there are reports way from 1937 regarding mesomorphism in bio-polymers.⁶ Formation of polymeric liquid crystals was predicted in 1956 by Flory.⁷ But the subject received real recognition due to pioneering work by Kwolek and her coworkers in DuPont de Nemours Inc., which led to lyotropic LCP⁸⁻¹⁰. Synthetic polyamides, with all linear -1,4- (para) disubstituted structures, were found to show mesomorphism above a critical concentration in solution. Fibres formed from this solution had remarkably high

tensile strength and bending modulus. This development gave impetus to the search in many fibre producing companies for the fibre spun from liquid crystalline melts (thermotropic LCs) which could have extraordinary mechanical properties.

The research in thermotropic LCs was initiated from a desire to increase the mechanical properties, heat resistance and fire retardance of poly(ethylene terephthalate) [PET] fibres and plastics by increasing the aromatic character through copolymerisation. The first observations of thermotropic liquid crystalline behaviour in polymers were made independently by Kuhfuss and Jackson¹¹⁻¹³ as well as Roviello and Sirigu.¹⁴ The former group described a series of copolymers generated through the reaction between PET and 4-acetoxy benzoic acid which exhibited the phenomenon of opaque melts, low melt viscosities and anisotropic properties. This triggered considerable research interest in this class of polymers.

1.2 CAUSE OF LIQUID CRYSTALLINITY

It is interesting to know what is the cause for this intermediate state to ensue between an anisotropic solid and truly isotropic liquid. This is due to the existence of rigid anisotropic structural elements known as *mesogens*.^{15,16} Most mesogenic molecules conform to the generic type



Mesogens do not conform to a specific chemical structure but comprise of *para* disubstituted aromatics (1,4-phenylene; 4,4'-biphenylene; 1,4- and 2,6-naphthalene) coupled to rigid groups (X) such as ester, azoxy, azomethine, nitron, ethene and ethyne. The condition for a structural element to be a mesogen is that the length to diameter ratio i.e. axial/aspect ratio must exceed 3.

At present our understanding of polymeric liquid crystals is largely derived from studies of monomeric liquid crystals.^{17,18} The intrinsic differences between the two arise from the chain character present in polymeric materials. It can be assumed, akin to low molecular mass liquid crystals, that even in polymeric liquid crystals the rigid elongated shape of molecules and the anisotropic intermolecular forces associated with that shape are the key parameters responsible for the formation of stable liquid crystalline state.

1.3 CLASSIFICATION

Liquid crystallinity can be induced either by thermal effects or by solvation. Accordingly, the polymers are classified as in **Figure 1.1**.

1.3.1 Lyotropic Liquid Crystal Polymers

In these systems the mesomorphism is observable within definite range of concentration in solution. These are the first generation liquid crystalline polymeric systems, of which *KEVLAR*⁸⁻¹⁰ is well known.

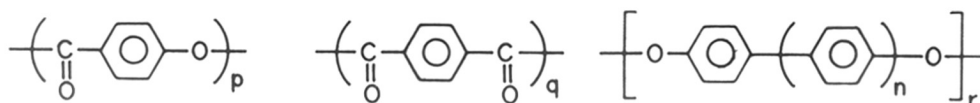
1.3.2 Thermotropic Liquid Crystal Polymers

These are the second generation high performance systems. In this the mesomorphic transitions are sensitive to temperature. Based on linking of mesogenic moiety in the polymer the liquid crystal polymers are divided into two types (**Figure 1.2**): main chain and side chain systems.

1.3.2.1 Main chain liquid crystal polymers

Here mesogen is jointed together as part of backbone of the polymer. Commercialised main chain LCPs are classified into three types, from their structures, as follows:

Type I: Flow Temperature > 320°C



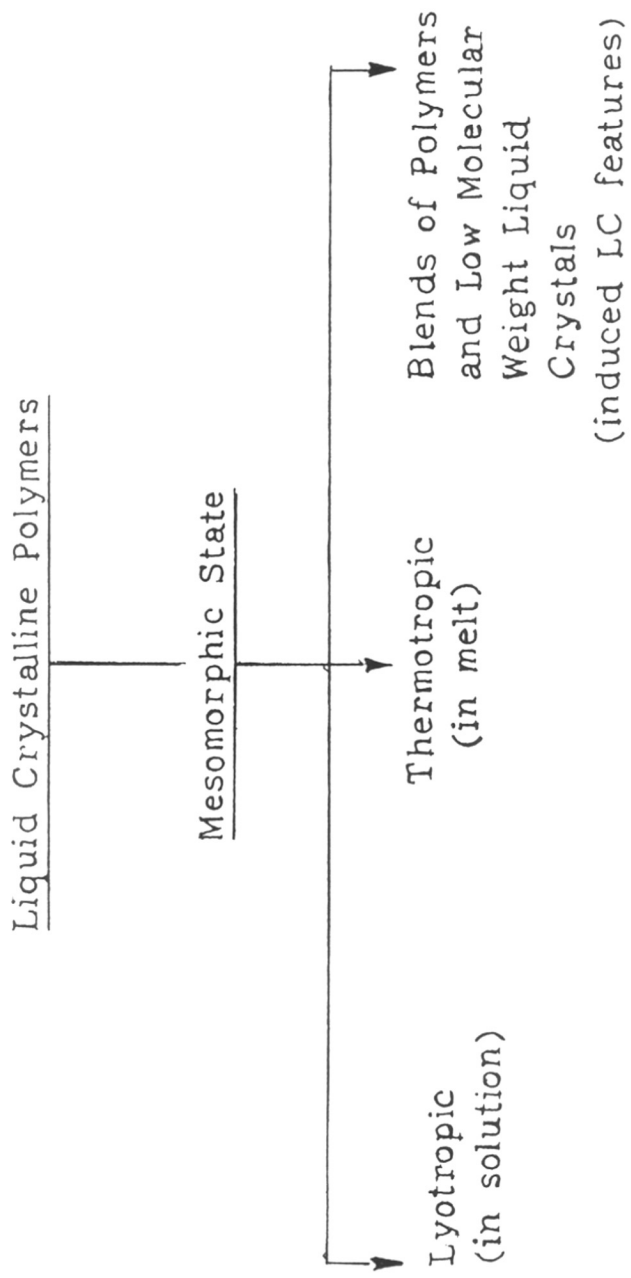
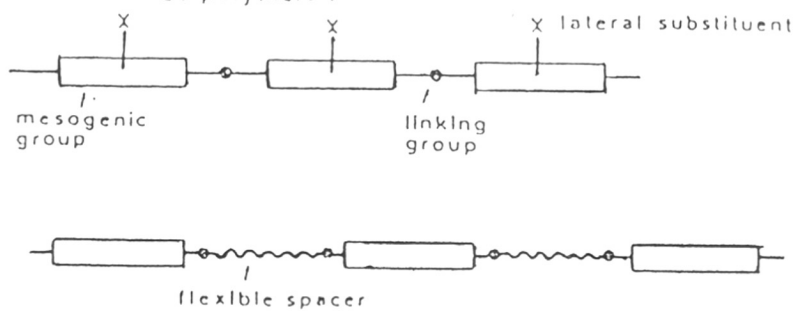


FIGURE 1.1 CLASSIFICATION OF LIQUID CRYSTALLINE POLYMERS

Main chain LC polymers :



Side chain LC polymers :

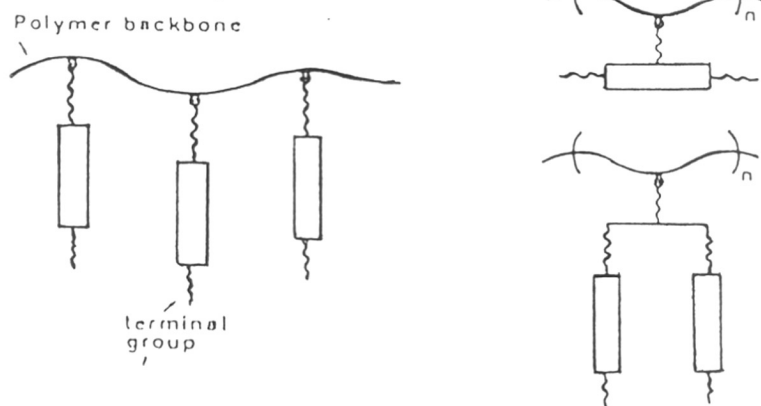
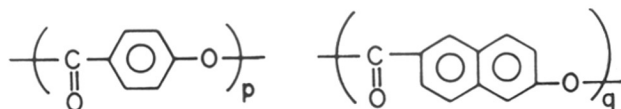
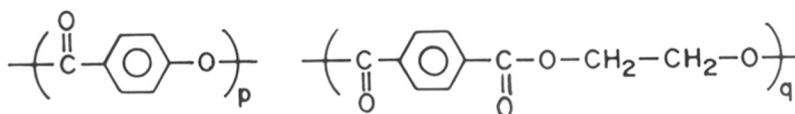


FIGURE 1.2 THERMOTROPIC POLYMERS WITH EITHER MAIN CHAIN OR SIDE CHAIN MESOGENIC UNITS

Type II : Flow Temperature > 220°C



Type III : Flow Temperature > 120°C



1.3.2.2 Side chain liquid crystal polymers

As the name indicates, these have the rod like moiety secured to the polymer backbone in the form of a pendant or as a constituent of the side chain. Side chain polymers essentially consist of three interrelated components: back-bone, spacer and mesogen. Mesogen unit needs to be rod like. Ultimate properties of the polymer originate from a synergistic fusion of all the three structural moieties.¹⁹⁻²²

1.3.3 Classification Based On Molecular Order

Liquid crystalline structures can be organised into several classes, in a manner akin to the organisation of crystalline materials into cubic, triclinic, monoclinic etc. The major liquid crystalline topologies are shown in **Figure 1.3**.

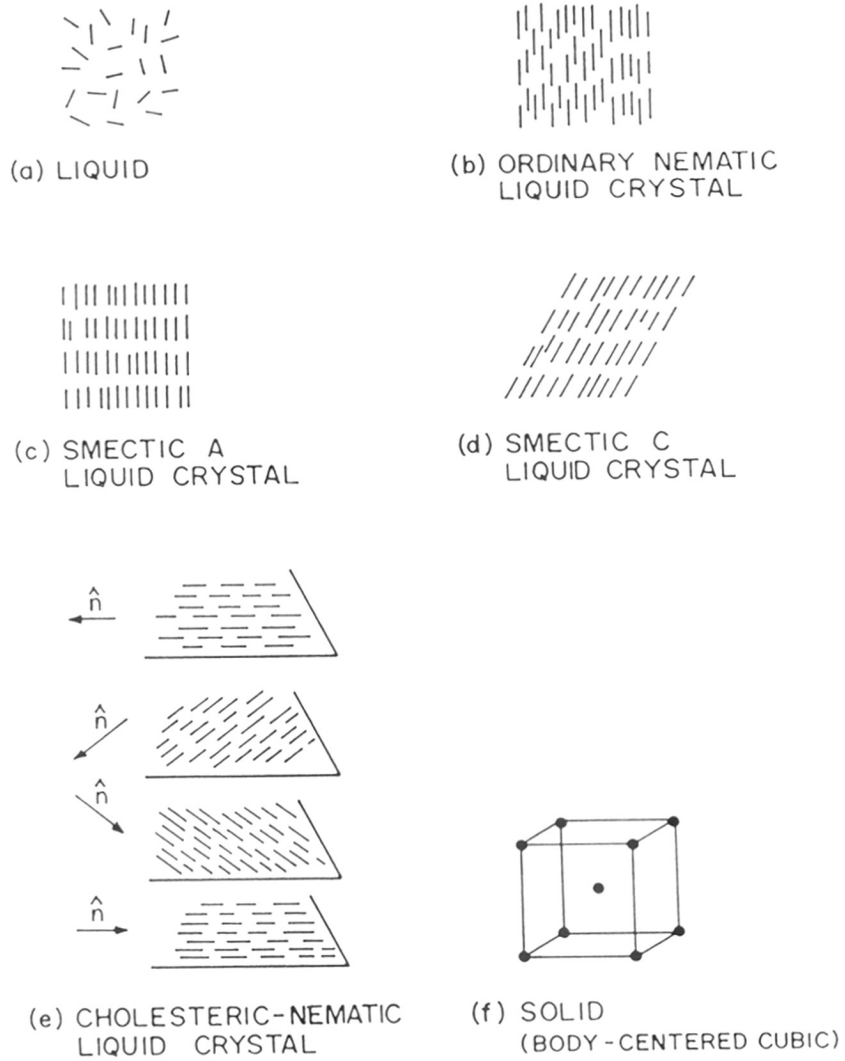


FIGURE 1.3 MAJOR LIQUID CRYSTALLINE TOPOLOGIES.

1.4 POLYMORPHISM IN THERMOTROPIC MATERIALS

Most thermotropic liquid crystalline materials are known to be polymorphous. i.e. they show more than one type of phase between a true solid and a liquid.^{17,23} An increase in temperature results in progressive destruction of order. Thus mesophase with increasing order are observable closer to the solid phase. The order of occurrence of mesophase with increase in temperature may be represented as:

Solid ----> Smectic B ----> Smectic C ----> Smectic A ----> Nematic ----> Isotropic

1.5 THEORY

Two classical approaches known are: (i) *Lars Onsager's Virial model*^{24,25} concerning isolated rigid rods and (ii) *Flory's Lattice model*^{26,27} regarding concentrated solution of connected rigid rods.

1.5.1 Virial Model

Onsager's theory based on virial expansion showed that a solution of hard asymmetric particles, such as long rods, should separate into two phases above a critical concentration. This is related to the axial ratio of particles. Such a phase separation is only due to shape asymmetry and is independent of intermolecular attractive forces. However, the drawback of this approach is that it can not be extended to highly asymmetric particles.

1.5.2 Lattice Model

Lattice theory has been successfully applied to polymeric materials. It is applicable to polydisperse systems, to mixtures of rod like polymers with random coils and to some semi-rigid chains.

$$V_p^* = \frac{8}{x} \quad (1.1)$$

This relation is widely used to represent the threshold volume fraction for the appearance of a stable anisotropic phase. $V_{(p)}^*$ is the volume fraction of polymer solution of hard rods (no intermolecular attraction) of axial ratio x .

Figure 1.4 represents variation of volume fraction of isotropic V_p and anisotropic phases V_p^* with x . These curves merge at $x = 6.42$. This is the calculated minimum value of x for stable nematic order in a melt of hard rods. In monodisperse polymers V_p/V_p^* is in the range 1.3 to 1.6. The ratio will be higher for polydisperse polymers.

DiMarzio²⁸ discussed the spontaneous ordering of linear polymer molecules having a rigid rod shape in solution as well as in the melt and concluded that orientational ordering would occur as a consequence of asymmetry of the particles, without an additional requirement of any attractive interactions among the particles being involved. Both these theories also yield a critical order parameter given by:

$$S = \frac{1}{2} \langle 3 \cos^2 \theta - 1 \rangle \quad (1.2)$$

where S is a measure of degree of ordering with respect to the principal direction (director). This parameter varies from 0 to 1. $S = 1$ for perfect alignment; for completely random isotropic phase $S = 0$ and for perpendicular arrangement it is $1/2$.

1.6 STRUCTURE-PROPERTY RELATIONSHIP

It is sensible and productive to prepare different types of polymers with mesogenic units in order to understand the interdependence of structure and properties observable in LCPs. Experimentation can generate innumerable liquid crystal systems (Figure 1.5).

The rigid rod of the chain can be accommodated by at least two "para" linked aromatic rings like 1,4-phenylene, 2,6-naphthalene or "trans" 1,4-cyclohexylene rings. The rings can be connected by rigid links such as azomethine (-CH=N-), azo (-N=N-), azoxy (-N=N-), ester (-C=O-) in addition to the biphenylene type linking.²⁹ These links help to maintain

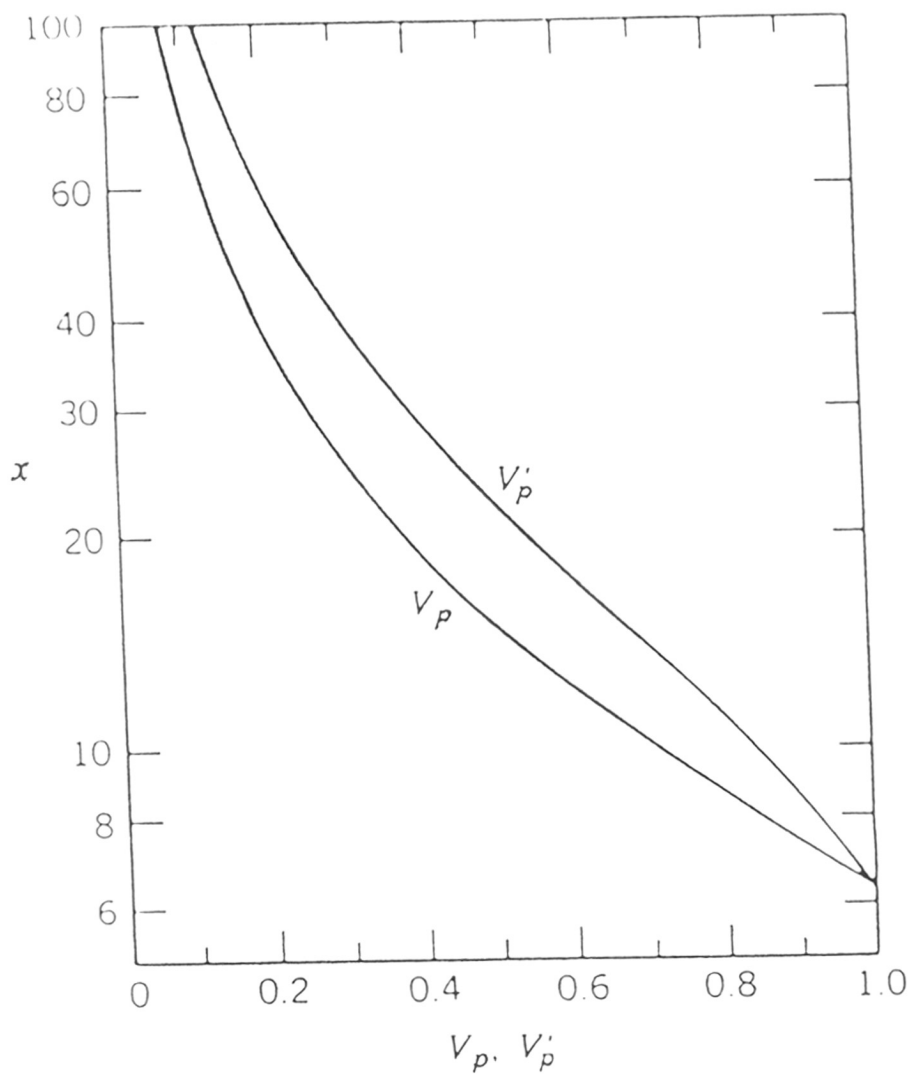
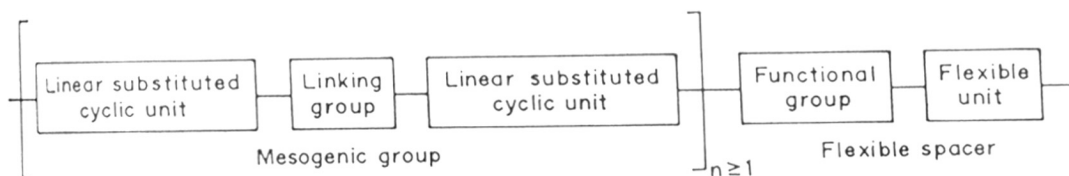


FIGURE 1.4 VARIATION OF VOLUME FRACTION OF ISOTROPIC AND ANISOTROPIC PHASES WITH THE AXIAL RATIO

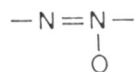
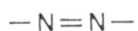
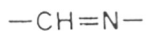
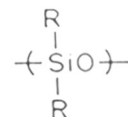
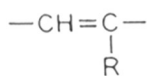
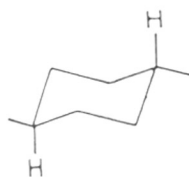
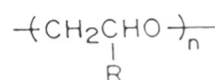
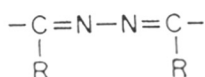
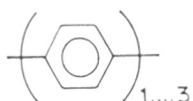


Linear substituted
cyclic unit

Linking
group

Functional
group

Flexible
unit



(R = H, alkyl)

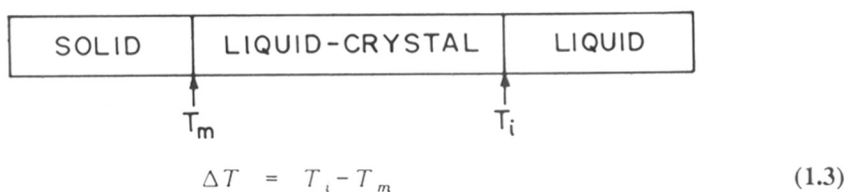
FIGURE 1.5

STRUCTURE - PROPERTY RELATIONSHIP OBSERVABLE IN LIQUID CRYSTAL POLYMERS.

linearity and planarity of the aromatic rings. The mesogen can be asymmetrically substituted by replacing hydrogen with groups like F, Cl, Br, CH₃, OCH₃, phenyl etc. Ester and ether groups are normally observed connecting units to bridge mesogen and the disrupter. Recent investigations also show the presence of amide, imine³⁰, carbonates as the bridging groups. Disrupter or spacer is frequently polymethylene³¹⁻³⁴. In this approach, a rigid element is formed with an overall length that is substantially greater than the diameter of aromatic rings.

1.7 MESOPHASE STABILITY

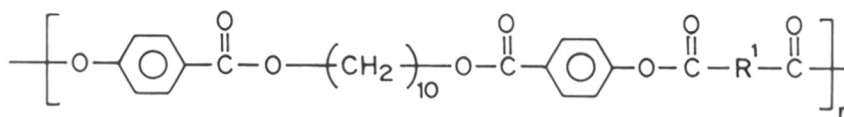
The nature and thermal stability of mesophase is a function of all the structural units present in the main chain. It is expressed in equation (1.3) and can be represented as follows.



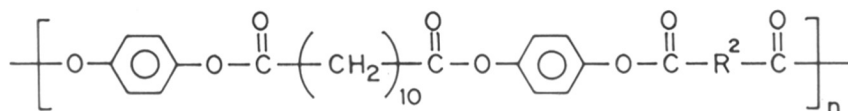
where, T_i is clearing temperature and T_m is melting temperature.

1.7.1 Effect of mesogenic links on mesophase stability

Mesogenic polymers with ester mesogenic links have been studied extensively.²⁹ Mesophase stability is affected by number of ester links, direction³⁵ of linking and arrangement of ester links e.g.



SMECTIC ; $\Delta T = 23$

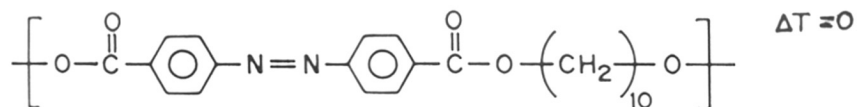


NEMATIC ; $\Delta T = 72$

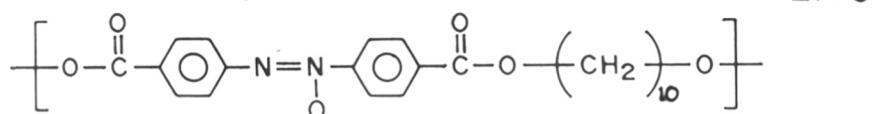
On changing the direction of linking the extent of conjugation is altered and therefore the stability is affected.

1.7.1.1 Azo and azoxy links

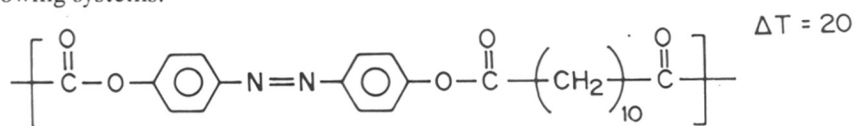
Diad mesogens with azo and azoxy links have been found to show stable liquid crystal phase.³⁶⁻³⁹ However, when such mesogens are terminated with carboxyl group, the mesophase stability is limited and either monotropic⁴⁰ or non-LC polymers are formed.⁴¹



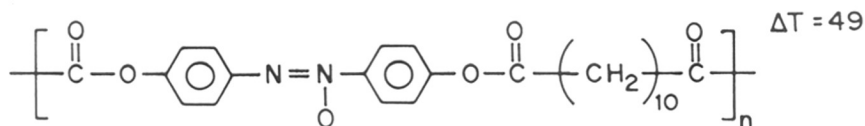
NON L. C.



However, mesophase is formed if the direction of linking of carboxyl group is changed as in case of following systems:



NEMATIC



1.7.1.2 Trans vinylene links

The behaviour of trans vinylenes are similar to that of azo and azoxy compounds due to the similarities in size and geometry.⁴² Mesogens of same length with the same spacer group but having azo and azoxy linking unit in one and stilbene type linking in the other differ in their stability. The stability in the former is enhanced by the presence of polar linking groups.

RR

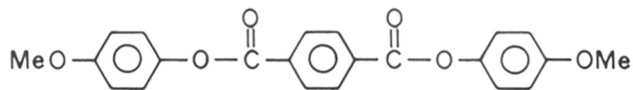
678-674; 541.124(043)

LOD

TH-1054

1.7.2 Effect of central group

Polarity, planarity and rigidity of the central group influence mesophase stability.⁴³

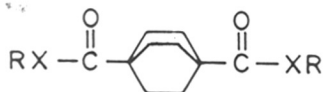


I

$$T_m = 209^\circ\text{C}$$

$$T_i = 285^\circ\text{C}$$

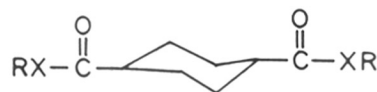
When central phenyl ring is replaced by A T_{N-I} reduces by 16°C while replacement by B reduces T_{N-I} by 40°C .



A

$$T_m = 152^\circ\text{C}$$

$$T_i = 269^\circ\text{C}$$



B

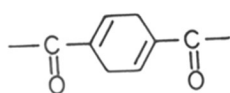
$$T_m = 142^\circ\text{C}$$

$$T_i = 245^\circ\text{C}$$

This indicates that rigidity is more effective than the presence of π electrons in the central group. If the cyclohexane moiety is replaced by 1,4-cyclohexadiene and 1,3-cyclohexadiene, then the polyesters

1,4-cyclohexadiene

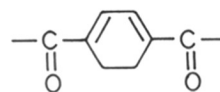
C



$$T_{N-I} = 273^\circ\text{C}$$

1,3-cyclohexadiene

D



$$T_{N-I} = 251^\circ\text{C}$$

show higher T_{N-I} than the polyester containing cyclohexane, but the nematic phase of C is stable relative to D. The reason probably lies in the non-planarity of double bonds in 1,3-cyclohexadiene.

Effect of bent monomer is extensively studied. Erdemir⁴⁴ et.al discovered that the isophthalic acid/hydroquinone/4-hydroxy benzoic acid (IA/HQ/4-HBA) copolyester formed only isotropic melt if IA exceeded 67 percent. Jin et.al⁴⁵ observed that terephthalic acid/resorcinol/4-hydroxy benzoic acid (TA/RE/4-HBA) polyester loses LC character if TA/RE units exceed 33 percent. Jackson⁴⁶ reported that hydroquinone/terephthalic acid/3-hydroxy benzoic acid (HQ/TA/3-HBA) does not form a mesophase when 3-HBA content exceeds 50 percent. Cai and Samulski⁴⁷ observed that increased concentration of 1,4-phenylene unit in the form of 4-HBA in IA/HQ polyester expands the mesophase range. Samulski⁴⁸ reported that 2-chloro hydroquinone/terephthalic acid (Cl-HQ/TA) and 2-methyl hydroquinone (Me-HQ/TA) polyesters are not liquid crystalline but the corresponding polyesters with 2,5-thiophene dicarboxylic acid unit exhibited liquid crystallinity over a wide range.

1.7.3 Effect of substitution on the mesogen

Substitution on the mesogen reduces coplanarity and the aspect ratio of the mesogen. Steric factors associated with such groups may hinder the interactions required for better packing between the chains. However, polar substitution helps to increase intermolecular interactions.

Effect of *t-butyl* substitution on Poly(hydroquinone-terephthalate) is seen in⁴⁹ Table 1.1.

t-Butyl Substitution, mole%	Temperature Range, °C	Transition Type
0	300-460	Solid-solid
10	368-460	Solid-solid
40	326-405	Crystal-nematic
60	325-391	Crystal-nematic

Effect of type and composition of substituted comonomer on temperature range of nematic state in random copolyester of PET is presented in⁴⁶ Table 1.2.

Comonomer m-substituent	Amount mole %	Thermal property Temperature range of nematic state
H	0.19	Non LC
H	0.46	220 -> 350
H	0.65	310 -> 350
Cl	0.35	180 - 240
Cl	0.50	190 - 240
Cl	0.53	190 - 260

1.7.4 Effect of flexible spacer

All structural moieties of the repeat unit excepting the mesogenic unit may be termed as a spacer. Flexible spacers based on *poly(methylene)* chains are very common.³¹⁻³⁴ Recently, spacers of *poly(siloxane)*⁵⁰⁻⁵² and *poly(ethylene oxide)*⁵³ segments have been studied. Flexible spacers decouple the mesogenic unit, which decreases both melting and clearing temperatures. There is a typical odd-even relationship between transition temperature and the number of carbon atoms in^{54,55} the spacer chain, as shown in Figure 1.6.

1.8 DEPRESSING MELTING TEMPERATURE

Melting temperature (T_m) is thermodynamically defined as,

$$T_m = \frac{\Delta H_f}{\Delta S_f} \quad (1.4)$$

where, ΔH_f = Heat of fusion; ΔS_f = Entropy of fusion

This has important implications in the design of LCPs. Based on theoretical prediction and the structural features so far discussed, it can be said that homopolymerisation of rigid units present in the mesogen would generate liquid crystalline polymers. Many aromatic polyesters with rigid backbones have been synthesised and examined to verify this.⁵⁶⁻⁵⁸

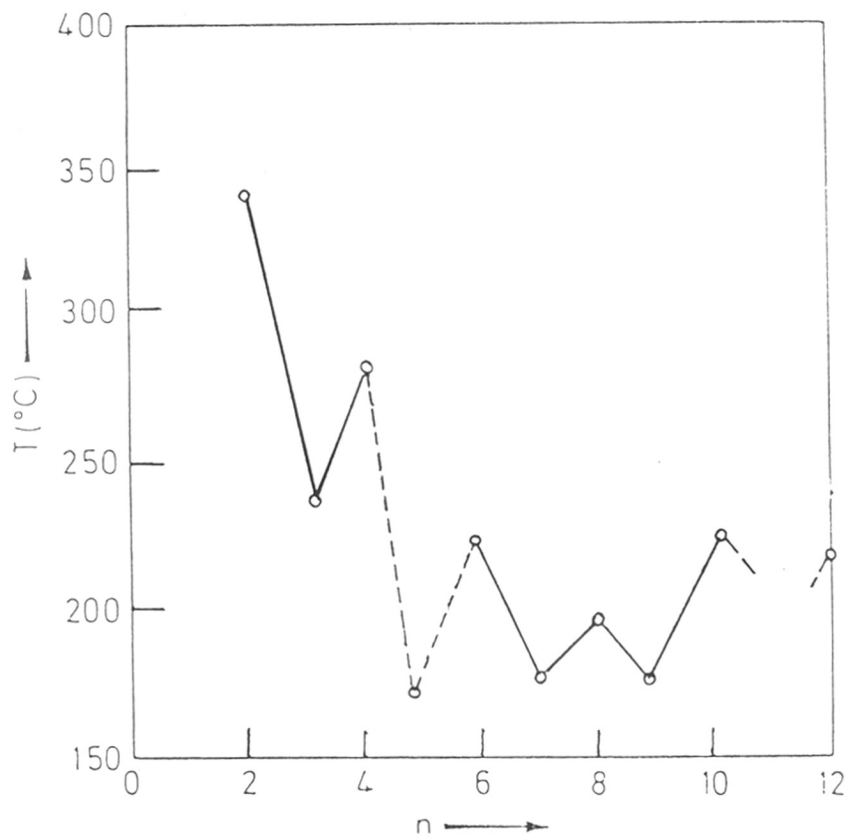


FIGURE 1.6 DEPENDENCE OF TRANSITION TEMPERATURE ON SPACER LENGTH

However, such rod like moieties tend to be infusible, largely intractable crystalline solids. Liquid crystalline properties were observed for oligomers of poly (1,4-phenylene) with $n = 7$ while decomposition occurred⁵⁹ prior to melting for $n > 7$. Melting temperatures of $610^{\circ}C$ and $600^{\circ}C$ were noted for poly(1,4-oxy benzoate) and poly(1,4-phenylene terephthalate) respectively.⁴⁶ Hence, the problem of polymer design is to reduce the melting temperature to obtain liquid crystalline phase below decomposition temperature and preferably in the temperature range suitable for most processing equipments. The nature of crystallites in solidified LCPs was examined by Blundell.⁶⁰ He proposed that there is little change in general configuration of LCP after T_m as against vast disorder experienced during the melting of conventional polymer. This will be clear from **Figure 1.7**.

Lower ΔH_f and ΔS_f were noted for LCPs as compared to a conventional thermoplastic polymer such as PET. Low ΔH_f is directly related to low level of molecular cohesion within crystallites; whereas low ΔS_f is a direct consequence of chain stiffness. Given that ΔS_f is low, the ΔH_f must also be low. Otherwise, T_m would be too high and the system will be intractable. Thus, chain irregularity and chain stiffness are two distinct properties that can be separately designed into the LCPs. This can be achievable in the following ways⁶¹⁻⁶³: (Figure 1.8)

1. Use, in relatively small mole fraction, of nonlinear structural units (kinks) such as resorcinol, isophthalic acid, 3-hydroxy benzoic acid in combination with their linear counterparts seems to be the general approach.⁶⁴⁻⁶⁶ Presence of 1,3-disubstituted rings destroys linearity. Regular packing of chains is sterically hindered. This drops down the melt transition temperature. Control of composition is very critical in such cases.
2. Use of flexible bonds and sequences increases the entropy of the melt.⁶⁷⁻⁷¹
3. Frustrated chain packing.^{72,73}

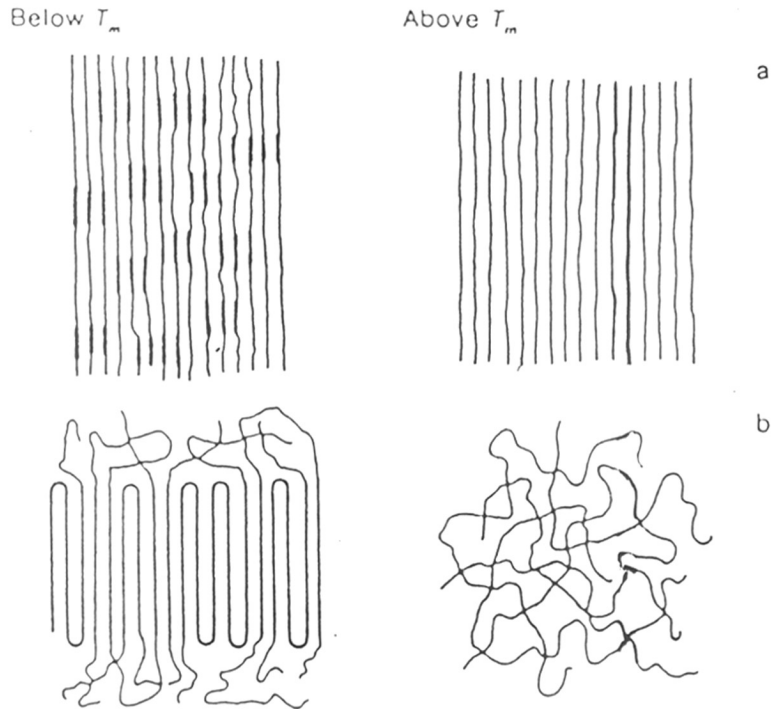


FIGURE 1.7 BLUNDELL'S SCHEMATIC DIAGRAM OF THE MORPHOLOGIES ABOVE AND BELOW THE CRYSTAL MELTING POINT FOR (A) RIGID CHAIN NEMATIC POLYMER, AND (B) CONVENTIONAL POLYMER WITH CHAIN FOLDED LAMELLAR CRYSTALS

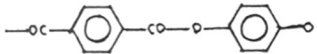
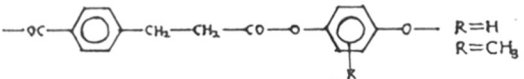
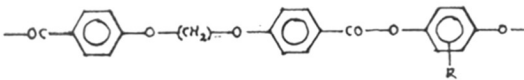
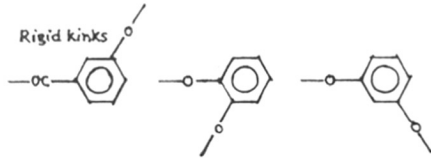
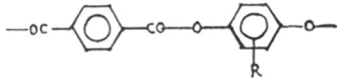
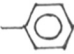
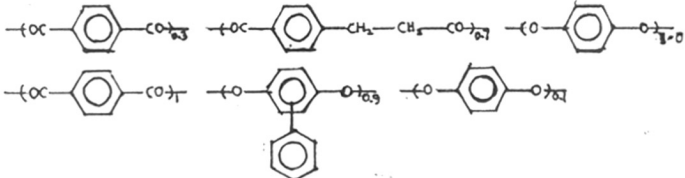
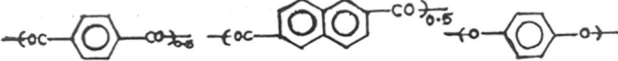
Polymer	Melting point (°C)
<p>Basic structure</p> 	600
<p>Introduction of disruptors Flexible spacers</p>  <p>R=H R=CH₃</p>	425 387
 <p>m=2, R=H m=2, R=CH₃ m=1, R=CH₃</p>	362 316 210
<p>Rigid kinks</p>  <p>~20 mol %</p>	<400
<p>Substitution of the aromatic rings</p>  <p>R=CH₃ R= </p>	>400 ~340
<p>Copolymerization</p> 	315 315
<p>Introduction of Crank-shaft units</p> 	~400

FIGURE 1.8 STRATEGIES FOR LOWERING T_m IN MAIN CHAIN LCPs

4. Copolymerisation: Copolymerisation leads to either an isotropic or an LC melt, depending on the copolymer composition.^{46,74,75} This is a key difference between LCPs and low molecular mass LCs.
5. Use of substituents: Asymmetric substitution of mesogen decreases the melting temperature by way of decreasing the aspect ratio and crystallisability.^{49,76}

1.9 SYNTHESIS

Main Chain Liquid Crystal polyesters are condensation polymers. Condensation proceeds by step polymerisation mechanism. All step polymerisations fall into two groups depending on the type of monomer employed.

1. Two different bifunctional monomers are used:



2. Both functional groups are present in a single monomer:



The synthesis could be conducted either at low or at high temperatures.

1.9.1 Low temperature methods

1.9.1.1 Schautten-Baumann reaction

This is a well known condensation reaction between an organic acid halide and compounds having active hydrogen such as phenols, thiols, amines etc.⁷⁷ This reaction can be conducted in the melt, solution or by interfacial methods.

1.9.1.2 Interfacial polymerisation

This method consists of reaction between a fast reacting intermediate and a normal reactant at the interface of two immiscible liquid phases, one of which is preferably water. The second phase consists of diacid halide dissolved in an organic solvent such as dichloromethane, carbon tetrachloride, hexane and xylene. Reaction can be carried out both in stirred and unstirred systems.⁷⁷

1.9.1.3 Solution polymerisation

This is carried out in a single liquid which is inert to both the reactants. The liquid can be any organic solvent without reactive functional groups. A tertiary amine is necessary as an acid acceptor. The product polymer remains either in solution or precipitates out. This method can be used to prepare many classes of polymers such as polyamides, polyureas, polyphenyl esters etc.

1.9.2 High temperature melt method

When appropriate bifunctional compounds such as diacids and diols are condensed, a linear polyester is formed with the loss of small molecule as a bi-product. Sufficiently high molecular weight polymers can be synthesised if stoichiometrically equivalent amounts of extremely pure intermediates are condensed and proper care is taken to remove non-polymeric bi-product. High temperature and reduced pressure form an integral part of these polycondensation methods.⁷⁸ Ester interchange method has the greatest commercial application. These methods are summarised in **Figure 1.9**.

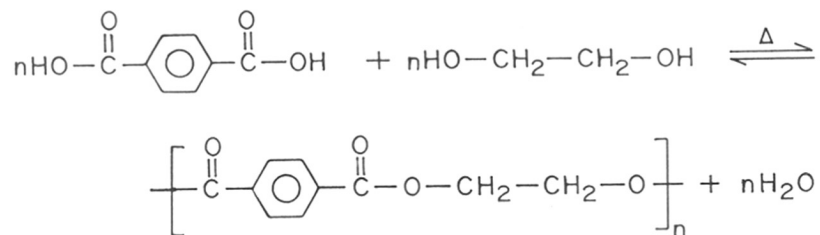
High temperature polycondensation of polyesters faces drawbacks such as low reaction rate, incomplete removal of bi-product and thermal instability. These are equilibrium reactions. In order to reach high conversion, bi-product removal is achieved by heat, stirring and reduced pressure. Also, side reactions should be absent and exact stoichiometric equivalence has to be assured.

1.10 CHEMICAL KINETICS AND KINETIC ANALYSIS

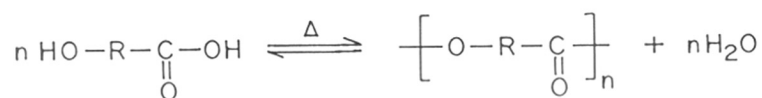
1.10.1 Basic Concepts of Kinetics

Chemical kinetics ^{79,80} deals with chemical transformations and may be defined as the study of chemical systems whose composition changes with time. These changes may take place in the gas, liquid or solid phase of a substance. A reaction occurring in a single

A. DIRECT ESTERIFICATION



B. SELF CONDENSATION OF HYDROXY ACIDS



C. DOUBLE ESTER INTERCHANGE

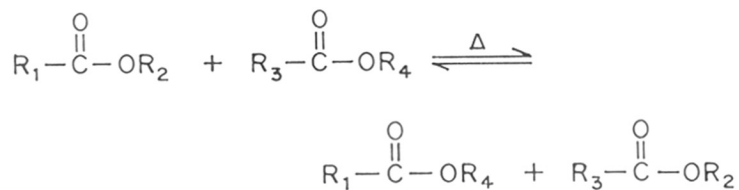
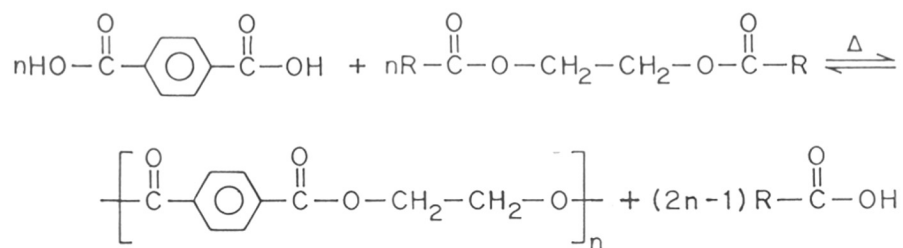
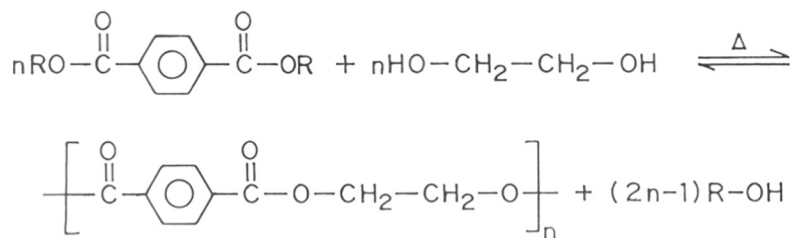
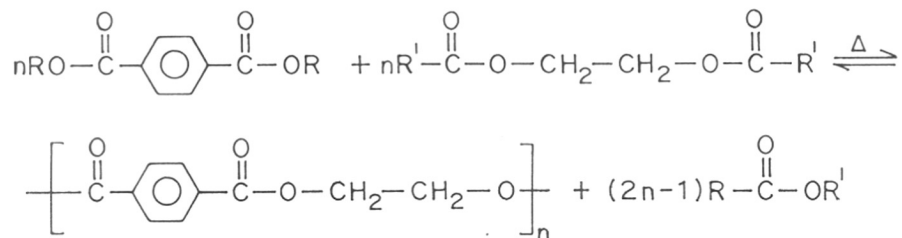


FIGURE 1.9 SCHEMES FOR THE SYNTHESIS OF POLYESTERS

...Continued on the next page

D. ESTER INTERCHANGE :

ACIDOLYSISALCOHOLYSISESTEROLYSIS

phase is usually referred to as a homogeneous reaction, while a reaction which takes place at an interface between two phases is known as a heterogeneous reaction. Chemical change that takes place in any reaction may be represented by a stoichiometric equation such as:



where a and b denote the moles of reactants A and B that react to form c and d moles of product C and D.

1.10.2 Rate Equation

The change in composition of reaction mixture with time is the rate of reaction. The rate of consumption of reactants represented by equation (1.5) is

$$R = -\left(\frac{1}{\alpha}\right)\frac{d[A]}{dt} = -\left(\frac{1}{b}\right)\frac{d[B]}{dt} \quad (1.6)$$

or the rate of formation of products is

$$R = \left(\frac{1}{c}\right)\frac{d[C]}{dt} = \left(\frac{1}{d}\right)\frac{d[D]}{dt} \quad (1.6a)$$

where R = rate of formation of products; t = reaction time etc.

Thus, the rate of overall reaction depends on the concentration of reactants. Therefore, in general, R may be expressed as a function of concentration of reactants as

$$R = k[A]^a[B]^b \quad (1.7)$$

This equation is rate equation or a rate expression wherein, a and b denote the order of reaction with respect to A and B respectively. The overall order of a reaction is given by $n = a + b$. The constant k is the rate constant and has the units of $(\text{concentration})^{n-1} \text{time}^{-1}$.

Zero order reaction

$$R = k[A]^0 = k \quad (1.8)$$

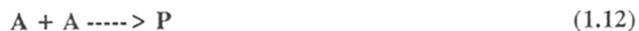
First order reaction of the type



$$R = k[A]^1 \quad (1.10)$$

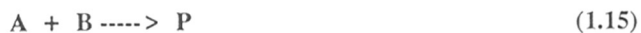
$$[A]_t = [A]_0 e^{(-kt)} \quad (1.11)$$

Second order reaction



$$R = k[A][A] = k[A]^2 \quad (1.13)$$

$$\frac{1}{[A]_t} = \frac{1}{[A]_0} - 2kt \quad (1.14)$$



$$R = k[A][B] \quad (1.16)$$

$$\frac{1}{([A]_0 - [B]_0)} \ln \frac{([B]_0[A]_t)}{([A]_0[B]_t)} = kt \quad (1.17)$$

The rate equation for 'n'th order reaction is

$$R = k[A]^n \quad (1.18)$$

integrated form of this is

$$\frac{1}{n-1} \left(\frac{1}{[A]_t^{n-1}} - \frac{1}{[A]_0^{n-1}} \right) = kt \quad (1.19)$$

1.10.3 Order and Molecularity

Order is an experimentally determined quantity and can take non-integer values. The values between -2 and 3 are usually noted. Negative orders imply the contribution of inhibitor in the rate equation while the complexity of a reaction is implied by fractional orders. Molecularity of a reaction specifies the number of reactants that are involved in the reaction step. Reaction is classified as uni, bi, ter-molecular etc. depending on its molecularity. A number of methods used to determine reaction order are:

1.10.3.1 Van't Hoff Method

When the order 'n' is unknown, a Van't Hoff plot can be constructed to deduce the reaction order. If,

$$-\frac{d[A]}{dt} = k[A]^n \quad (1.20)$$

Then,

$$\left\{ \text{then, } -\log \frac{d[A]}{dt} = \log k + n \log [A] \right. \quad (1.21)$$

In this method, the logarithm of rate is plotted against the logarithm of concentration of reactant. The slope of the graph gives the order of a reaction. **Figure 1.10** shows a typical Van't Hoff plot.

1.10.3.2 Reaction Half Life Method

Reaction Half Life ($t_{1/2}$) is defined as the time required for the concentration of a reactant to reach one half of its initial concentration.

$$t_{(1/2)} \propto \frac{1}{[A]_0^{n-1}} \quad (1.22)$$

where n = order of reaction; $[A]_0$ = initial concentration

1.10.3.3 Experimental method

Experimental data is fitted in different rate law plots corresponding to different orders. The proper choice of order is that for which rate constant is constant at different times.

1.10.3.4 Initial Rates

Order can be determined from initial rates i.e. rate for different initial concentration of reactant. A plot of logarithm of initial rate against logarithm of corresponding initial concentration gives reaction order from the slope.

1.10.3.5 Ostwald's Isolation Method

This depends on the approximation that when a reactant is taken in large excess, there is no perceptible change in its concentration during the course of the reaction. If the rate law is

$$-\frac{d[A]}{dt} = k_2[A][B] \quad (1.23)$$

and if $[B]$ is in excess then, $[B] = [B]_0$ and rate equation simplifies to

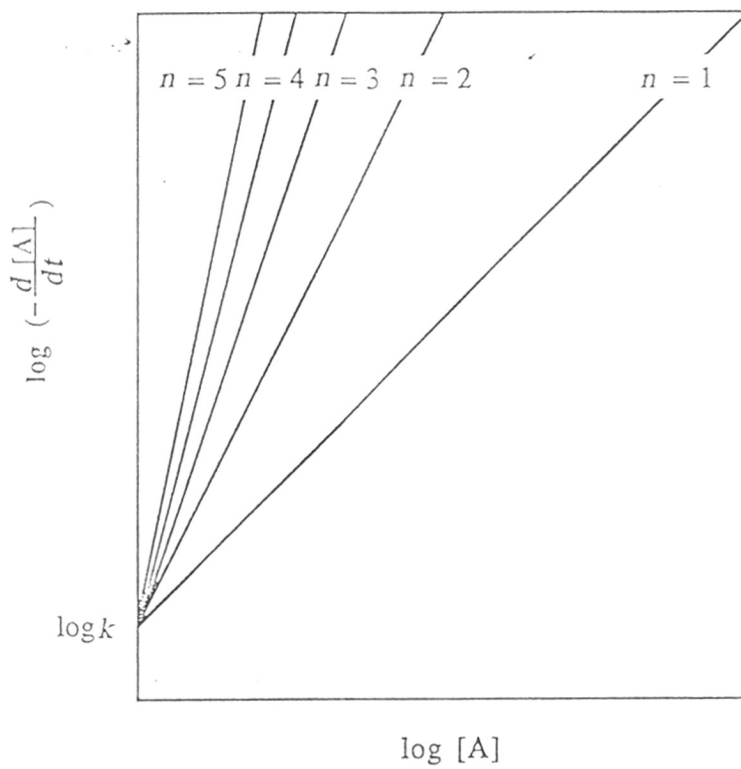


FIGURE 1.10 VAN'T HOFF PLOT OF $\log (-d[A]/dt)$ VERSUS $\log [A]$ FOR VARIOUS REACTION ORDERS

$$-\frac{d[A]}{dt} = k_1[A] \quad (1.24)$$

This technique of isolating in turn the contributions of various components can be used in unravelling a complex reaction mechanism.

1.10.4 Complex reactions

A series of elementary reactions constitute a mechanism of a complex reaction. Complex reactions can be divided into several classes: (i) Opposing or reversible reactions [equation (1.25)]; (ii) Consecutive reactions [equation (1.26)]; (iii) Parallel reactions [equation (1.27)] and (iv) Mixed reactions.



It is difficult to obtain exact solution for many complex reactions. It may therefore become necessary to use approximate treatments such as steady state, Laplace transform, determinant method etc. However, when analytical solutions are impossible to obtain either directly or by using approximation methods, a numerical solution is generally possible.

1.10.5 Steady state approximation

This method is commonly applied to solve some cumbersome reactions. It was originally proposed by Bodenstein⁸¹ and further developed by Semenov.⁸² Complex analytical treatment is simplified by assuming the rate of change of some reaction intermediate to be equal to zero. Mathematically,

$$\frac{d[A]_t}{dt} = 0 \quad (1.28)$$



then, under steady state condition

$$\frac{d[B]}{dt} = -k_2[B] + k_1[A] = 0 \quad (1.30)$$

1.10.6 Temperature dependence of rate constants

Rate expressions are simple functions of reactant concentrations with a characteristic rate constant 'k'. If rate equation is correctly formulated, the rate constant should be independent of concentration of species appearing in the rate law. It should also be independent of time. It does, however, depend strongly on temperature. This behaviour was described by Arrhenius⁸³ in 1889 on the basis of numerous experimental rate measurements. This dependence is given by Arrhenius equation as follows:

$$k(T) = A e^{\frac{-E_{(act)}}{RT}} \quad (1.31)$$

1.11 KINETICS OF STEP POLYMERISATION

Many of the principle features of polycondensation reaction have unresolved despite their great technological importance. There are uncertainties regarding the order of reaction and whether it is markedly dependent on the medium, incidence of equilibrium in condensation and influence of the rate of by-product removal etc. These uncertainties arise because the studies have been conducted primarily in complicated bulk medium provided by pure reactants.

Kinetics of polyesterification have been reported by Lenz⁸⁴, Davies and Hill⁸⁵⁻⁸⁷, Rolfe and Hinshelwood⁸⁸, Dostal and Raff^{89,90}, Flory⁹¹ and others but exceedingly varied results have been noted. Few researchers are of the view that polyesterification should be a second order reaction since these are essentially bimolecular; or second order in the early stages and third order in the later stages of reaction. Tang Au-Chin and Yao Kuo-Sui⁹² proposed a mechanism for the catalysis of polyesterification by hydrogen ion which leads to an intermediate order of 2.5. Makay-Bodi⁹³ grouped diacids into two different groups on the basis of the dissociation constants (pK_1 and pK_2).

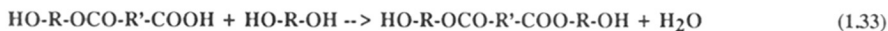
Quantitative theoretical basis of kinetics and mechanism of polycondensation reaction between dicarboxylic acid and dibasic alcohol are attributable to Flory.⁹⁴ He suggested that polycondensation proceeds under the catalytic activity of carbonyl groups and postulated trimolecularity for reaction in the absence of an external catalyst. A review of existing kinetics literature leads to the following conclusions : (1) The similarities between simple esterification and polyesterification are accepted unequivocally; (2) The reactivity of functional groups is independent of chain length; (3) Monomers are the most prevalent species at every instant during polycondensation reaction; (4) Condensation kinetics of aromatic diacids and diols have not been investigated; (5) There are very few published reports on kinetics of acidolysis of all aromatic LCPs.⁹⁵⁻⁹⁸

1.11.1 Analysis of polymerisation kinetics

The primary aim of kinetic analysis is the determination of mechanism by which system changes its composition. This involves determination of order and rate coefficients and provides Arrhenius parameters which should be rationalised in terms of thermodynamics of the process. Step polymerisation proceeds by a relatively slow increase in molecular weight of polymer. The first step is the reaction of diol and diacid monomers to form a dimer,



dimer then forms trimer by reaction with diol monomer,



and also with diacid monomer,



dimer reacts with itself to form a tetramer,



Trimer and tetramer react further. The reaction can be expressed as a general reaction:



Reaction mixture consists of diols, diacids and hydroxy acid molecules of varied lengths and any molecule with hydroxyl group can and will react with any molecule having carboxylic acid group. Thus, the rate of step polymerisation is the sum of the rates of all these intermediate reactions between molecules of various sizes.^{99,100} Kinetic analysis of such a difficult system is simplified by assuming that reactivities of both functional groups of a bifunctional monomer are the same and that each functional group reacts independent of the other irrespective of the chain length. These assumptions allows the treatment of polyesterification in a manner similar to esterifications.

1.11.2 Kinetic Expressions

The diacid monomer doubles up as the catalyst for the reaction. The rate is therefore

$$\frac{-d[\text{COOH}]}{dt} = K[\text{COOH}]^2[\text{OH}] \quad (1.37)$$

for stoichiometrically equivalent amounts of diacid and diol,

$$- \frac{d[M]}{dt} = k[M]^3 \quad (1.38)$$

[M] = concentration of hydroxyl and carbonyl groups at time t

$$- \frac{d[M]}{[M]^3} = K dt \quad (1.39)$$

integration of this yields

$$2Kt = \frac{1}{[M]^2} - \frac{1}{[M_0]^2} \quad (1.40)$$

[M₀] = initial concentration of hydroxyl and carbonyl groups. If "p" is fractional conversion, concentration of functional group reacted at time t is M₀p; concentration of unreacted functional group M, is (M₀ - M₀p).

$$[M] = [M_0](1 - p) \quad (1.40a)$$

combining equations (1.40) and (1.40a), we get

$$\frac{1}{(1 - p)^2} = 2[M_0]^2 kt + 1 \quad (1.41)$$

when catalyst is added, rate expression changes to,

$$[M_0]kt = \frac{1}{(1 - p)} - 1 \quad (1.42)$$

This is a rate expression for second order reaction.¹⁰¹ The plot of 1/(1-p) against time is a straight line slope of which gives the rate of reaction.

1.12 THERMODYNAMIC FORMULATION OF RATE EQUATIONS

The treatment of reaction rates described here is based on the concept that there exists a 'Transition state' or an 'Activated complex' between the initial and the final state. It exists at the highest point of potential energy surface in the reaction path from initial state to the final state through the lowest energy barrier (Figure 1.11). In the theoretical treatment of rate processes by Arrhenius⁸³, Eyring^{102,103}, Evans and Polanyi, the activated complex was regarded as being in equilibrium with the reactants.¹⁰⁴ Modern development of the theory of reaction rates have come from Arrhenius equation,

$$\ln k = \ln A - \frac{E}{RT} \quad (1.43)$$

where k = rate constant; T = reaction temperature; E = activation energy and A = frequency factor. A and E are independent of temperature provided the temperature range under consideration is small.

Two theories were put forth as a consequence of this relation between rate constant and temperature^{105,106} are : (1) *Collision theory* and (2) *Theory of absolute reaction rates*.

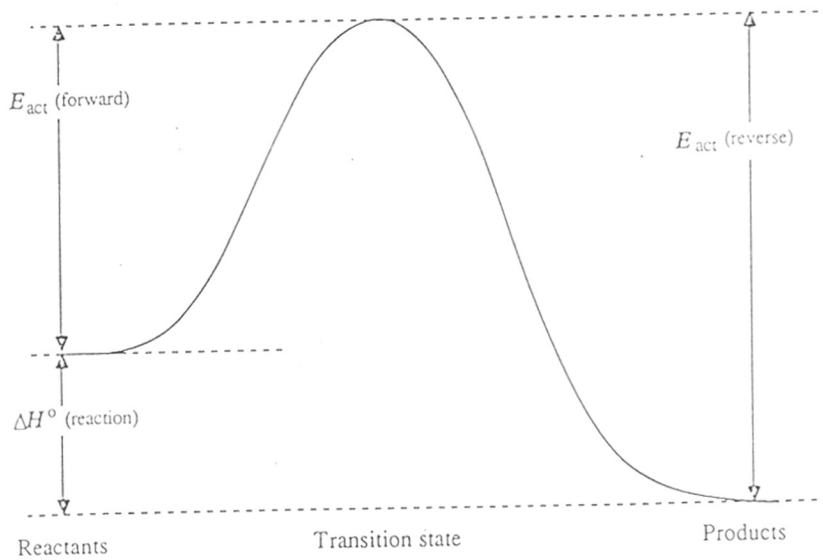
1.12.1 Collision Theory

Rate constant is given by the following expression:

$$k = Z e^{-\frac{E}{RT}} \quad (1.44)$$

where the exponential term represents concentration of activated molecules and

$$Z = \pi \left(\frac{1}{2} \sigma_A + \frac{1}{2} \sigma_B \right)^2 v_{relative} n_A n_B \quad (1.45)$$



$E_{\text{act}}(\text{forward})$ Activation energy of forward reaction
 $E_{\text{act}}(\text{reverse})$ Activation energy of reverse reaction
 $E_{\text{act}}(\text{forward}) - E_{\text{act}}(\text{reverse}) = \Delta H^\circ$

FIGURE 1.11 ENTHALPY DIAGRAM FOR A CHEMICAL REACTION

This gives the number of molecules colliding per unit volume per unit time (collision frequency). σ_A and σ_B are reactive cross sections of colliding molecules, n_A and n_B are moles of A and B respectively and v_{relative} is relative velocity of colliding molecules.

Collision theory agrees well only in reactions between simple molecules in gaseous state. There are many so called 'slow' reactions in solution which have rates much slower than that predicted by the equation (1.44). Collision theory also fails in case of reversible reactions.



$$k_1 = Z_1 e^{-\frac{E}{RT}} \quad (1.47)$$

$$k_2 = Z_2 e^{-\frac{E}{RT}} \quad (1.48)$$

$$K^* = \frac{k_1}{k_2} = e^{-\frac{E_1 - E_2}{RT}} \quad (1.49)$$

$(E_1 - E_2)$, the difference in activation energies of forward and backward reactions, is therefore the difference in the heat content of products and reactants. Collision theory then leads to the following expression,

$$k = Z e^{-\frac{\Delta H}{RT}} \quad (1.50)$$

where ΔH is heat of activation. This can be true only at absolute zero or when change in entropy during the reaction is negligible. Equation (1.44) thus is:

$$k = P Z e^{-\frac{E}{RT}} \quad (1.51)$$

where P is the steric/probability factor. Equation (1.49) takes the form:

$$K^* = \frac{k_1}{k_2} = \frac{P_1}{P_2} e^{-\frac{\Delta H}{RT}} \quad (1.52)$$

since $Z_1/Z_2 = 1$. This equation indicates that in addition to the number of collision (Z), orientation during collision (P) too governs the rate of reaction. Change in free energy is related to equilibrium constant^{105,106} of a reaction by:

$$\Delta G^* = -RT \ln K^* \quad (1.53)$$

$$K^* = e^{-\frac{\Delta G^*}{RT}} \quad (1.54)$$

$$\Delta G^* = \Delta H - T \Delta S^* \quad (1.55)$$

where ΔG^* is free energy of activation, ΔH^* is enthalpy of activation and ΔS^* is entropy of activation.

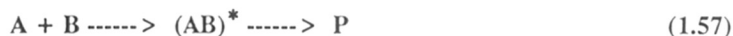
$$K^* = e^{\frac{\Delta S^*}{R}} e^{-\frac{\Delta H^*}{RT}} \quad (1.56)$$

On comparing equation (1.52) and (1.56) it bears out that the term P_1/P_2 accounts for the entropy of activation. Therefore, the free energy too is an important factor in the reaction and not just the enthalpy of activation alone as implied in equation (1.49). A case in point is the denaturation of proteins where the energy of activation is exceptionally high,¹⁰⁷ in excess of 100 kCal/mole, but the reaction proceeds favourably even at ambient temperatures because the reaction is accompanied by a large increase in entropy. On the other hand, condensation of vapour is relatively slow despite a small or zero heat of activation. Here, the

change is accompanied by marked decrease in entropy.

1.12.2 Theory of Absolute Reaction Rates

Collision theory fails in many cases because it treats the molecules as hard spheres and does not allow them any kind of freedom. This theory takes into consideration the degrees of freedom associated with a molecule by way of partition functions. Consider the following reaction,



where $(AB)^*$ represents the activated complex. It differs from the ordinary molecules in that it has no stable equilibrium state and exists only momentarily at some potential energy maximum. The theory assumes that the activated complex is in equilibrium with the reactant molecules A and B. Hence, equilibrium constant can be related to the energy of activation by the following equation,

$$K^* = \frac{[AB^*]}{[A][B]} = \frac{Q_{AB}^*}{Q_A Q_B} e^{-\frac{E_0}{kT}} \quad (1.58)$$

where K^* = equilibrium constant; Q = partition function; E_0 = activation energy.

Partition function can be factorised into contributions corresponding to translational, rotational and vibrational modes. Activated complex (AB^*) has $[3(N_A + N_B) - 6]$ modes of vibration if it is nonlinear. One of these vibrations is of different character from the rest, since it corresponds to a loose vibration which allows the complex to dissociate into products. Normal mode of vibrational partition function is q_v

$$q_v = \frac{1}{1 - e^{-\frac{h\nu}{kT}}} \quad (1.59)$$

The above relation changes for loose vibration ($\nu = 0$) to

$$\lim_{h\nu \ll kT} \frac{1}{1 - e^{-\frac{h\nu}{kT}}} = \frac{1}{1 - \left(1 - \frac{h\nu}{kT}\right)} = \frac{kT}{h\nu} \quad (1.60)$$

Substituting this value in equation (1.58), we get

$$\frac{[AB^*]}{AB} = \frac{Q_{*AB}}{Q_A Q_B} \frac{kT}{h\nu} e^{-\frac{E_0}{RT}} \quad (1.61)$$

$Q_{*AB}/Q_A Q_B$ corresponds to $[3(N_A + N_B) - 7]$ modes of vibration and $kT/h\nu$ corresponds to loose vibration; where, k = Boltzmann constant, T = temperature, h = Planck constant and ν = vibration frequency. Rearranging equation (1.61) gives:

$$\nu \frac{[AB^*]}{[A][B]} = k = \frac{Q_{*AB}}{Q_A Q_B} \frac{kT}{h} e^{-\frac{E_0}{RT}} \quad (1.62)$$

Comparing equation (1.58) with equation (1.62) gives,

$$k = \frac{kT}{h} K^* \quad (1.63)$$

Thermodynamically, free energy is related to equilibrium constant as follows,

$$\Delta G^* = -RT \ln K^* \quad (1.64)$$

Taking antilogarithm of equation (1.64), we get:

$$K^* = e^{-\frac{\Delta G^*}{RT}} \quad (1.65)$$

Equation (1.63) therefore, changes to

$$k = \frac{kT}{h} e^{-\frac{\Delta G^*}{RT}} \quad (1.66)$$

Above equation can also be written as

$$k = \frac{kT}{h} e^{\frac{\Delta S^*}{R}} e^{-\frac{\Delta H^*}{RT}} \quad (1.67)$$

Experimental activation energy obtained from Arrhenius plot is not exactly the heat of activation mentioned in the above equation. Actual relation¹⁰⁸ between the two is as follows,

$$E_{\text{exp}} = \Delta H^* + RT \quad (1.68)$$

Substituting this value for (ΔH^*) leads to the following equation

$$k = e \frac{kT}{h} e^{\frac{\Delta S^*}{R}} e^{-\frac{E_{\text{exp}}}{RT}} \quad (1.69)$$

where, k = rate constant; T = absolute reaction temperature; k = Boltzmann constant; h = Planck's constant; R = gas constant; E_{exp} = experimental activation energy and ΔS^* = Entropy of activation. Frequency factor "A" can be calculated if the above equation is compared with Arrhenius equation,

$$A = e \frac{kT}{h} e^{\frac{\Delta S^*}{R}} \quad (1.70)$$

In terms of relation of frequency factor and entropy of activation (ΔS) the rate of reaction is lower than that given by collision theory if (ΔS) is negative, since probability of formation of the activated complex is low. The probability of formation of activated complex is high when (ΔS) is positive and therefore the rate is greater than that given by collision theory.

1.13 CHARACTERISATION

Combination of various analytical techniques is intrinsic to complete characterisation of liquid crystal polymers.

1.13.1 Differential Scanning Calorimetry

Differential Scanning Calorimeter (DSC) is widely used for thermal characterisation of polymeric materials. In this technique sample and the reference are heated/cooled simultaneously at a predetermined rate. The differential power supplied to the sample, to annul any temperature difference which might arise between the two during a thermal transition, is monitored against temperature in power compensation device (Perkin Elmer). In heat flux type DSC (Mettler), a temperature difference between sample and reference is measured as a differential voltage which is later converted to the actual heat flow. A typical thermogram so obtained shows peaks corresponding to glass transition, melting, crystallisation, solid-liquid crystal and liquid crystal-liquid crystal etc. During the transformation of a material from solid to liquid crystal or liquid crystal to isotropic liquid state, there are characteristic changes in physical and mechanical properties, morphology and also thermodynamic variables.¹⁰⁹

The instrument can measure heat of fusion, heat of crystallisation, percent crystallinity, time of crystallisation (isothermal technique) etc. It has been observed that liquid crystal polymeric structures produce a melt which tends to be cloudy instead of being clear. On further heating, a temperature is reached at which the cloudy melt changes to a clear melt. This corresponds to the transition temperature at which the molecular orientation of the

liquid crystal phase breaks up and anisotropic melt transforms into the transparent isotropic melt. In liquid crystalline materials the transitions are independent of thermal history of the material.¹⁰⁰ Liquid crystal-isotropic transition and liquid crystal-liquid crystal transition are almost reversibly observed on cooling the isotropic liquid while supercooling is observed for solid-liquid crystal and solid-solid transitions.

A typical odd-even relationship between number of carbon atoms in the flexible spacer and the transition temperature is observed in polymeric materials as in low molecular liquid crystals.^{54,55,111} The enthalpy changes associated with melting of polymers are lower than those observed for small molecules of similar chemical structure.¹¹²

1.13.2 Optical Microscopy

The liquid crystalline phases can be identified from the textures characteristic of different types of phases.^{113,114} When viewed under crossed polariser in polarising microscope nematic phase shows typical threaded or Schlieren texture. Cholesteric polymers show planar texture with oily streaks. Focal conic or fan shaped texture are characteristic of smectic phases. Pretreatment is often necessary to see textures easily in polymeric materials.¹¹⁵ It may take several days to develop textures due to high viscosity of polymeric materials.

1.13.3 X-Ray Analysis

A system for identification of type of mesophases from the diffraction pattern is developed by DeVries.¹¹⁵ Diffraction pattern of a powder sample can be divided into inner rings at small diffraction angle which are indicative of longer layer spacings. The outer rings at large angles correspond to shorter spacing in the lateral packing arrangement of molecules. Appearance of a broad halo or a sharp ring is a measure of order present in the structure.

Studies of thermotropic polymers by Wide Angle X-ray Diffraction, WAXD, in the liquid crystalline state are useful in the identification of the structure of the liquid crystalline melt.

In WAX diffraction patterns, nematic structures produce a diffuse broad ring which corresponds to average intermolecular spacing of approximately 4 to 6 \AA on a flat film diffractogram. Similar diffuse halo is seen for isotropic liquid phase. Therefore, it is assumed that there is lack of lateral periodic order. At small angles, nematic patterns may present a diffuse ring corresponding to distances which are very close or equal to the length of repeat unit. This shows that there is no order along molecular long axes. Nematic phases are characterised by one broad halo in the wide angle scattering region which could imply short range positional order. Cholesteric mesophases in general resemble the nematic mesophases when observed by both small angle X-ray diffraction and WAXD.

Smectic structure is characterised by one more reflection in the small angle scattering region (15-50 \AA) which is sharp and a broad halo in the wide angle region (4-5 \AA). The pattern in the small angle region is due to smectic layers. The wide angle halo is due to two dimensional fluid state within the smectic layers. Detailed structural information is possible if the sample is in well oriented monodomain form.

REFERENCES

1. O.Z. Lehman, *Phys. Chem.*, **4**, 462 (1889).
2. F. Reinitzer, *Monatsh. Chem.*, **9**, 421 (1888).
3. L. Gattermann, *Liebigs. Ann. Chem.*, **347**, 347 (1906).
4. L. Gattermann, *Liebigs. Ann. Chem.*, **357**, 313 (1908).
5. D. Vorlander, "Chemische Kristallographic der Flussigkeiten", p-90, Akad. Verlagsges:Leipzig (1924).
6. F.C. Bowden, *Proc. R. Soc. London. Ser.B*, **123**, 274 (1937).
7. P.J. Flory, *Proc. R. Lond. Ser. A*, **234**, 60, 73 (1956).
8. S.L. Kwolek, Du Pont, B. P. 1,198,081 (1966).
9. S.L. Kwolek, Du Pont, B. P. 1,283,064 (1968).
10. S.L. Kwolek, P.W. Morgan, J.K. Schaijge and L.W. Gulrich, *Macromolecules*, **10**, 1390 (1977).
11. H.F. Khufuss and W.J. Jackson, Eastman Kodak Co. B.P. 1,435021 (1972).
12. H.F. Khufuss and W.J. Jackson, *J. Polym. Sci., Polym. Chem. Ed.*, **14**, 2043(1976).
13. H.F. Khufuss and W.J. Jackson, *J. App. Polym. Sci.*, **25**, 1685 (1980).
14. A. Roviello and A. Sirigu, *J. Polym. Sci., Polym. Lett. Ed.*, **13**, 455 (1975).
15. G.W. Gray, "Molecular structure and properties of liquid crystals," Academic Press Ltd., London, England (1962).
16. G.W. Gray, *Mol. Cryst., Liq. Cryst.*, **21**, 161 (1973).
17. F.D. Saeva "Liquid crystals: The fourth state of matter", Marcel Dekker Inc., New York (1979).

18. E.B. Priestley, P.J. Wojtowicz and P. Sheng "Introduction to liquid crystals", Plenum Press, New York (1976).
19. V.P. Shibaev and N.A. Plate, Polym. Sci. USSR, **19**, 1068 (1978).
20. H. Ringsdorf and A. Schneller, Brit. Polym. J., **13**, 43 (1981).
21. H. Finkelmann and G. Rehage, Adv. Polym. Sci., **60/61**, 69 (1984).
22. N.A. Plate, R.V. Talroze and V.P. Shibaev, Polym. J., **19**, 135 (1987).
23. W.H. de Jeu in "Physical properties of liquid crystalline materials", ed. Gordon and Breach, Science Publishers, Inc. London (1980).
24. L. Onsager, Ann. N.Y. Acad. Sci., **51**, 627 (1949).
25. S.L. Kwolek, P.W. Morgan and J.R. Schaefgen, in Encyclopedia of Polymer Science and Engineering (ed. H.F. Mark), Wiley, New York, **9**, 1 (1987).
26. P.J. Flory, Adv. Polym. Sci., **59**, 1 (1984).
27. P.J. Flory and G. Ronca, Mol. Cryst.; Liq. Cryst., **54**, 289, 311 (1979).
28. E.A. DiMarzio, J. Chem. Phys., **35**, 658 (1961).
29. C.K. Ober, J.I. Jin and R.W. Lenz, Adv. Polym. Sci., **59**, 103 (1984).
30. A. Blumstein, K.N. Sivaramakrishnan, R.B. Blumstein and S.B. Clough, Polymer, **23**, 479 (1982).
31. A. Roviello and A. Sirigu, Macromol. Chem., **183**, 895 (1982).
32. A.C. Griffin and S.J. Havens, J. Polym. Sci., Polym. Lett. Ed., **18**, 259 (1980).
33. A.C. Griffin, Mol. Cryst., Liq. Cryst., Letters, **49**, 239 (1979).
34. W.R. Krigbaum, J. Asrar, H. Toriumi, A. Ciferri and J. Preston, J. Polym. Sci., Polym. Lett. Ed., **20**, 109 (1982).

35. Jung-Il. Jin, H.S. Choi, and E.J. Choi, *J. Polym. Sci., Part B; Polym. Phys.*, **28**, 531 (1990).
36. Van Luyen and L. Strzelecki, *Eur. Polym. J.*, **16**, 299 (1980).
37. A.C. Griffin and S.J. Havens, *J. Polym. Sci., Polym. Phys. Ed.*, **19**, 951 (1981).
38. R.W. Lenz, Jung-Il Jin and K.A. Feichtinger, *Polymer*, **24**, 327(1983).
39. J.I. Jin, S. Antoun, C. Ober and R.W. Lenz, *Br. Polym. J.*, **12**, 132 (1980).
40. K. Iimura, N. Koide and R. Ohta, *Rep. Prog. Polym. Phys. Jap.*, **24**, 231 (1981).
41. A. Blumstein, K. Sivaramakrishnan, S.B. Claughand R.B. Blumstein, *Mol. Cryst., Liq. Cryst., Letters*, **49**, 255 (1979).
42. C. Noel, L. Monnerie and B. Fayolle, *Br. Polym. J.*, **13**, 55 (1981).
43. M.J.S. Dewar and R.M. Riddle, *J. Am. Chem. Soc.*, **97**, 6658 (1975).
44. A.B. Erdemir, D.J. Johnson and J.G. Tomka, *Polymer*, **27**, 441 (1986).
45. J.-I. Jin, S.H. Lee and H.J. Park, *Polym. Prepr.*, **28**, 122 (1987).
46. W.J. Jackson, Jr., *Br. Polym. J.*, **12**, 154 (1980).
47. R. Cai and E.T. Samulski, *Macromolecules*, **27**, 135 (1994).
48. R. Cai, J. Preston and E.T. Samulski, *Macromolecules*, **25**, 563 (1992).
49. Z.G. Li, J.E. McIntyre, J.G. Tomka and A.M. Voice, *Polymer*, **34**(9), 1946 (1993).
50. B.-W. Jo, J.-I. Jin and R.W. Lenz, *Eur. Polym. J.*, **18**, 233 (1982).
51. B. Millaud, C. Strazielle, *Mol. Cryst., Liq. Cryst., letters*, **49**, 299 (1979).
52. H. Ringsdorf and A. Schrieller, *Br. Polym. J.*, **13**, 43 (1981).
53. B. Fayolle, C. Noel and J. Billard, *J. Phys. (Paris)*, **40**, C3-485 (1979).
54. A. Roviello and A. Sirigu, *Eur. Polym. J.*, **15**, 61 (1979).

55. A. Roviello and A. Sirigu, *Makromol. Chem.*, **183**, 895 (1982).
56. S.K. Varshney, *Rev. Macromol. Chem. Phys.*, **C26**, 551 (1986).
57. T.S. Chung, *Polym. Engg. Sci.*, **26**, 901 (1986).
58. N. Koide, *Mol. Cryst., Liq. Cryst.*, **139**, 47 (1986).
59. J. Preston, *Angew. Makromol. Chemie.*, **109/110**, 1 (1982).
60. D.J. Blundell, *Polymer*, **23**, 359 (1982).
61. B.P. Griffin and M.K. Cox, *Br. Polym. J.*, **12**, 147 (1980).
62. J. Cao, J.G. Tomka, J.E. McIntyre, *Polymer*, **34-7**, 1471 (1993).
63. M.G. Dobb and J.E. McIntyre, *Adv. Polym. Sci.*, **60/61**, (1984).
64. F. Navarro and J.L. Serrano, *J. Polym. Sci. A., Polym. Chem.*, **30**, 1789 (1992).
65. Jung- Il Jin, S.H. Lee, H.J. Park and Il-Joong Kim, *Polymer J.*, **21**, 615 (1989).
66. W.A. MacDonald and J.G. Ryan, *Eur. Pat. (ICI)*, 275164 (1988).
67. H.F. Khufuss and W.J. Jackson, *U.S. pat. (Eastman Kodak Co.)* 3778410 (1973).
68. B.Y. Shin and I.J. Chung, *Polym. Engg. and Sci.*, **30**, 13 (1990).
69. B.Y. Shin and I.J. Chung, *Polym. Engg. and Sci.*, **30**, 22 (1990).
70. Jung- Il Jin, C.-S. Kang and J.-H. Chang, *J. Polym. Sci. A., Polym. Chem.*, **31**, 259 (1993).
71. R.W. Lenz, *Polymer J.*, **17(1)**, 105 (1985).
72. B.-W. Jo and Jung-Il Jin and R.W. Lenz, *Makromol. Chem. Rapid. Commun.*, **3**, 23 (1982).
73. G.W. Claudann, *U.S. Pat. (Celanese Co.)*, 4161470 (1979).
74. W.J. Jackson, Jr. and U.C. Morris, *Brit. Pat. 2002404; U. S. Pat. 4169933*.

75. G.W. Claudann, Brit. Pat. 1585511; U.S. Pat.4067852.
76. M.H.B. Skovby, R. Lessel and J. Kops., J. Polym. Sci. A., Polym. Chem., **28**, 75 (1990).
77. P.W. Morgan,"Condensation Polymers: By Interfacial and Solution Methods", Interscience Publishers (1965).
78. L.B. Sokolov,"Synthesis of Polymers by Polycondensation", Isreal Program for Scientific Translations, Jerusalem, Chapter 1 (1968).
79. S. Glasstone, K.J. Laidler and H. Eyring,"Theory of Rate Processes", McGraw Hill, New York (1941).
80. J.I. Steinfeld,"Chemical Kinetics and Dynamics" Prentice - Hall, Inc., New Jersey, p.32 (1989).
81. M. Bodenstein, Z. Physik. Chem., **85**, 329 (1913).
82. N.N. Semenov, Zhur. Fiz. Khim., **17**, 187 (1943).
83. S. Arrhenius, Z. Physik. Chem. (Leipzig), **4**, 226 (1889).
84. R.W. Lenz, Ind. Eng. Chem., **61**, 67 (1969).
85. M. Davies and D.R.J. Hill, Trans. Faraday. Soc., **49**, 395 (1953).
86. M. Davies, Trans. Faraday. Soc., **34**, 410 (1938).
87. M. Davies, Reserch Supplement, **2**, (1949).
88. R.T. Rolfe and C.N. Hinshelwood, Trans. Faraday. Soc., **30**, 935 (1934).
89. H. Dostal and R. Raff, Monatsh, **68**, 188 (1936).
90. H. Dostal and R. Raff, Monatsh, **68**, 117 (1936).
91. P.J. Flory, J. Am. Chem.Soc., **59**, 466 (1937).

92. Tang Au-Chin and Yao Kuo-Sui, *J. Polym. Sci.*, **35**, 219 (1959).
93. E. Makey-Bodi, *J. Polym. Sci.*, C **16**, 3709 (1968).
94. P.J. Flory, "Principles of Polymer Chemistry", Cornell Univ. Press, Ithaca, New York, (1953).
95. J. Mathew, R.V. Bahulekar, R.S. Ghadage, C.R. Rajan, S. Ponrathnam and S.D. Prasad, *Macromolecules*, **25**, 7338 (1992).
96. J. Mathew, R.S. Ghadage, S. Ponrathnam and S.D. Prasad, *Macromolecules*, **27**, 4021 (1994).
97. I. Vulic and T. Schulpen, *J. Polym. Sci. A., Polym. Chem.*, **30**, 2725 (1992).
98. D.B. Cotts and G.C. Berry, *Macromolecules*, **14**, 930 (1981).
99. P.E.M. Allen and C.R. Patrick, "Kinetics and Mechanism of Polymerisation Reactions", John Wiley and Sons (1974).
100. G. Allen and J.C. Bevington, "Comprehensive Polym. Sci", **5**, Chapter 2, Pergamon Press, Oxford (1989).
101. F.W. Billmeyer, Jr., "Textbook of Polymer Science", John Wiley & Sons Inc., New York (1984).
102. H. Eyring and A.E. Stearn, *Chem. Rev.*, **24**, 253 (1939).
103. J. Eyring, *J. Chem. Phys.*, **3**, 107 (1935).
104. M.G. Evans and M. Polanyi, *Trans. Faraday Soc.*, **31**, 875 (1935).
105. K.J. Laidler, "Theories of Reaction Rates", McGraw Hill, New York (1969).
106. I. Amdur and G.G. Hammes, "Chemical Kinetics: Principles and Selected Topics", McGraw Hill Inc. (1966).
107. A.E. Stearn, *Ergebnisse Enzymforsch*, **7**, 1 (1938).

107. A.E. Stearn, *Ergebnisse Enzymforsch*, **7**, 1 (1938).
108. K.J. Laidler, Glasstone and J. R. Barrante, "Physical Chemistry for the Life Sciences", Prentice Hall, Inc., New Jersey (1977).
109. P. Navard, *Macromolecules*, **25**, 7172 (1992).
110. W.R. Krigbaum and F.J. Salaris, *Polym. Sci., Polym. Phys. Ed.*, **16**, 883 (1978).
111. A. Roviello and A. Sirigu, *Polym. J.*, **14**, 9 (1982).
112. B. Wunderlich and J. Grebonicz, *Adv. Polym. Sci.*, **60/61**, 1 (1984).
113. N.H. Hartshrone, "The Microscopy of Liquid Crystals", Microscope Publications Ltd., London (1974).
114. D. Demus and L. Richter, "Textures of Liquid Crystals", Verlag Chemie, Weinherim (1978).
115. J.N. Hay, *Brit. Polym. J.*, **3**, 74 (1971).
116. A. DeVries, *Mol. Cryst., Liq. Cryst.*, **10**, 31 (1970).

CHAPTER - 2

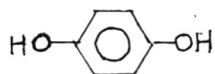
CHAPTER - 2

EXPERIMENTATION

Wholly aromatic polyesters were synthesised from aromatic diacids and diacetates by acidolysis type melt transesterifications. Similarly, three component copolyesters were synthesised by partially replacing either the diacid or the diacetate with other diacids and diacetates. Simultaneously, the kinetics of transesterification were monitored by estimating the rate of evolution of bi-product, acetic acid. Once the rate of generation of acetic acid became negligible under normal pressure, the reactions were taken to high conversion by continuing the reactions under reduced pressure. The polyesters formed were purified to remove reactants, catalyst residues (if any) and were characterised by differential scanning calorimetry (DSC) for thermal analysis, polarising microscopy (PM) for optical analysis and x-ray diffraction methods of analysis. The experimental kinetic data was analysed for rate, order of reactions, activation energies etc. Six uncatalysed and catalysed homopolyesterifications and two copolyesterification were investigated.

2.1 MATERIALS

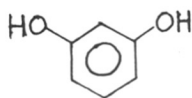
2.1.1 1,4-Benzene diol (Hydroquinone)



Empirical formula	$C_6 H_6 O_2$
Molecular weight	110.11
Melting point	$172^\circ C$

1,4-Benzene diol [hydroquinone] was obtained from M/S Loba Chemie Indo-Astranal Co., Mumbai, India.

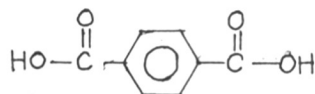
2.1.2 1,3-Benzene diol (Resorcinol)



Empirical formula	$C_6H_6O_2$
Molecular weight	110.11
Melting point	109-110°C

It was obtained from Aldrich Chemical Co.

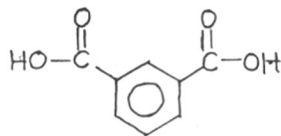
2.1.3 1,4-Benzene dicarboxylic acid (Terephthalic acid)



Empirical formula	$C_8H_6O_4$
Molecular weight	166.13
Melting point	> 300°C

It was obtained from M/S Koch-Light Laboratories Ltd. (England). It was used as received.

2.1.4 1,3-Benzene dicarboxylic acid (Isophthalic acid)



Empirical formula	$C_8H_6O_4$
Molecular weight	166.13

Melting point 341-343° C

It was obtained from Aldrich Chemical Co. Meta substituted (1,3-) monomers were used with the objective of introducing kinks in the linear polymer chain.

2.2 Catalysts

2.2.1 Zinc acetate

Empirical formula $\text{Zn}(\text{CH}_3\text{CO}_2)_2$

Molecular weight 219.50

This AR grade chemical was used after sufficient drying.

2.2.2 Sodium acetate

Empirical formula $\text{CH}_3\text{CO}_2\text{Na}$

Molecular weight 82.03

This AR grade chemical was used after sufficient drying.

2.2.3 Dibutyl tin oxide

Empirical formula $[\text{CH}_3(\text{CH}_2)_3]_2\text{Sn} = \text{O}$

Molecular weight 248.92

Melting point $> 300^\circ \text{C}$

GR grade sample was obtained from Fluka Chemie. and was used as received.

2.2.4 Dibutyl tin dilaurate

Empirical formula $[\text{CH}_3(\text{CH}_2)_{10}\text{CO}_2]_2\text{Sn}[(\text{CH}_2)_3\text{CH}_3]_2$

Molecular weight 631.56

LR grade sample was obtained from Fluka Chemie. and was used as received.

2.3 ACETYLATION OF DIOLS

Aromatic diols were acetylated to the respective diacetates with acetic anhydride so as to prepare the polyesters by the acidolysis route.

2.3.1 Acetic anhydride

Empirical formula	$C_4H_6O_3$
Molecular weight	102.09
Density	1.082 gm/mL
Boiling Point	138-140° C

Acetic anhydride was obtained from M/S S.D. Fine Chemicals Pvt. Ltd., Mumbai, India.

2.3.2 Hydroquinone diacetate

Empirical formula	$C_{10}H_{10}O_4$
Molecular weight	194.19
Melting point	121-123° C

Acetic anhydride (2 mole; 204 mL) was added with stirring to hydroquinone (1 mole; 110 g) and a drop of concentrated sulphuric acid was added to catalyse the reaction. The slurry homogenised to a clear solution. This was poured on to ice water. The white precipitate so obtained was filtered and washed several times with water to remove acetic acid generated during the reaction. It was recrystallised from mixed solvent system of water-methanol and dried in vacuum oven for 12 hours at 80° C; mp: 121-123° C; yield: 85 percent.

2.3.3 Resorcinol diacetate

Empirical formula	$C_{10}H_{10}O_4$
Molecular weight	194.19
Boiling point	146° C /12 torr

Resorcinol (1 mole; 110.0 g) was dissolved in sodium hydroxide (2 mole; 80.0 g). Acetic anhydride (2 mole; 204 mL) was added to this solution with stirring. Product phase separated as brown coloured oil which settled at the bottom. This was separated using a separating funnel and purified by vacuum distillation. Yield: 90 percent.

2.4 POLYESTERIFICATION

Stoichiometrically equivalent amounts of diacetate and diacid were polymerised by acidolysis method of melt polyesterification. Polymerisation reactions were conducted in a 60 mL capacity glass reactor (**Figure 2.1**). Reaction mixture was heated in a furnace coupled to a programmable temperature controller. Continuous overlay of inert gas (N_2) was maintained to avoid oxidative degradation of the mixture. Reaction mixture was stirred at a fixed rotations per minute using a constant speed stirrer to ensure constant rate of agitation and to facilitate removal of bi-product, acetic acid.

Reaction kinetics was studied by quantitatively monitoring the amount of acetic acid collected with respect to the time in side arm of the reactor. Rate of reaction was studied as a function of temperature, catalyst and also with respect to the monomer composition, in case of copolymers.

After the kinetic data collection was completed under normal pressure, the reactions were continued under reduced pressure for a definite period of time to realise high molar mass polymer by removing the last traces of acetic acid. Product was then isolated, crushed and purified to remove starting materials.

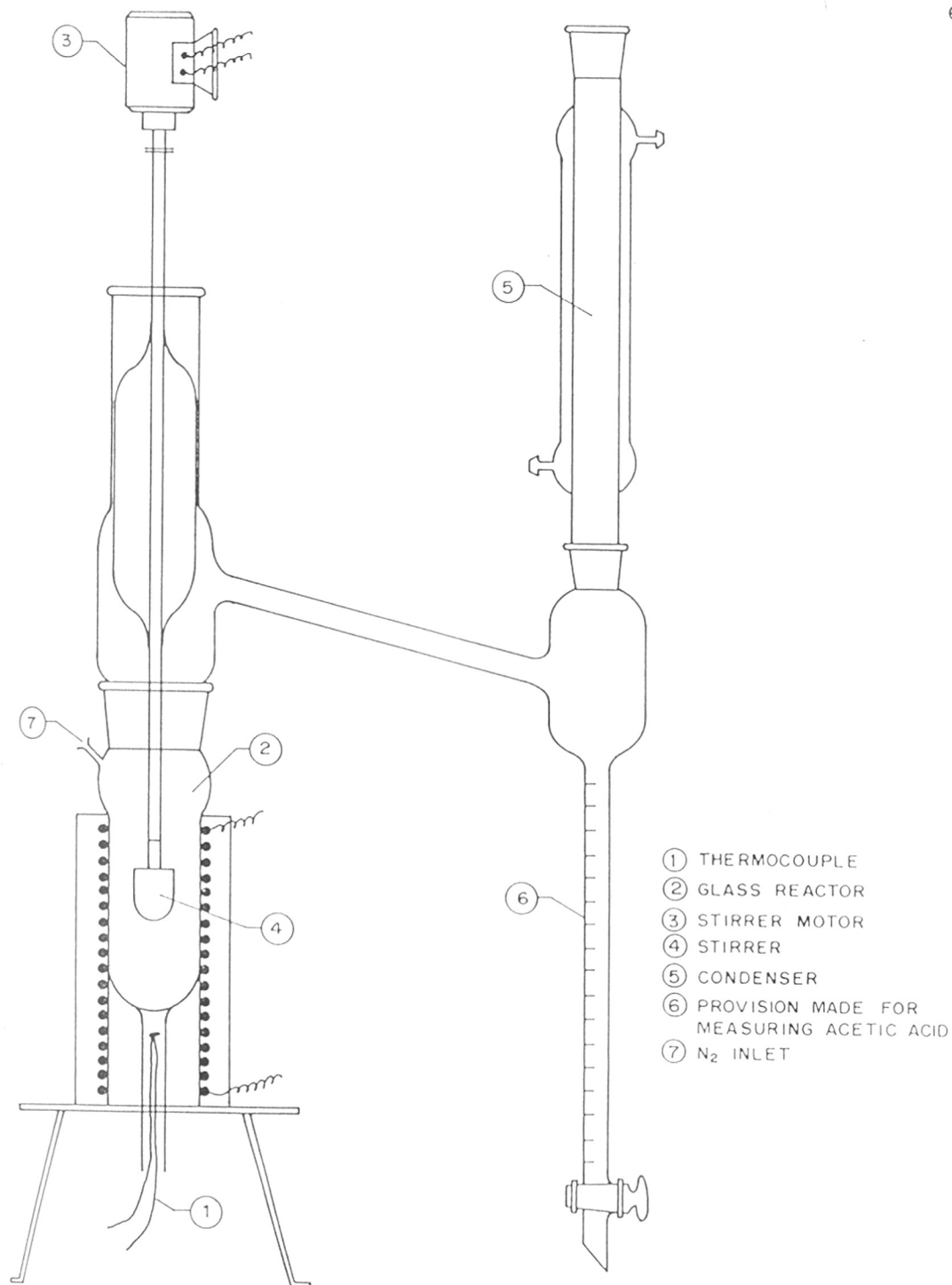


FIGURE 2.1 EXPERIMENTAL SETUP FOR MELT ACIDOLYTIC TRANSESTERIFICATION REACTIONS

2.5 OPTIMISATION OF REACTION PARAMETERS

Preliminary studies conducted to standardise certain reaction parameters such as temperature, catalyst, stirring speed, heating rate etc. This was achieved by carrying out reactions isothermally at various temperatures in the range 260 to 320° C using four different catalysts. Optimum heating rate and stirring speed were identified from the reactions carried out by varying these two parameters.

The following optimum reaction conditions were arrived at for further experimentation from the results of above reactions.

Reaction temperature	:	280, 290, 300, 310 and 320° C
Catalyst	:	Dibutyl tin oxide (1 mole %)
Stirring speed	:	300 rpm
Heating rate	:	10° C / minute
Homopolyester systems	:	<u>U</u> ncatalysed and <u>C</u> atalysed <u>H</u> ydroquinone <u>t</u> erephthalate (HTU and HTC) <u>H</u> ydroquinone <u>i</u> sophthalate (HIU and HIC) <u>R</u> esorcinol <u>t</u> erephthalate (RTU and RTC)
Copolyester systems	:	HIT and HRT

2.6 CHARACTERISATION

Polymers synthesised were subjected to following characterisations.

2.6.1 Differential Scanning Calorimetry (DSC)

The polyesters were analysed for thermal characteristics on Mettler DSC-30 coupled with TA-4000 data processor. 5 to 10 mg of sample was heated or cooled at 20° C

per minute and corresponding thermograms were recorded simultaneously. Depending on these preliminary scans, samples were subjected to different thermal histories in order to confirm the cause and nature of the transitions observed in those scans. Thermal parameters like glass transition temperature (T_g), mesophasic transition temperature (T_m), isotropisation temperature (T_i) and the corresponding enthalpy change (ΔH) and entropy change (ΔS) of transitions were calculated.

2.6.2 Polarising Microscopy (PM)

Optical observations were made with a Leitz Laborlux 12 POLS polarising microscope. Sample was heated at $5^\circ C$ per minute and observed under crossed polariser to see if birefringence is observed at temperatures corresponding to the transitions noted on differential scanning calorimeter. Morphology of mesophases and transition to different types of mesophases was studied with respect to temperature and time.

2.6.3 X-ray diffraction

Powder diffraction patterns were recorded at room temperature on PW-1730 Philips X-ray diffractometer. Slit collimated Ni filtered Cu-K α radiation of wavelength 0.15406 nm was generated by voltage and current settings at 40 KV and 16 mA respectively. High temperature X-ray analysis was carried out on an assembled instrument at 40 KV and 20mA.

2.6.4 Kinetic analysis

Experimental data collected at different temperatures in the form of volume of acetic acid condensed with time was analysed to determine percent conversion and degree of polymerisation. The data was also subjected to regression analysis in which rate plots corresponding to first, second, two and a half and third order rate law plots were plotted to determine precisely the order of reaction. Further analysis were conducted to estimate rate constant, activation energy for each system.

2.6.5 Thermodynamic analysis

Thermodynamic parameters of reaction like heat of activation (ΔH), entropy of activation (ΔS) and frequency factor etc. were calculated from the relation between specific reaction rate and experimental activation energy as predicted by the "*theory of absolute reaction rates*".

* * * * *

CHAPTER - 3

* * * * *

CHAPTER - 3

3.1 INTRODUCTION

Main chain all-aromatic thermotropic polyesters can be derived from 1,4-phenylene units¹. 'Xydar' and 'Vectra' are commercially successful thermotropic liquid crystal polyesters synthesised by polyesterification between aromatic diacids and diacetates. The melting temperatures of wholly aromatic polyesters based on 1,4-disubstituted benzenes are too high to be melt processed by conventional equipments^{2,3}. Melt processable thermotropic rigid-rod polyesters are obtained by structure randomisation through copolymerisation with comonomers having either substituents or kinks, to suppress the crystal-mesophase transition below the decomposition temperature. Prior to the synthesis of copolyesters it is imperative that the kinetics of the individual homopolyesterification processes be examined in isolation to estimate the probability of such randomisation.

polyesterifications between diacids and diols can be brought forth by a variety of means. Uncatalysed polyesterification of diacids with diols at high temperatures is inadequate to generate high molecular weight aliphatic polyesters^{4,5}. Also, this method is unsuited to less stable alkylidene and cycloalkylidene diphenols such as Bisphenol-A.^{6,7} Linear polyesters have been prepared from a mixture of diphenol, dicarboxylic acid and lower aliphatic dicarboxylic acid.⁵ Polyesterification procedures to generate high molecular weight polyesters, which have evolved over the years, use at least one reactive monomer such as acid chloride (Schautten-Baumann reaction)⁸⁻¹⁰, diacetate (acidolysis) and diphenate (alcoholysis).

The diacetate and diphenate reactions can be conducted in solution, melt or in a slurry at high temperature in an inert atmosphere¹¹. The only shortcoming with diacetate route is the limited solubility and reactivity of the diacid which dictates the reaction time

required to achieve the desired high molecular weight polyester. The limitations with the diphenate route are the additional step of preparing the diaryl ester of the diacid and the handling of a corrosive bi-product, phenol.⁴

The kinetics of polyesterification reactions between aliphatic diacids and diols in solution have been extensively investigated.^{12,13} Quantitative theoretical foundations of the kinetics and mechanism are attributable to Flory¹⁴. He extended the assertions of Rolfe and Hinshelwood¹⁵ on catalytic role of carbonyl groups to polycondensations and offered a rationale for trimolecularity of the reaction. This kinetic picture extends the esterification reaction further to polyesterification and proposes independence of reactivities of the functional groups on the molecular size¹⁴. Subsequent researches have noted differing kinetic orders. Davies¹⁶ and Korshak et Al^{17,18} found the reaction to be bimolecular. Davies and Hill¹⁹ investigated the reversibility of the reaction due to hydrolysis and concluded on a variable reaction order. Tang Au Chin et Al²⁰ found a direct proportionality to the concentration of hydrogen ion arising from the dissociation of carboxylic acid groups. Polyesterification of a specific group of weak diacids was shown to have an order of 2.5. Further proof has been obtained in an extensive investigation by E. Makay-Bodj²¹.

Reports of kinetic investigation of acidolysis in the melt, which has commercial implications (liquid crystalline polyesters, polyarylates), have been rather few. Vulic and Schulpen²² studied the acidolysis kinetics in the melt between 4-acetoxy benzoic acid (OB), 4,4'-biphenyl diacetate (BPDA) and terephthalic acid (TPA) with and without catalyst. Mathew et Al^{23,24} reported a detailed kinetics investigation of melt acidolysis of 4-acetoxy benzoic acid [OB] either alone or in the presence of poly(ethylene terephthalate) [PET] to synthesise poly(4-oxy benzoate) or PET-OB respectively.

This scarcity of published literature is surprising because the mechanism of acidolysis is known²⁵⁻²⁷ since 1958 and over the past two decades synthesis of thermotropic all aromatic polyesters by this route have been thoroughly investigated^{28,29}. There are many uncertainties about kinetic order of the reaction, activation energy etc. of the reaction in the melt. This dearth in open literature on kinetics of melt polyesterification reaction between aromatic monomers leading to main chain liquid crystalline polyesters (LCPs) can be attributed to the intrinsic mechanistic complexity of reaction. Complications derive from the high temperature needed to maintain the copolyesters in the molten state. Side reactions may occur at these high temperatures leading to chain growth or chain scission or changes in the chemical nature of end groups, insolubility of diacids or stoichiometric imbalances due to sublimation of reactants, diffusion constraints which limit the effective removal of bi-product and influence the reaction rate.

The major aim of this study is to evolve a detailed kinetic investigation of the acidolysis reaction between well known 1,4- and 1,3-benzene disubstituted acids and acetates which are the major constituents in thermotropic liquid crystalline polyesters.

The study was carried out with the following objectives: (1) Kinetic analysis of the synthesis of catalysed and uncatalysed poly(hydroquinone-terephthalate) (HT); (2) Kinetic analysis of the synthesis of catalysed and uncatalysed poly(hydroquinone-isophthalate) (HI); (3) Kinetic analysis of the synthesis of catalysed and uncatalysed poly(resorcinol-terephthalate) (RT); (4) Comparison of kinetic behaviour between catalysed and uncatalysed reactions; (5) Effect of type of the diacetate and the diacid monomer on the reaction kinetics; (6) To see whether simple kinetic laws are valid in melt/slurry as in solution polymerisation.

The work is presented as follows: Experimental kinetic data of reactions of above mentioned systems is collected. Kinetic analysis is then attempted. Complexity in reaction

due to heterogeneous medium provided by high melting diacids is explained. The role of 1 mole % dibutyl tin oxide as a catalyst is defined. The thermodynamic functions like entropy, enthalpy and free energy of activation are calculated. Lastly, characterisation of oligomers using optical, thermal and X-ray diffraction methods is presented.

3.2 EXPERIMENTAL

3.2.1 Materials

Hydroquinone diacetate (HQDA) and resorcinol diacetate (RDA) were prepared by acid/base catalysed method of acetylation using acetic anhydride respectively. HQDA was purified by recrystallisation from mixed solvent system of methanol and water. Purity was checked by differential scanning calorimeter and high performance liquid chromatography and was found suitable for polymerisation. RDA was purified by distillation under reduced pressure. Terephthalic acid (TPA) and isophthalic acid (IPA) were used as received.

3.2.2 Preparation of polymers

Melt condensation was carried out in a specially designed 60 mL capacity glass reactor^{23,24}. Stoichiometric molar equivalents of reactants was charged into the reactor and electrically heated rapidly to the reaction temperature and then maintained isothermally (till the end of the reaction) by means of a multi-step programmable temperature controller. Reactants were continuously agitated at constant rpm (300) by means of a power compensating DC motor to facilitate the removal of bi-product, acetic acid. A steady stream of nitrogen gas was continued through the system to avoid thermal degradation.

Reaction kinetics was studied isothermally over a temperature range from 270°C to 320°C at intervals of 10°C. The moles of acetic acid collected was recorded relative to

reaction time and this data for a few typical experiments are presented in Tables 3.1-3.4. The initial kinetics of polycondensation, wherein acetic acid distilled out under normal pressure, alone was investigated and hence a change in volume of reaction was considered to be negligible for further analysis. Reaction was allowed to proceed further under reduced pressure and the bi-product was collected to take the polymerisation to high conversion. At the end, the product was isolated, crushed and purified free from the starting monomers by extraction with solvents and washing with sodium bicarbonate, water and drying under vacuum.

3.2.3 Measurements

Polyesters were characterised on Shimadzu IR spectrophotometer. Optical analysis was carried out under crossed polarisers using Leitz Laborlux 12 POLS polarising microscope. Samples were heated on Leitz Weitzlar hot stage. Thermal transitions were recorded on Mettler DSC-30 interfaced with TA-4000 data processor. Standard Indium (In) was used for enthalpy calibration. Temperature calibration was done using a three metal standard of In-Pb-Zn. 5-10 mg of sample was analysed at the rate of 20° C in the heating and cooling mode. Powder X-ray diffraction patterns were recorded on PW-1730 Philips X-ray diffractometer. Slit collimated Ni filtered Cu Ka radiation of wavelength 0.15406 nm was generated by voltage and current settings of 40 KV and 16 mA respectively. Samples were run in the range 5 to 40°. High temperature X-ray diffraction analysis was conducted on an assembled instrument at 40 KV and 20 mA.

3.3 RESULTS AND DISCUSSION

The rate of polymerisation for a second order reaction between a diacetate and a diacid can be expressed in terms of generation of acetic acid as follows

TABLE - 3.1

HIGH TEMPERATURE POLY-TRANSESTERIFICATION OF HYDROQUINONE DIACETATE [HQDA] AND TEREPHTHALIC ACID [TPA] WITHOUT CATALYST AT 320.0°C

Reaction time	Volume of side product	Fractional conversion	Degree of polymerisation
[Minutes]	mL	[P]	{1/(1-P)}
4.3	0.10	0.0175	1.0178
5.4	0.20	0.0350	1.0362
6.5	0.30	0.0524	1.0554
8.0	0.50	0.0874	1.0958
9.0	0.70	0.1224	1.1394
10.3	0.90	0.1573	1.1867
13.9	1.40	0.2448	1.3241
14.8	1.50	0.2622	1.3555
15.8	1.60	0.2797	1.3884
17.5	1.80	0.3147	1.4592
19.6	2.00	0.3497	1.5376
21.8	2.20	0.3846	1.6250
23.9	2.40	0.4196	1.7229
25.5	2.50	0.4371	1.7764
26.5	2.60	0.4545	1.8333
28.0	2.70	0.4720	1.8940
31.9	2.90	0.5070	2.0284
34.8	3.00	0.5245	2.1029
40.6	3.20	0.5594	2.2698
43.7	3.30	0.5769	2.3636
48.5	3.40	0.5944	2.4655
52.6	3.50	0.6119	2.5766

TABLE - 3.2

HIGH TEMPERATURE POLY-TRANSESTERIFICATION OF HYDROQUINONE DIACETATE [HQDA] AND ISOPHTHALIC ACID [IPA] WITHOUT CATALYST AT 280.0°C

Reaction time	Volume of side product	Fractional conversion	Degree of polymerisation
[Minutes]	mL	[P]	{1/(1-P)}
13.4	0.10	0.0175	1.0178
15.3	0.20	0.0350	1.0362
18.0	0.30	0.0524	1.0554
20.3	0.40	0.0699	1.0752
21.6	0.50	0.0874	1.0958
22.6	0.60	0.1049	1.1172
24.1	0.70	0.1224	1.1394
25.1	0.80	0.1399	1.1626
26.7	0.90	0.1573	1.1867
27.9	1.00	0.1748	1.2119
29.5	1.10	0.1923	1.2381
31.2	1.20	0.2098	1.2655
32.4	1.30	0.2273	1.2941
35.8	1.50	0.2622	1.3555
38.6	1.70	0.2972	1.4229
40.1	1.80	0.3147	1.4592
44.1	2.00	0.3497	1.5376
46.1	2.10	0.3671	1.5801
49.0	2.20	0.3846	1.6250
55.0	2.40	0.4196	1.7229
59.9	2.50	0.4371	1.7764

TABLE - 3.3

HIGH TEMPERATURE POLY-TRANSESTERIFICATION OF RESORCINOL DIACETATE [RDA] AND TEREPHTHALIC ACID [TPA] WITHOUT CATALYST AT 320.0°C

Reaction time	Volume of side product	Fractional conversion	Degree of polymerisation
[Minutes]	mL	[P]	{1/(1-P)}
1.5	0.10	0.0175	1.0178
2.2	0.20	0.0350	1.0362
2.7	0.30	0.0524	1.0554
3.4	0.40	0.0699	1.0752
4.1	0.50	0.0874	1.0958
6.5	0.90	0.1573	1.1867
7.0	1.00	0.1748	1.2119
7.5	1.10	0.1923	1.2381
8.1	1.20	0.2098	1.2655
9.4	1.40	0.2448	1.3241
9.8	1.50	0.2622	1.3555
10.5	1.70	0.2972	1.4229
11.1	1.80	0.3147	1.4592
11.7	1.90	0.3322	1.4974
12.3	2.00	0.3497	1.5376
12.9	2.10	0.3671	1.5801
13.4	2.20	0.3846	1.6250
14.4	2.40	0.4196	1.7229
15.0	2.50	0.4371	1.7764
16.4	2.70	0.4720	1.8940
17.0	2.80	0.4895	1.9589
18.1	3.00	0.5245	2.1029
19.5	3.20	0.5594	2.2698
20.5	3.30	0.5769	2.3636
21.0	3.40	0.5944	2.4655
21.8	3.50	0.6119	2.5766
22.7	3.60	0.6294	2.6981
25.7	3.80	0.6643	2.9792
27.5	3.90	0.6818	3.1429
30.1	4.00	0.6993	3.3256

TABLE - 3.4

HIGH TEMPERATURE POLY-TRANSESTERIFICATION OF RESORCINOL DIACETATE [RDA] AND TEREPHTHALIC ACID [TPA] WITH DIBUTYL TIN OXIDE [DBTO] CATALYST AT 320.0°C

Reaction time [Minutes]	Volume of side product mL	Fractional conversion [P]	Degree of polymerisation {1/(1-P)}
1.5	0.10	0.0175	1.0178
2.1	0.20	0.0350	1.0362
3.3	0.40	0.0699	1.0752
4.3	0.60	0.1049	1.1172
5.0	0.70	0.1224	1.1394
5.4	0.80	0.1399	1.1626
5.9	0.90	0.1573	1.1867
6.2	1.00	0.1748	1.2119
6.5	1.10	0.1923	1.2381
7.0	1.20	0.2098	1.2655
7.4	1.30	0.2273	1.2941
8.5	1.50	0.2622	1.3555
8.8	1.60	0.2797	1.3884
9.3	1.70	0.2972	1.4229
9.7	1.80	0.3147	1.4592
10.1	1.90	0.3322	1.4974
10.4	2.00	0.3497	1.5376
10.8	2.10	0.3671	1.5801
11.4	2.20	0.3846	1.6250
12.8	2.50	0.4371	1.7764
13.2	2.60	0.4545	1.8333
13.6	2.70	0.4720	1.8940
14.3	2.80	0.4895	1.9589
14.5	2.90	0.5070	2.0284
15.3	3.00	0.5245	2.1029
15.9	3.10	0.5420	2.1832
16.6	3.20	0.5594	2.2698
18.2	3.50	0.6119	2.5766
19.2	3.60	0.6294	2.6981
20.0	3.70	0.6469	2.8317
20.9	3.80	0.6643	2.9792
21.9	3.90	0.6818	3.1429
23.0	4.00	0.6993	3.3256
25.4	4.10	0.7168	3.5309

$$\frac{dx}{dt} = k_2[\text{COOH}][\text{OAc}] \quad (3.1)$$

where, [COOH] and [OAc] are the concentration of TPA and HQDA. For equimolar amounts of the diacid and the diacetate equation (3.1) changes to

$$\frac{dx}{dt} = k_2[C]^2 \quad (3.2)$$

where 'C' is the concentration of unreacted functional groups. If 'c₀' is the initial concentration and 'p' is fractional conversion then,

$$c = c_0(1 - p)$$

and so,

$$c_0 kt = \frac{1}{(1-p)} + \text{constant} \quad (3.3)$$

The concentration can not be expressed in absolute units since the molar volume of the reactants in the melt is not precisely known. A second order initial rate will be given on this basis, by numerical value of the rate constant itself but will have units moles per second^{23,24}.

3.3.1 Thermodynamic treatment of rate constant

The thermodynamic functions were calculated in accordance to the theory of absolute reaction rates³⁰ using following equations

$$k = e^2 \left(\frac{kT}{h} \right) e^{\frac{\Delta S^\ddagger}{R}} e^{-\frac{E_{\text{exp}}}{RT}} \quad (3.4)$$

$$E_{\text{exp}} = \Delta H^\ddagger + 2RT \quad (3.5)$$

The symbols ΔS^\ddagger , ΔH^\ddagger and E_{exp} represent the entropy, enthalpy and the experimental energy of activation respectively when two monomers react to form a dimer. Entropy of activation is usually negative for a second order bimolecular reaction³⁰ between two monomers to form a dimer.

3.3.2 Hydroquinone diacetate-terephthalic acid (HT) system

This polyesterification system deals with the preparation of wholly aromatic rigid rod poly(1,4-oxy phenylene oxy-1,4-carboxy phenylene) by acidolysis between hydroquinone diacetate (HQDA) and terephthalic acid (TPA)³¹. HQDA is molten while TPA is present as solid particles (30 μm) at the temperature range over which kinetics was investigated. The reaction between HQDA and TPA would first generate 4-(4-acetoxy-phenylene-1-oxy carboxy) benzoic acid. This could react with either TPA to form nonmelting 1,4-bis(4-carboxyl phenylene-1-carboxy oxy) benzene or with HQDA to form thermotropic 1,4-bis(4-acetoxy phenylene-1-oxy carboxy) benzene, which would be isotropic at the reaction temperature^{32,33} (**Figure 3.1**). Thus, the reaction medium is initially a slurry consisting of terephthalic acid crystals in a molten hydroquinone diacetate and changes gradually to solid state polycondensation due to the build-up of very high melting intermediates and eventually generates poly(1,4-phenylene terephthalate) having a melt transition around 600°C³⁴.

An attempt to fit the data into rate expressions corresponding to different orders showed that only second order could be fit most appropriately. The rate law plots corresponding to 1st, 2nd, 2.5th and 3rd order rate expressions are shown in **Figures 3.2-3.5** respectively. Regression analysis of experimental kinetic data generated the best fit for the second order rate law plot. It is apparent that the reaction follows second order kinetics since it is essentially bimolecular. A typical second order rate law plot for catalysed reactions between HQDA and TPA at different temperatures is shown in **Figure 3.6**. An induction

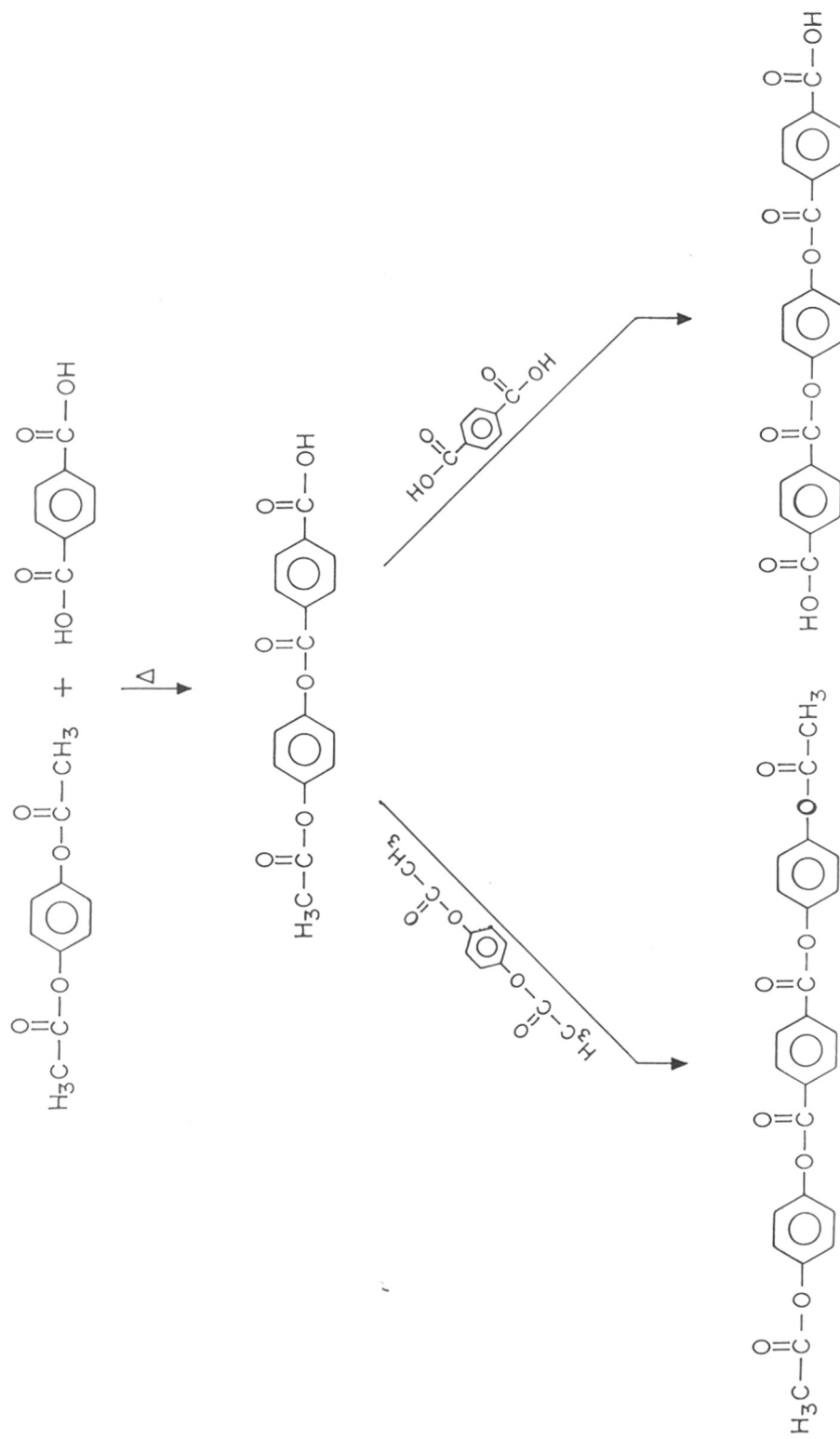


FIGURE 3.1 REACTION SCHEME FOR THE SYNTHESIS OF HT POLYESTER

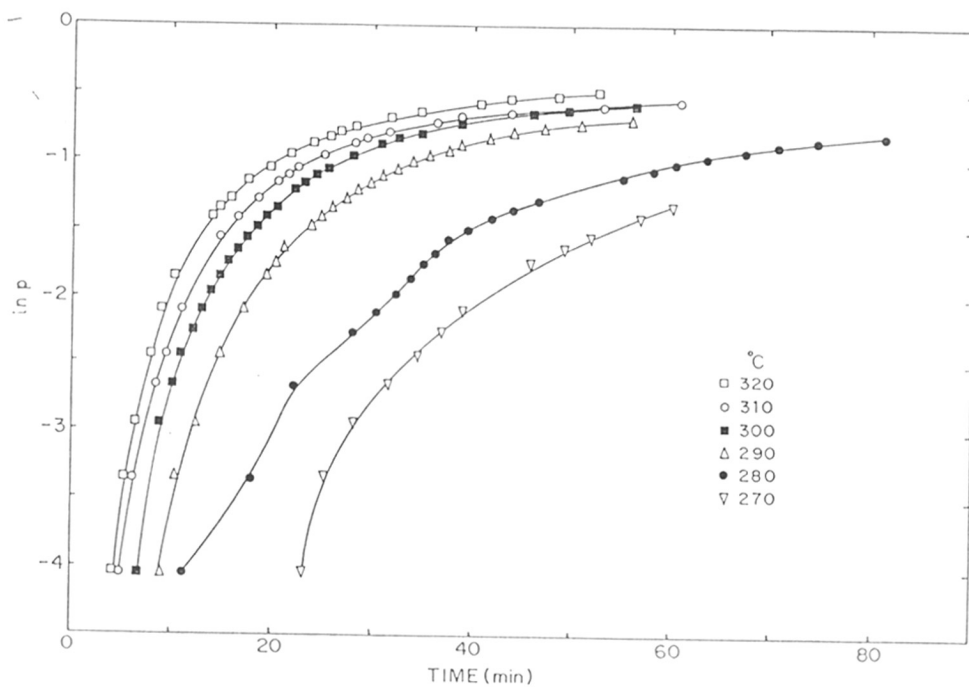


FIGURE 3.2 FIRST ORDER RATE LAW PLOT ILLUSTRATING THE EFFECT OF TEMPERATURE FOR HQDA/TPA UNCATALYSED REACTIONS

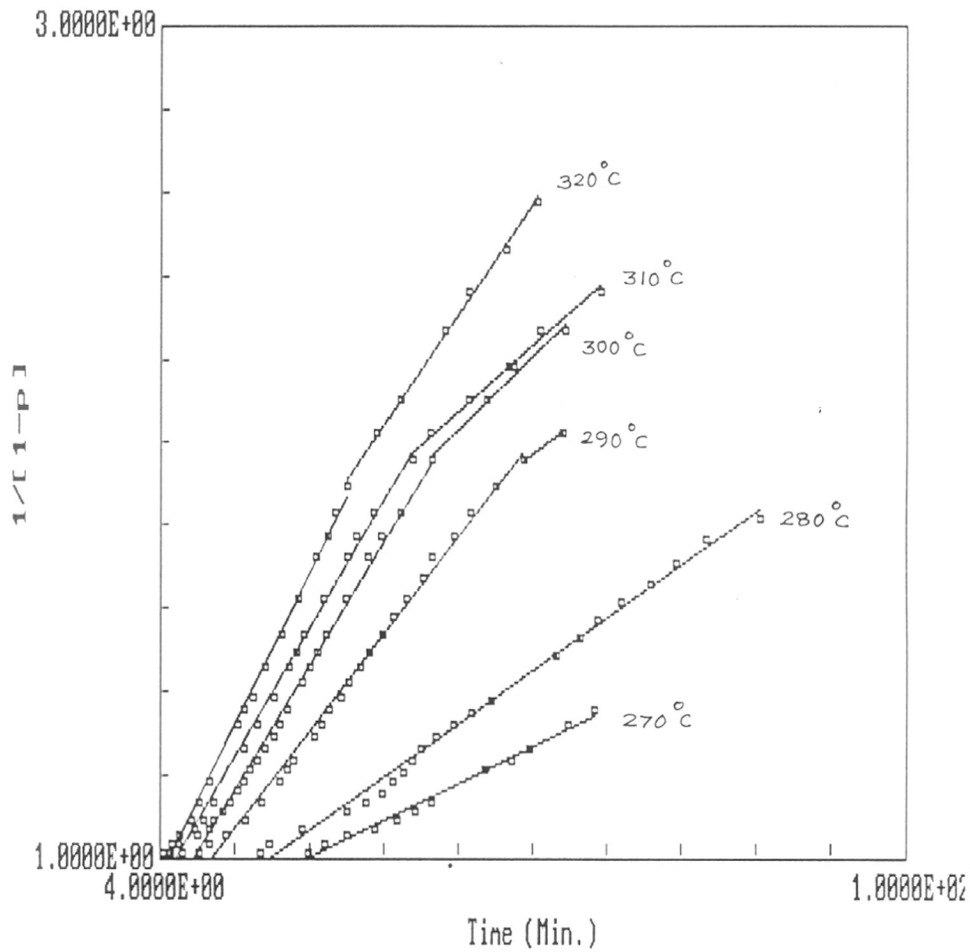


FIGURE 3.3 SECOND ORDER RATE LAW PLOT ILLUSTRATING THE EFFECT OF TEMPERATURE FOR HQDA/TPA UNCATALYSED REACTIONS

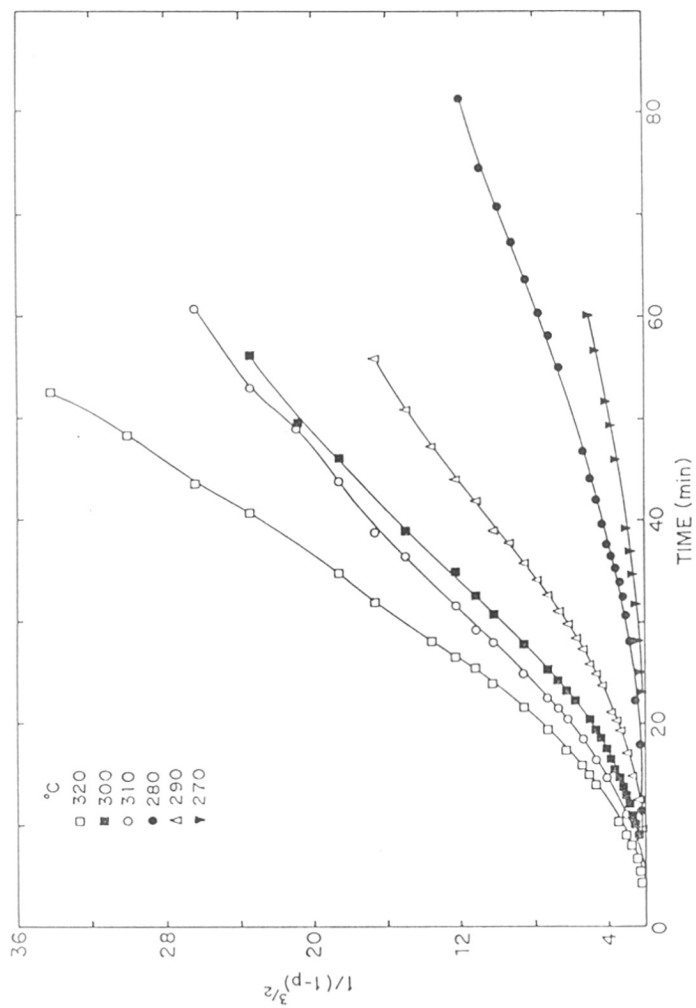


FIGURE 3.4 2.5 TH ORDER RATE LAW PLOT ILLUSTRATING THE EFFECT OF TEMPERATURE FOR HQDA/TPA UNCATALYSED REACTIONS

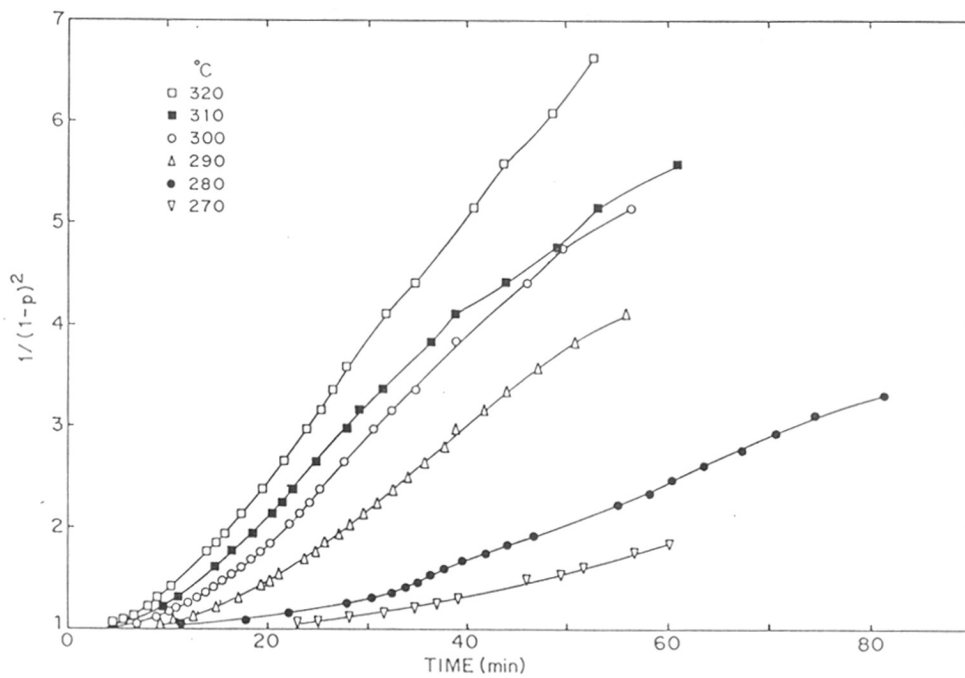


FIGURE 3.5 THIRD ORDER RATE LAW PLOT ILLUSTRATING THE EFFECT OF TEMPERATURE FOR HQDA/TPA UNCATALYSED REACTIONS

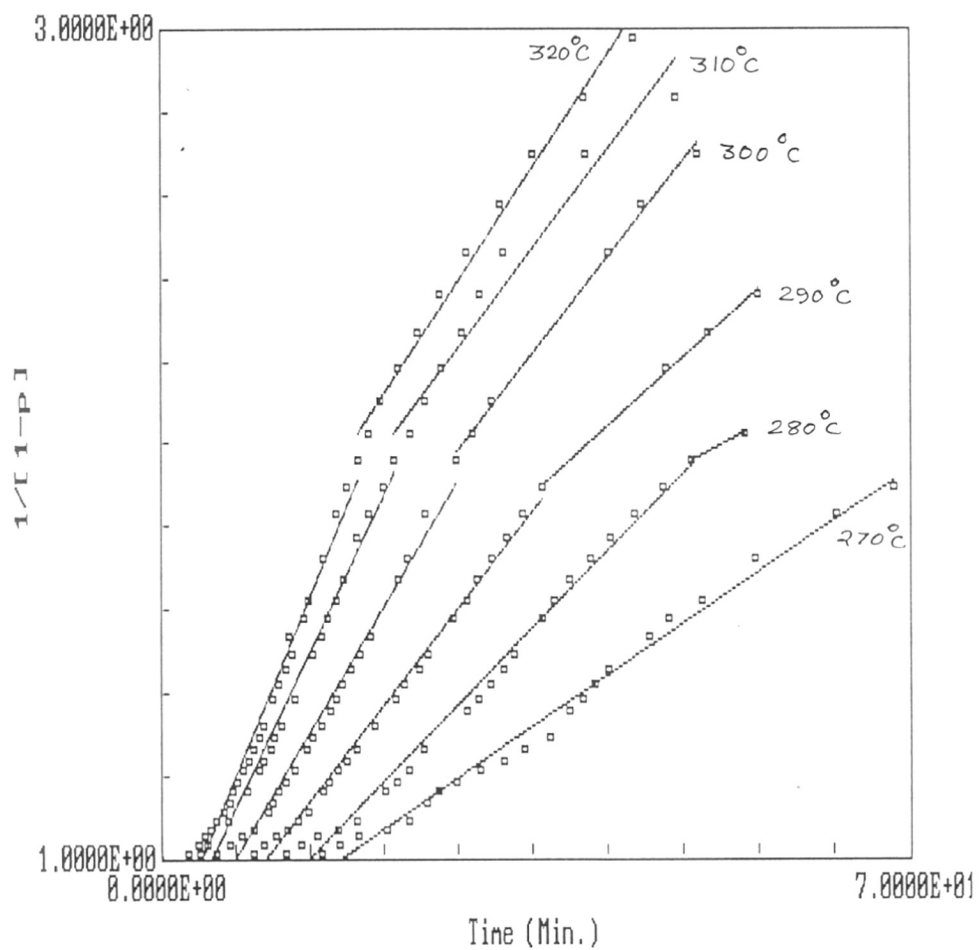


FIGURE 3.6 SECOND ORDER RATE LAW PLOT ILLUSTRATING EFFECT OF TEMPERATURE FOR HQDA/TPA CATALYSED REACTIONS

period is noted at all temperatures, which decreases progressively with increase in reaction temperature. The rate law plots show that the kinetics is adequately modeled for second order behaviour. This is true of both uncatalysed and catalysed reactions.

All catalysed and uncatalysed reactions are characterised by breaks in the second order plots indicating different kinetic behaviour in the two regions separated by the break. The breaks sharpen at higher reaction temperatures. The reactions follow the same order before and after the break. The plausible explanations for these breaks are: (i) the reactivity of the carboxylic acid group may depend on the degree of polymerisation; (ii) heterogeneous (lamellar) chain growth may occur within the precipitated oligomer by stepwise addition of the monomer and (iii) in catalysed reactions, the activity level of the catalyst could change with time. The most plausible explanation of a change in reaction order with time could not explain the breaks.

The polyesterification kinetics are altered by the ionisation of the dicarboxylic acid. While a direct correlation can not be found between the ionisation constant in a predominantly aqueous environment at an ambient temperature and the behaviour in melt at high temperatures, a striking similarity does seem to exist²¹. The polyesterification of diacids with low pK_1 (1.92 to 3.02), which would ionise quite extensively, fit into a second order kinetics while the polyesterification of diacids with high pK_1 , (4.21 to 4.57), which would ionise marginally, can be fit only into an order of 2.5. It is thus apparent that the former assumes a pseudo second order due to a excess in the hydrogen ion concentration. Ionisation constant of weakest diacid in the first group of relatively stronger diacids is 16 times that of the strongest diacid in the second group of weak diacids²¹. The pK_1 of two acids used in the present study, terephthalic acid and isophthalic acid³⁵ (3.54 and 3.62), are exactly half way between the two groups. Thus, this kinetic analysis extends the pK range over which the reaction follows a second order.

The rate was found to decrease after the break. Second order rate constants of the reaction prior to and after the break calculated from the slope of the corresponding kinetic plots are tabulated in **Table 3.5**. This decrease in the second region most probably results from a diffusion controlled reaction³⁶ due to increasing heterogeneity of the system arising from oligomer precipitation, as discussed earlier.

The activation energies were calculated from the slope of the Arrhenius plots shown in **Figures 3.7-3.10**. The value for the reaction prior to the break compares well with that observed for the self condensation of 4-acetoxy benzoic acid over a similar temperature range. A glance at activation energies of the HT system, of 18.88 kCal/mole initially and 16.22 kCal/mole after the break in **Table 3.8**, would imply that an increase in rate is to be anticipated after the break. This was not borne by the analysis. The decrease in enthalpy of activation must be accompanied simultaneously by a greater decrease in the entropy of activation. The overall increase in free energy of activation thus, is the probable cause for the decrease in the observed rate.

3.3.3 Hydroquinone diacetate-isophthalic acid (HI) system

In this polyesterification, the 1,4-dicarboxylic acid, TPA is replaced by the 1,3-dicarboxylic acid, isophthalic acid (IPA) (**Figure 3.11**). This diacid provides a kink of 120° and retards the alignment of the polymer chain as a rigid-rod. Partial substitution of linear 1,4-disubstituted monomers with such kinking comonomers over a definitive composition range is known to generate liquid crystallinity in wholly aromatic polyesters by disrupting packing and thereby causing a downturn in the melting temperature³⁷⁻³⁹. Both catalysed and uncatalysed reactions obey second order kinetics in the two regimes separated by the break

TABLE - 3.5

RESULTS OF KINETICS OF UNCATALYSED AND CATALYSED ACIDOLYSIS
BETWEEN HYDROQUINONE DIACETATE AND TEREPHTHALIC ACID

Polymn. Code	Temp./ °C	Induction period, min.	k [c ⁻¹ .t ⁻¹] Dimerisation	k [c ⁻¹ .t ⁻¹] Oligomerisation
<u>Uncatalysed Acidolysis</u>				
1T	320	4.3	0.00645	0.00457
2T	310	5.3	0.00543	0.00273
3T	300	6.7	0.00517	0.00302
4T	290	8.4	0.00405	0.00232
5T	280	14.7	0.00220	---
6T	270	18.2	0.00153	---
<u>Catalysed Acidolysis</u>				
1TC	320	3.0	0.0105	0.00647
2TC	310	3.7	0.00922	0.00567
3TC	300	5.6	0.00742	0.00552
4TC	290	8.5	0.00552	0.00395
5TC	280	10.6	0.00440	0.00235

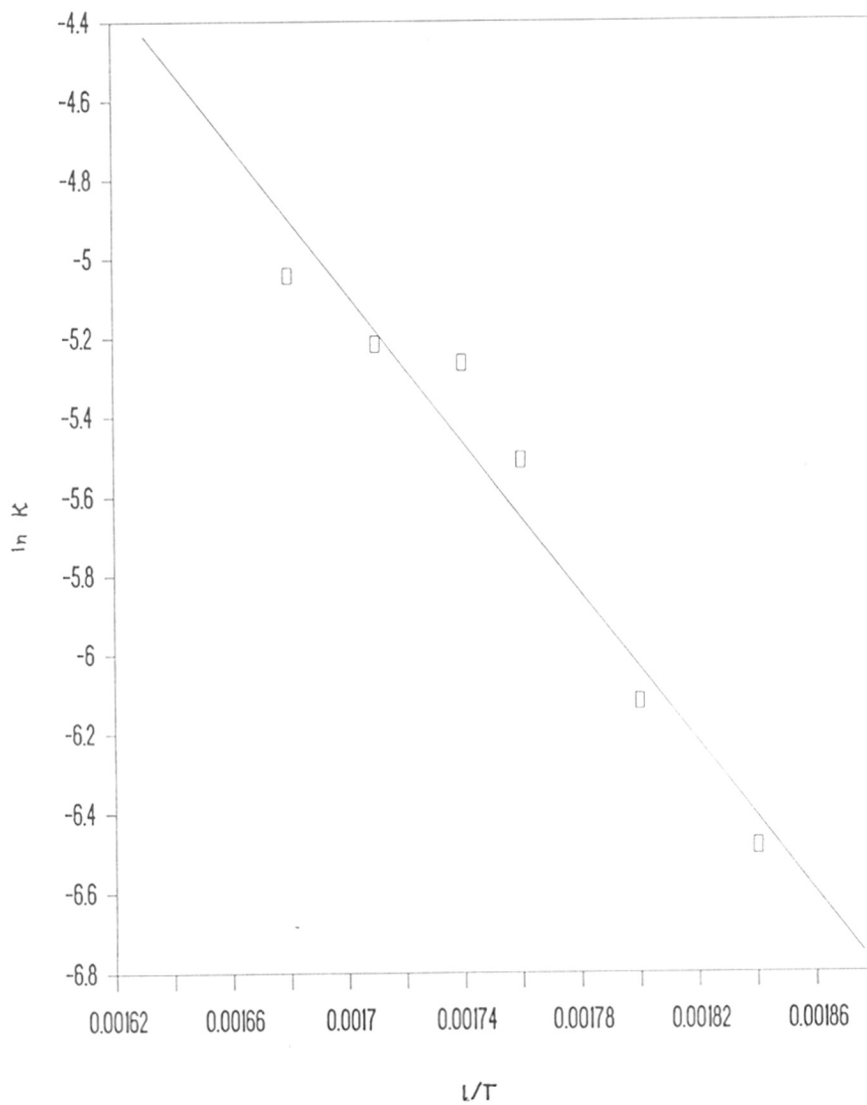


FIGURE 3.7 ARRHENIUS PLOT FOR HQDA/TPA UNCATALYSED REACTIONS PRIOR TO THE BREAK

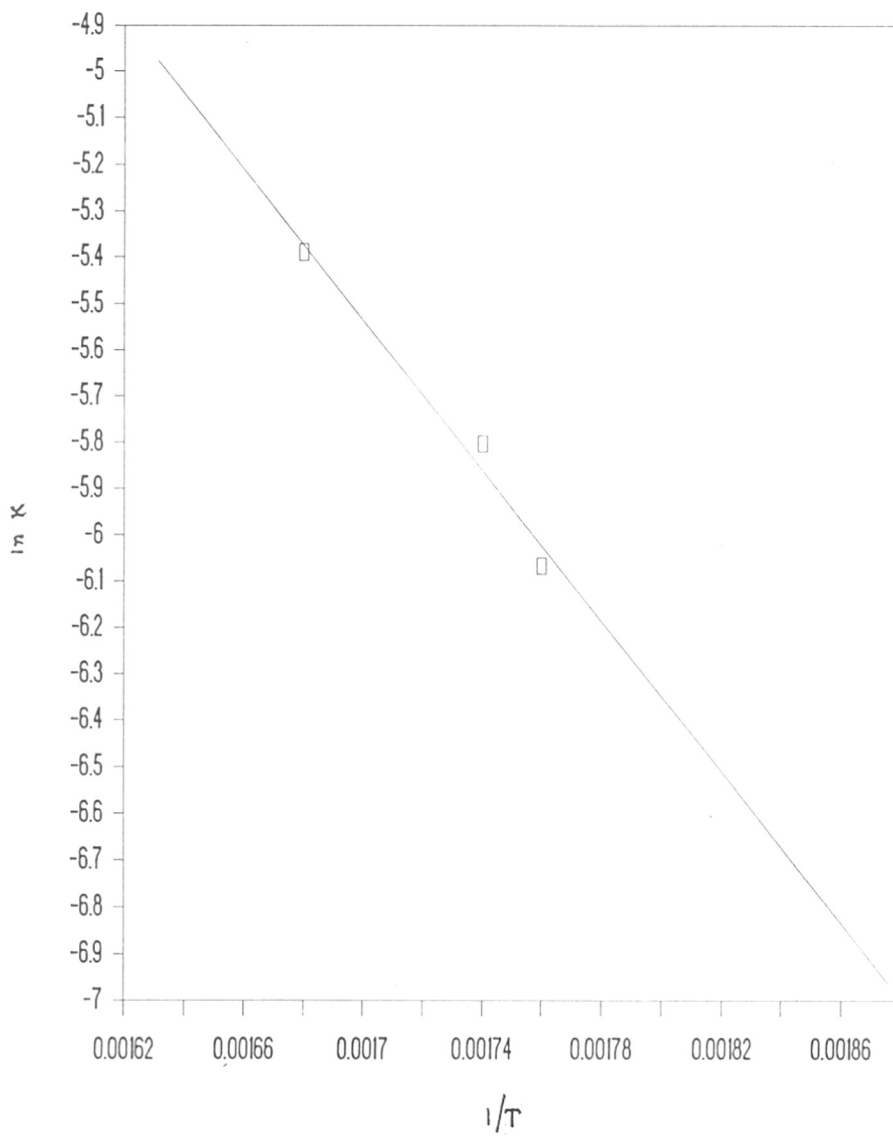


FIGURE 3.8 ARRHENIUS PLOT FOR HQDA/TPA UNCATALYSED REACTIONS AFTER THE BREAK

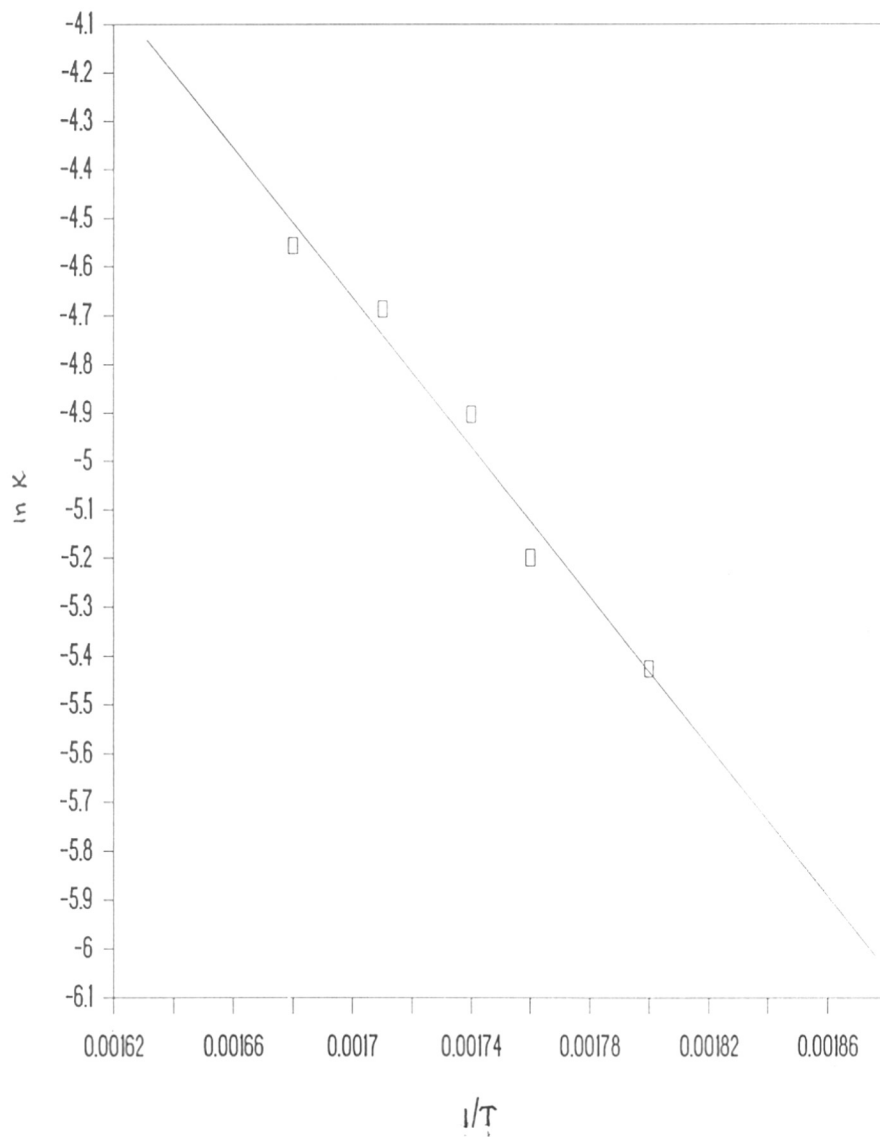


FIGURE 3.9 ARRHENIUS PLOT FOR HQDA/TPA CATALYSED REACTIONS PRIOR TO THE BREAK

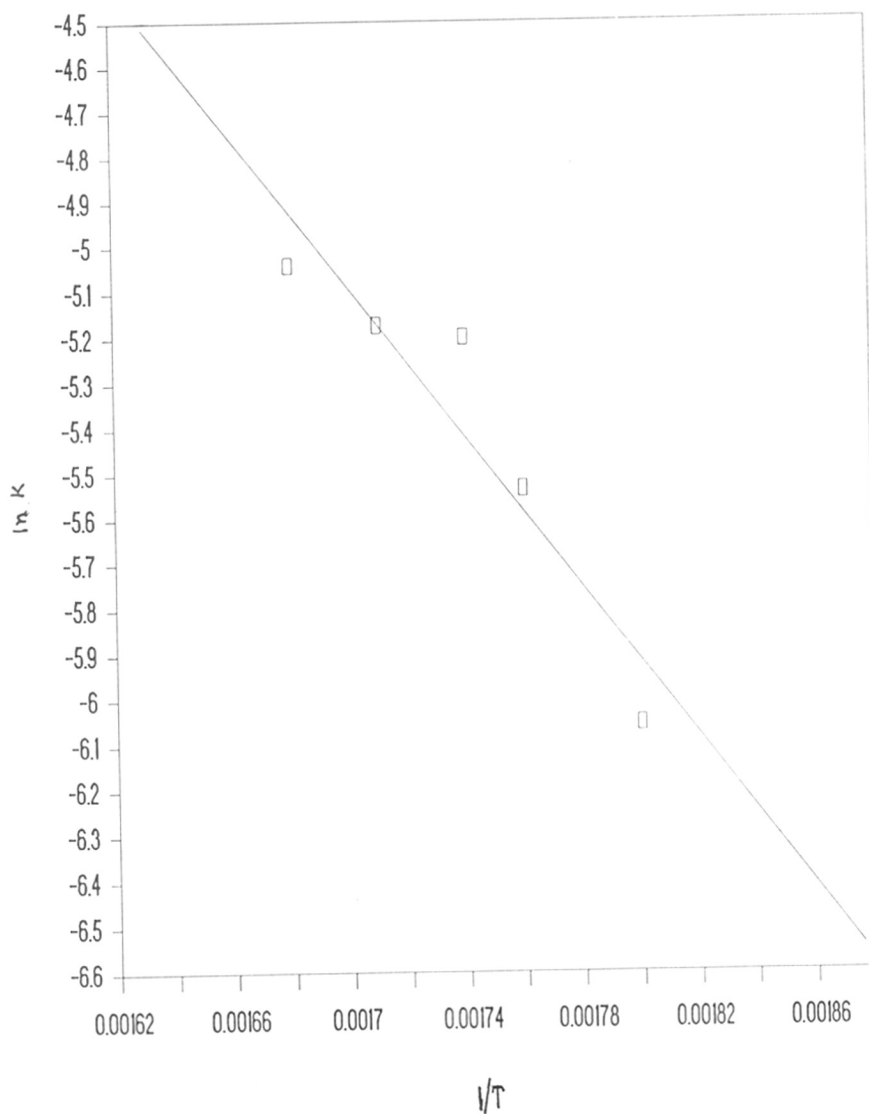


FIGURE 3.10 ARRHENIUS PLOT FOR HQDA/TPA CATALYSED REACTIONS AFTER THE BREAK

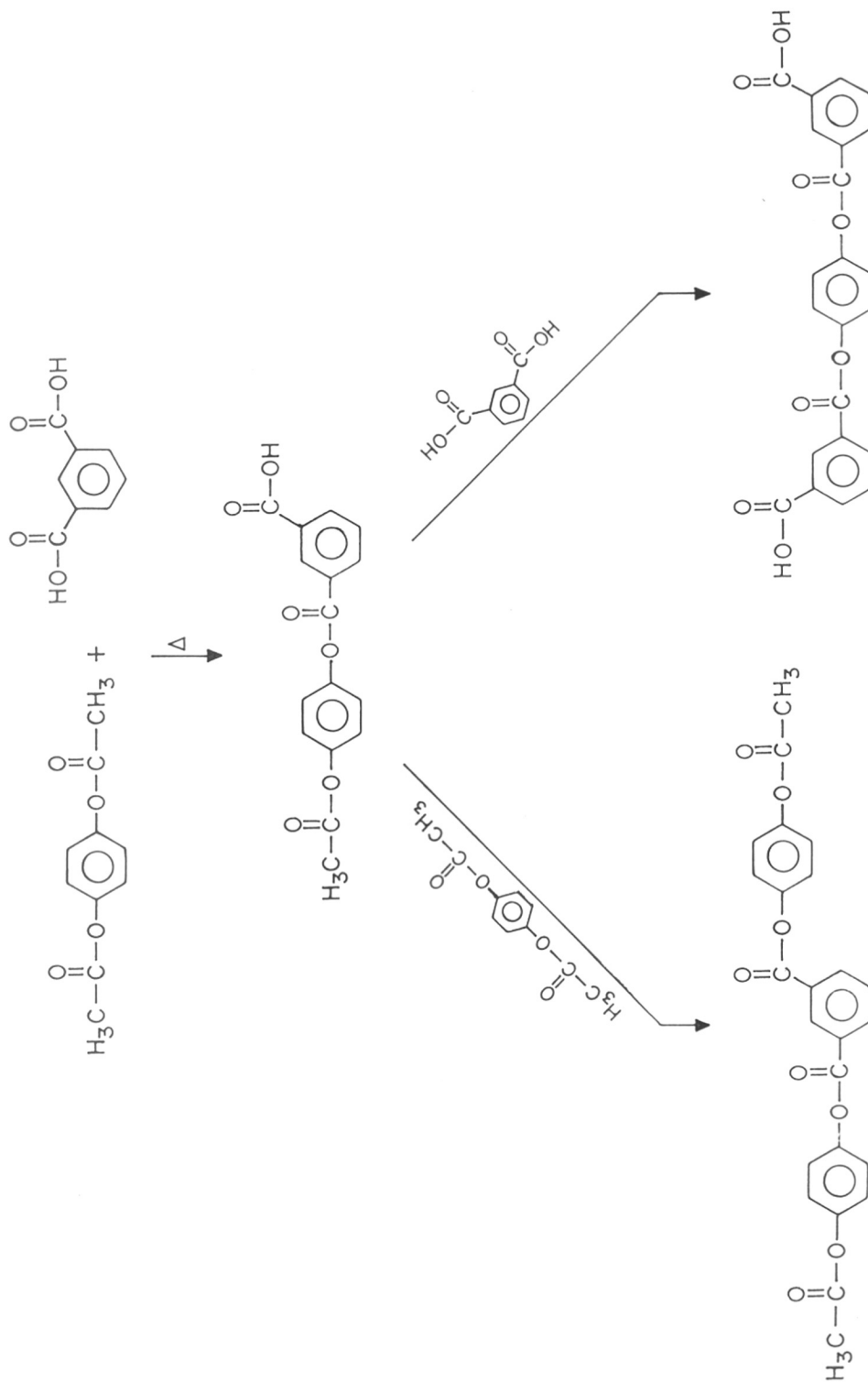


FIGURE 3.11 REACTION SCHEME FOR THE SYNTHESIS OF HI POLYESTER

over the entire temperature range of kinetic analysis, as evidenced from **Figures 3.12** and **3.13** respectively. It is clear from **Table 3.6** that rate constants in the two stages are only marginally higher from those of HT polyesterification.

In this system too, the melting point of the diacid (isophthalic acid) exceeds the reaction temperature. In a manner akin to the HT system, the reaction starts as a slurry and progressively increases in heterogeneity and ends up as solid state reaction due to continuous oligomer precipitation. The time over which these transformations occur ought to be inversely related to the reaction temperature. Since oligomers would come out of phase only when melting temperature exceeds the reaction temperature, the degree of polymerisation above which the changes should be noticed would increase with the reaction temperature. While such a clear trend was noticed in the self condensation of wholly aromatic 4-acetoxy benzoic acid, it was not so apparent in the reaction of aromatic diacids with aromatic diacetates probably because HI oligomers become nonmelting at a much lower degree of polymerisation than oxybenzoate oligomers.

As in HT system, the rate of the reaction decreases after the break for apparently similar reasons. However, in uncatalysed reaction the breaks are observed only at higher reaction temperatures of 300 and 320° C. Hence activation energy could be estimated only for the first stage prior to the break. This was estimated from Arrhenius plot (**Figure 3.14**) to be 17.69 kCal/mole.

3.3.4 Resorcinol diacetate-terephthalic acid (RT) system

Another kinking comonomer which could be employed to decrease the aspect ratio of a rigid-rod polyester is resorcinol diacetate (RDA), also known as 1,3-diacetoxy benzene. Thus, hydroquinone diacetate could be partially/totally replaced from the HT system (**Figure 3.15**). The kink introduced here is 120° as well. However, the direction of ester groups

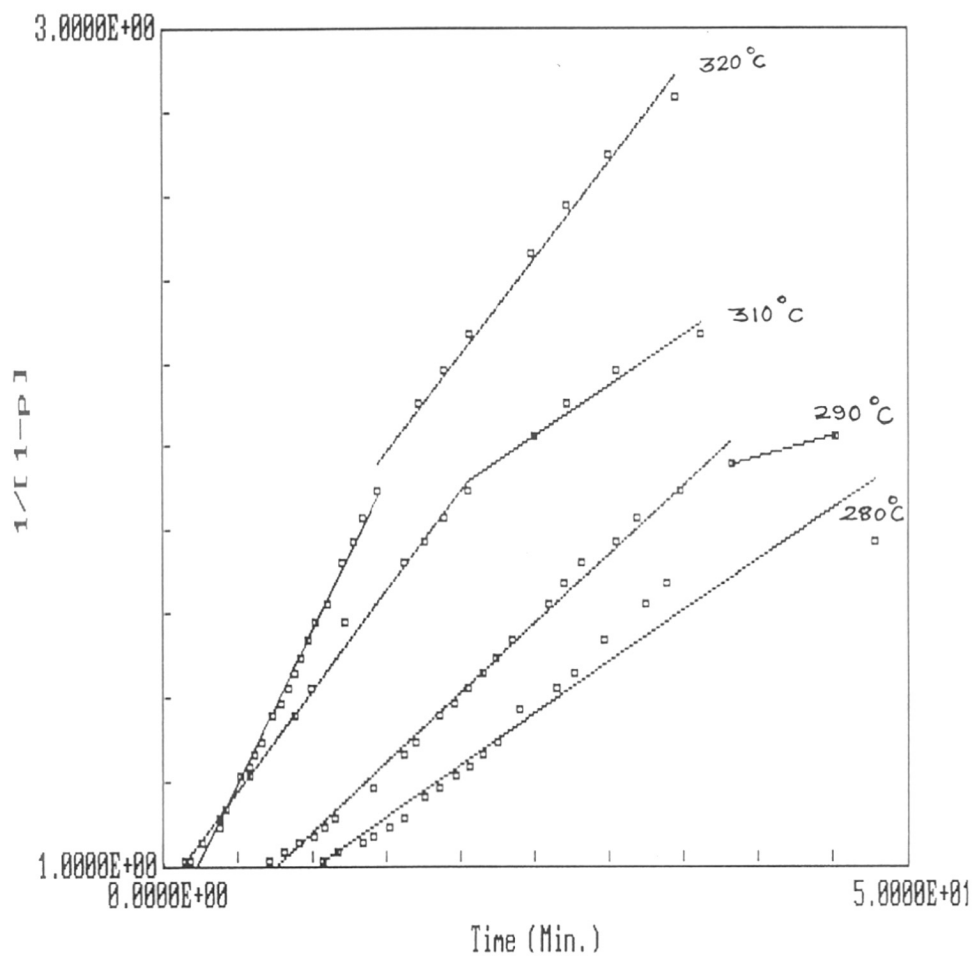


FIGURE 3.12 SECOND ORDER RATE LAW PLOT ILLUSTRATING EFFECT OF TEMPERATURE FOR HQDA/IPA CATALYSED REACTIONS

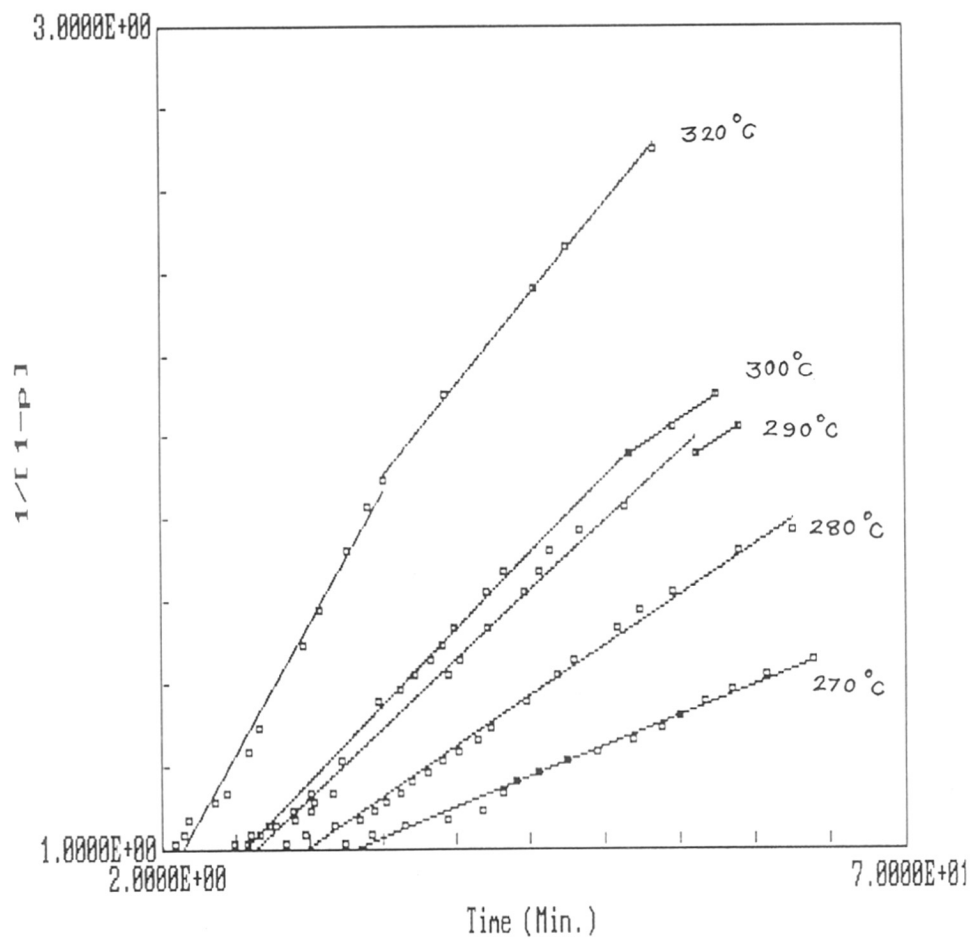


FIGURE 3.13 SECOND ORDER RATE LAW PLOT ILLUSTRATING EFFECT OF TEMPERATURE FOR HQDA/IPA UNCATALYSED REACTIONS

TABLE - 3.6

RESULTS OF KINETICS OF UNCATALYSED AND CATALYSED ACIDOLYSIS
BETWEEN HYDROQUINONE DIACETATE AND ISOPHTHALIC ACID

Polymn. Code	Temp./ °C	Induction period, min.	k [c ⁻¹ .t ⁻¹] Dimerisation	k [c ⁻¹ .t ⁻¹] Oligomerisation
<u>Uncatalysed Acidolysis</u>				
1I	320	3.1	0.00778	0.00537
2I	310	4.6	0.00363	---
3I	300	8.5	0.00452	0.00302
4I	290	9.0	0.00412	---
5I	280	11.9	0.00298	---
6I	270	15.2	0.00180	---
<u>Catalysed Acidolysis</u>				
1IC	320	1.7	0.0121	0.00768
2IC	310	1.3	0.00797	0.00400
3IC	300	4.5	0.00423	---
4IC	290	6.8	0.00550	0.00168
5IC	280	9.9	0.00408	---

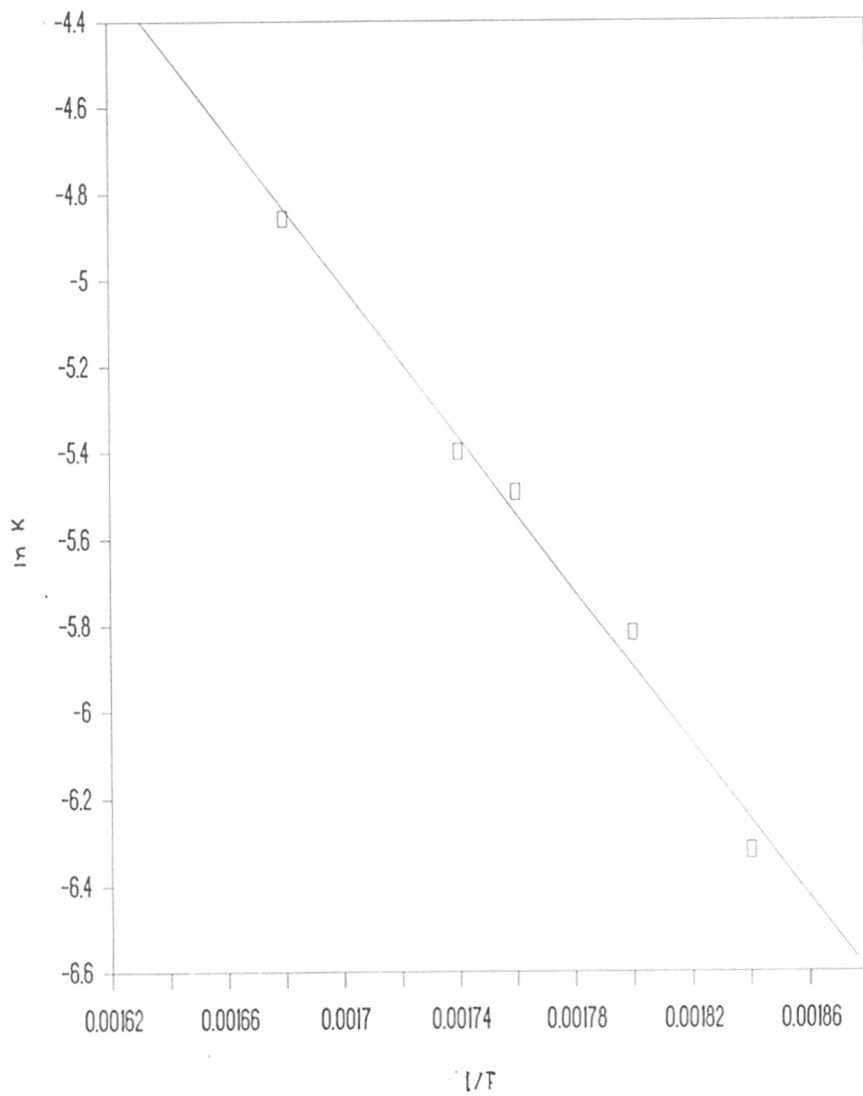


FIGURE 3.14 ARRHENIUS PLOT FOR HQDA/IPA UNCATALYSED REACTIONS PRIOR TO THE BREAK

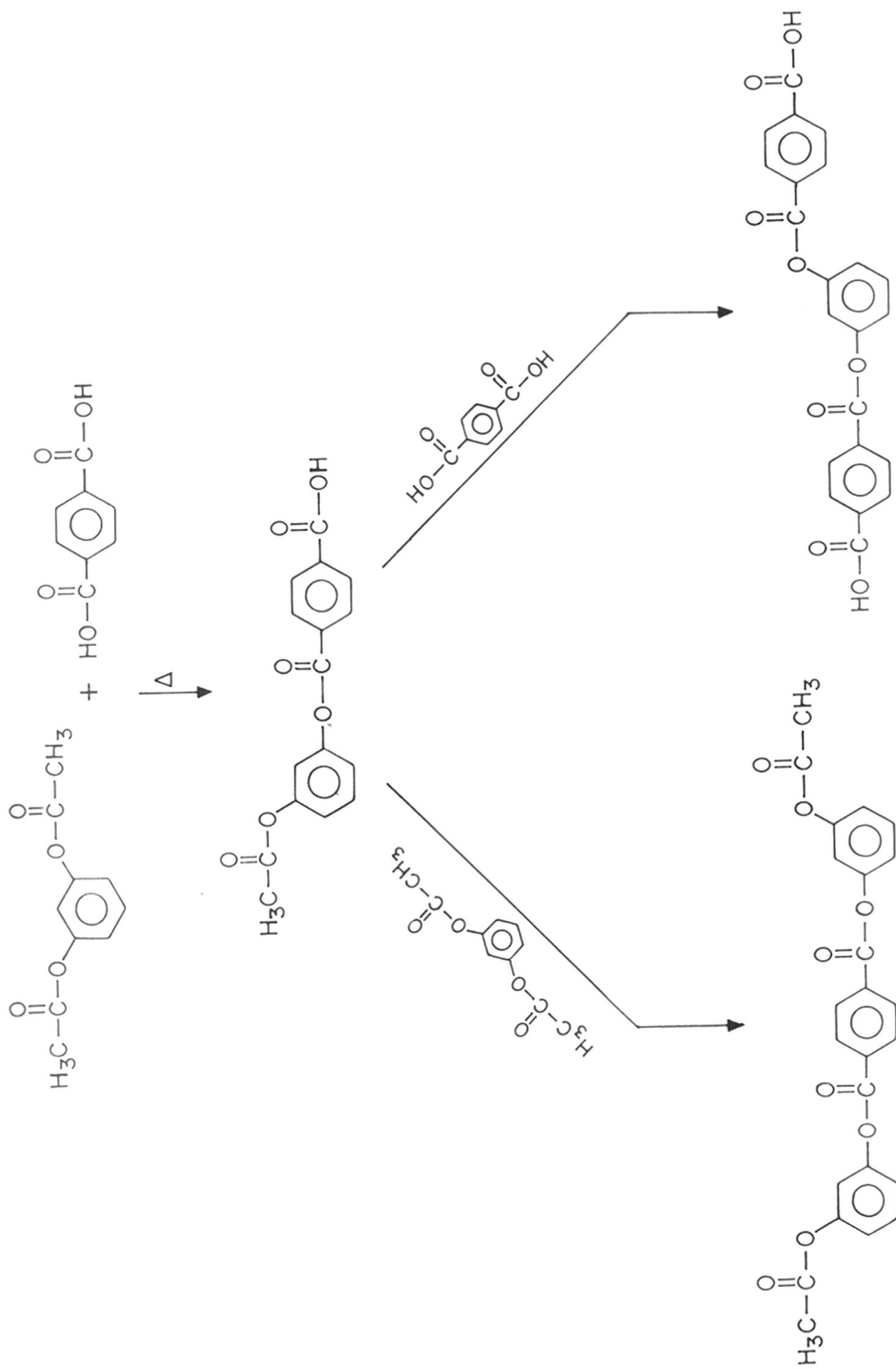


FIGURE 3.15 REACTION SCHEME FOR THE SYNTHESIS OF RT POLYESTER

relative to the kink along the polyester chain is exactly opposite to that in HI system. This is known to cause a significant difference in the extent of downturn in the transition temperature from that caused by replacement of terephthalic acid in HT polyester partially/totally with isophthalic acid⁴⁰⁻⁴².

Thorough regression analysis and the fits of rate law plots indicate that the experimental data of both catalysed and uncatalysed bimolecular reactions are most aptly described by second order kinetic law. Typical second order plots for catalysed and uncatalysed reactions, presented in **Figures 3.16** and **3.17** respectively, show that the induction period and breaks in second order kinetic plots are a feature of this transesterification reaction as well. While the kinetic order of the first stage is retained after the break, the rate of reaction increases in the second stage, despite an increase in the activation energy as seen in **Table 3.7**. Activation energies of the reactions prior to and after the break are calculated (**Table 3.8**) from the slope of Arrhenius plots shown in **Figures 3.18-3.21**. A similar trend was observed for the self polycondensation of 4-acetoxy benzoic acid^{23,24}. This points to the presence of an apparent 'compensation effect'⁴³ wherein the entropy of activation increases at a faster rate than the enthalpy of activation thereby driving the reaction in the forward direction. In the self condensation of 4-acetoxy benzoic acid the compensation effect, observed on oligomer precipitation, probably arose from the surface effects which increase the local concentration of the carboxylic acid units^{23,24}.

The transesterification reaction rates observed for the RT system are higher than those observed in the HT and HI systems under identical experimental conditions. The comparison of Arrhenius plots of uncatalysed HT, HI and RT system shows (**Figures 3.22** and **3.23**) that rate behaviour of HT and HI reactions are comparable while kinetics of RT system differs from the two. This difference is more pronounced in the oligomerisation stage. The

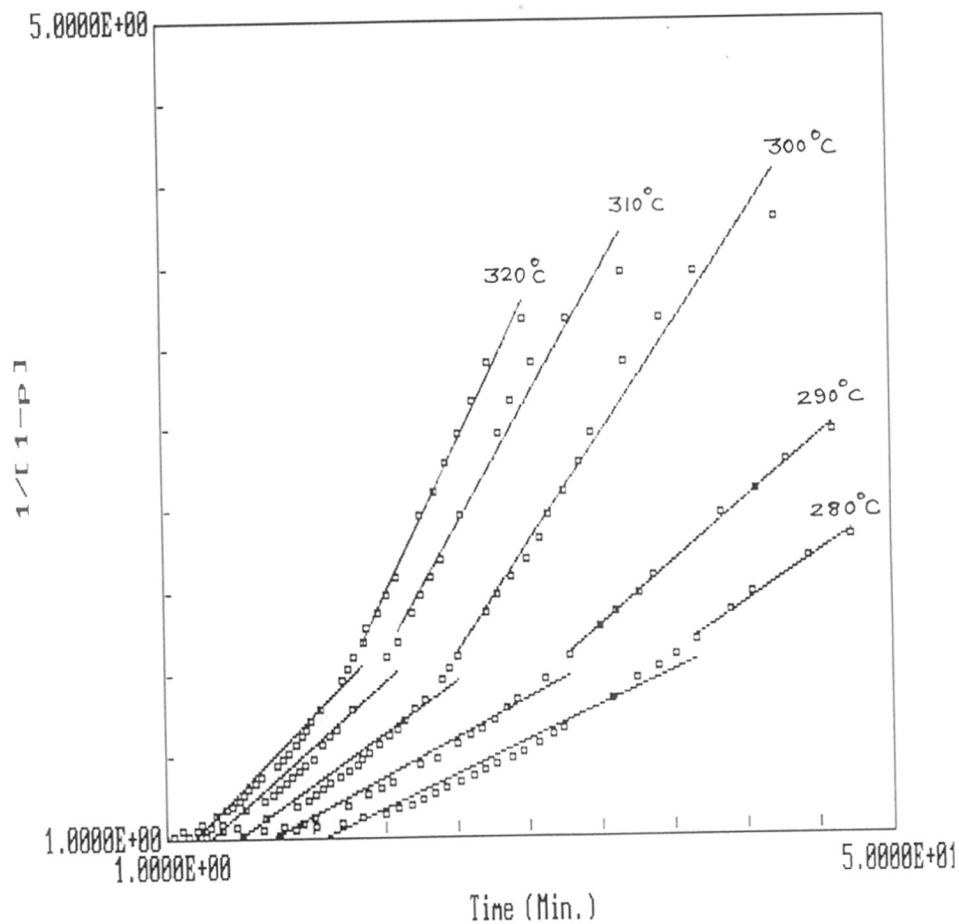


FIGURE 3.16 SECOND ORDER RATE LAW PLOT ILLUSTRATING EFFECT OF TEMPERATURE FOR RDA/TPA CATALYSED REACTIONS

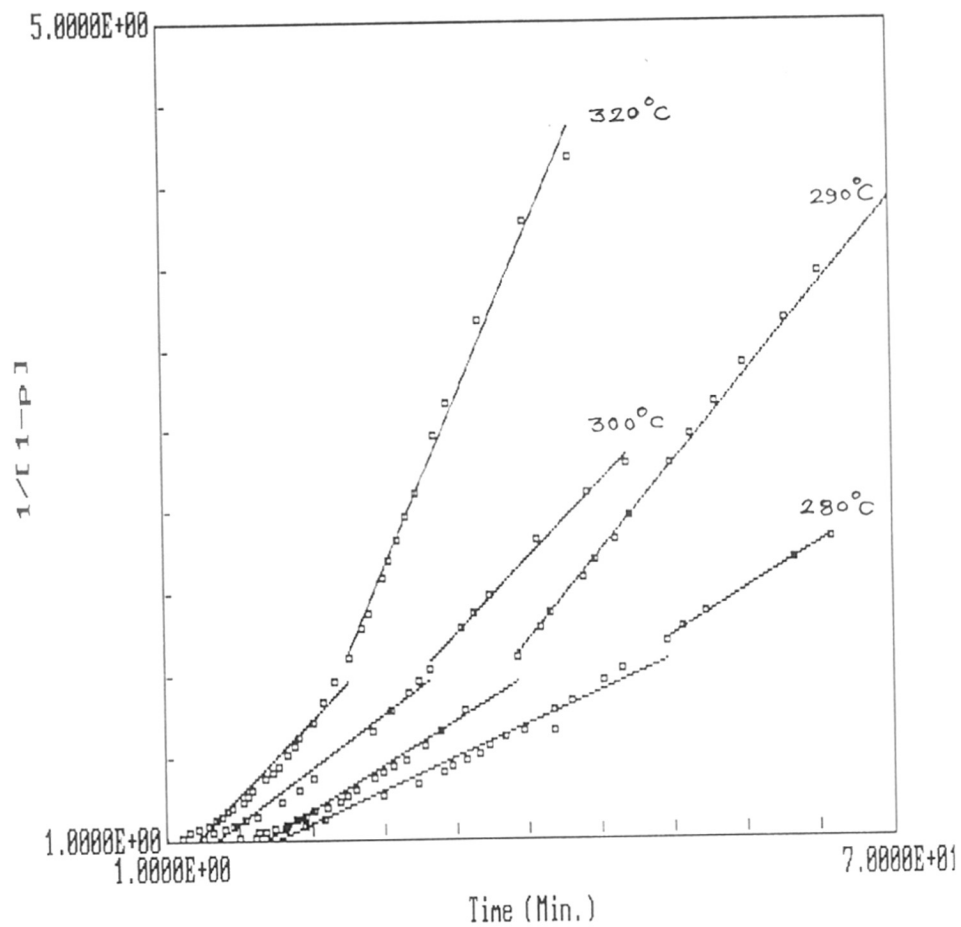


FIGURE 3.17 SECOND ORDER RATE LAW PLOT ILLUSTRATING EFFECT OF TEMPERATURE FOR RDA/TPA UNCATALYSED REACTIONS.

TABLE - 3.7
RESULTS OF KINETICS OF UNCATALYSED AND CATALYSED ACIDOLYSIS
BETWEEN RESORCINOL DIACETATE AND TEREPHTHALIC ACID

Polymn. Code	Temp./ °C	Induction period, min.	k [c ⁻¹ .t ⁻¹] Dimerisation	k [c ⁻¹ .t ⁻¹] Oligomerisation
<u>Uncatalysed Acidolysis</u>				
RT1	320	0.8	0.00985	0.0178
RT2	310	2.2	0.00890	0.0199
RT3	300	3.7	0.00635	0.00893
RT4	290	8.2	0.00550	0.0104
RT5	280	8.0	0.00388	0.00530
<u>Catalysed Acidolysis</u>				
RTC1	320	1.1	0.0124	0.0248
RTC2	310	2.1	0.00107	0.0200
RTC3	300	3.6	0.00912	0.0180
RTC4	290	5.9	0.00650	0.0100
RTC5	280	7.0	0.00568	0.00803

TABLE - 3.8
RESULTS OF KINETICS AND THERMODYNAMICS ANALYSIS OF ACIDOLYSIS
REACTIONS OF HT, HI AND RT POLYESTERS

Polymn. Code	AE _D kCal/mole	AE _O kCal/mole	ΔS_D eu	ΔS_O eu	ΔH_D kCal/mole	ΔH_O kCal/mole	$\frac{\ln A_O}{\ln A_D}$
HT	18.88	16.22	-41.30	-47.03	17.74	15.08	0.59
HTC	15.35	16.57	-46.76	-45.22	14.21	15.43	1.07
HI	17.69	-----	-43.66	-----	16.55	-----	----
HIC	17.51	37.65	-44.11	-----	16.37	36.51	2.59
RT	16.18	21.56	-45.63	-35.56	15.04	20.42	1.57
RTC	13.93	20.25	-48.83	-36.45	12.79	19.11	1.82

D = Dimerisation; O = Oligomerisation

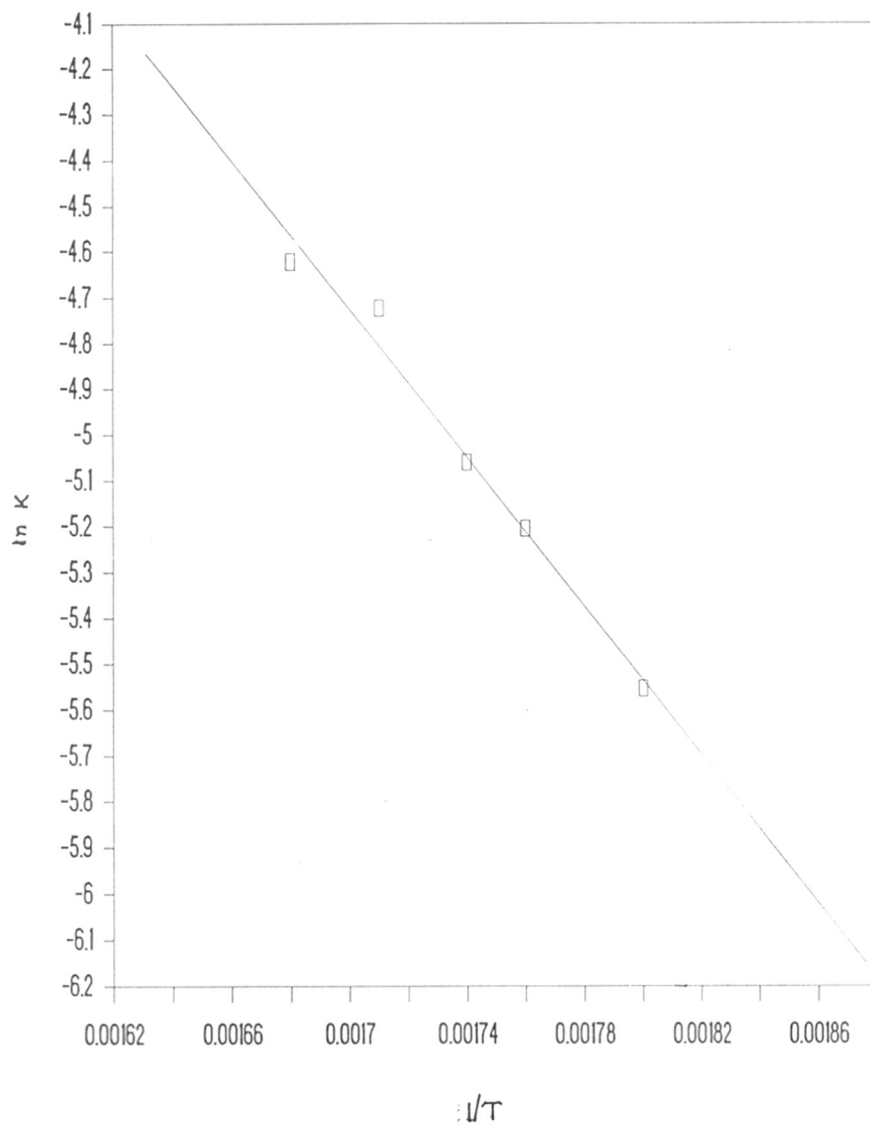


FIGURE 3.18 ARRHENIUS PLOT FOR RDA/TPA UNCATALYSED REACTIONS PRIOR TO THE BREAK

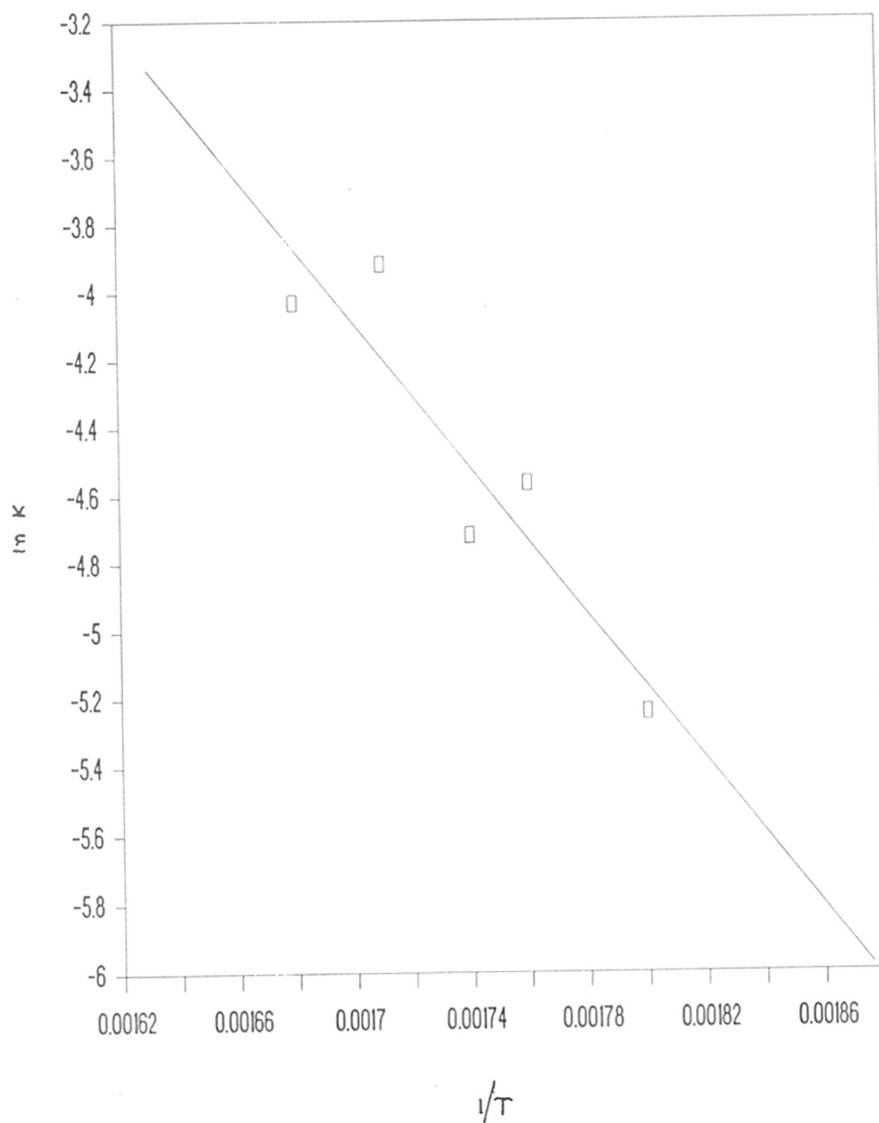


FIGURE 3.19 ARRHENIUS PLOT FOR RDA/TPA UNCATALYSED REACTIONS AFTER THE BREAK

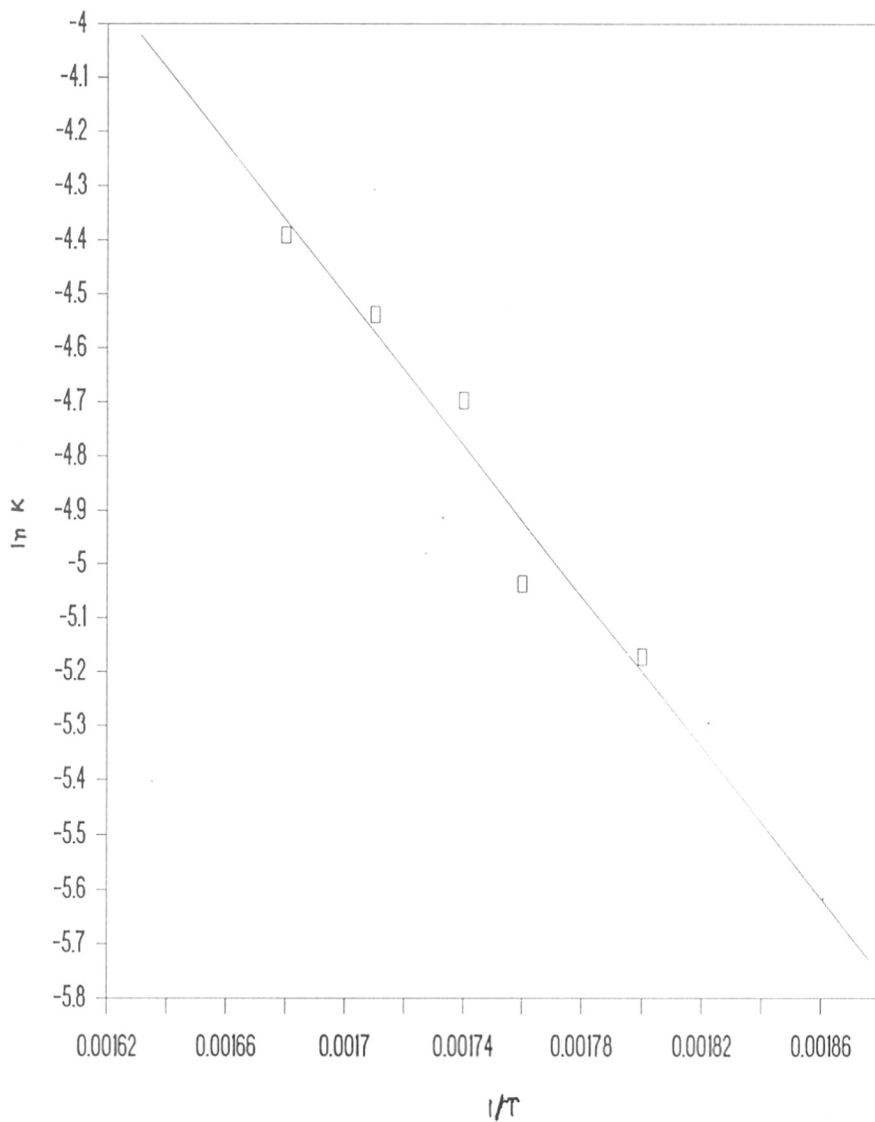


FIGURE 3.20 ARRHENIUS PLOT FOR RDA/TPA CATALYSED REACTIONS PRIOR TO THE BREAK

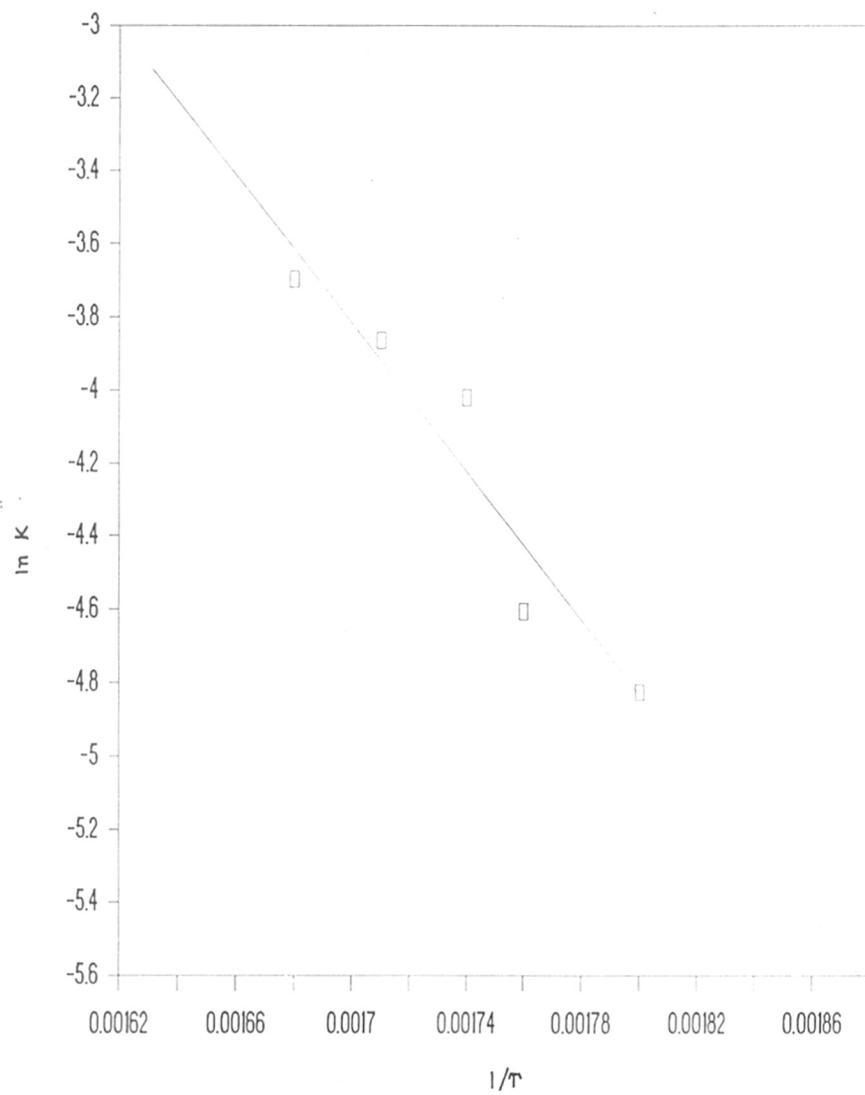


FIGURE 3.21 ARRHENIUS PLOT FOR RDA/TPA CATALYSED REACTIONS AFTER THE BREAK

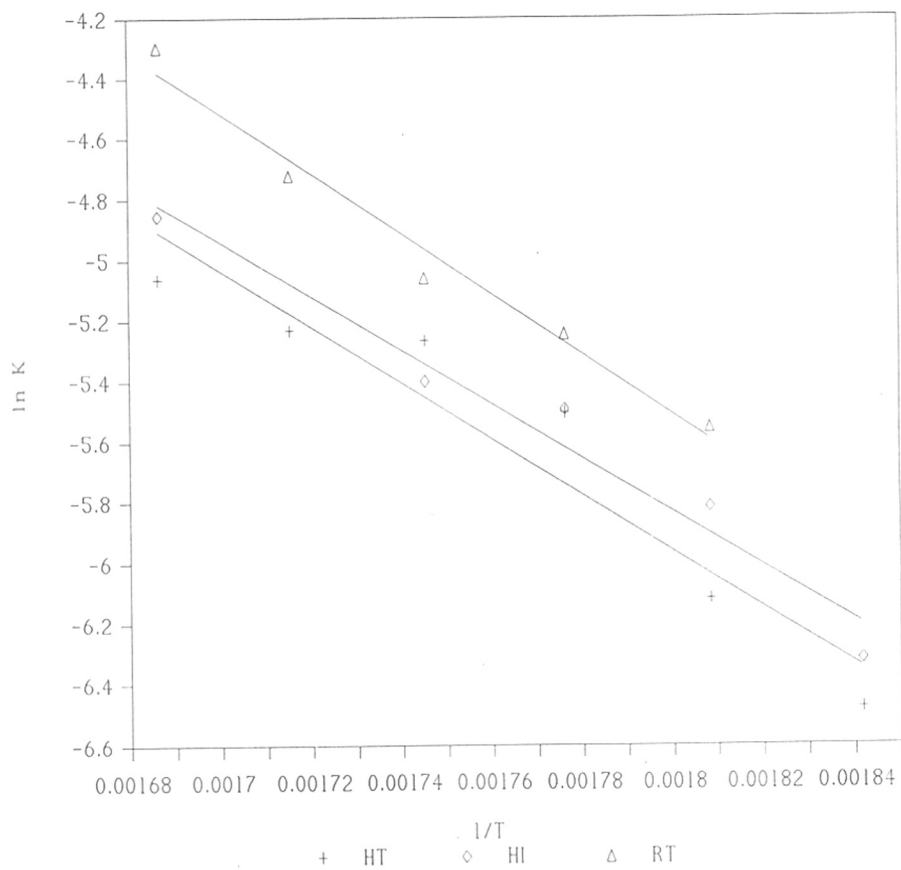


FIGURE 3.22 COMPARISON OF ARRHENIUS PLOTS OF FIRST STAGE UNCATALYSED REACTIONS OF HT, HI AND RT SYSTEMS

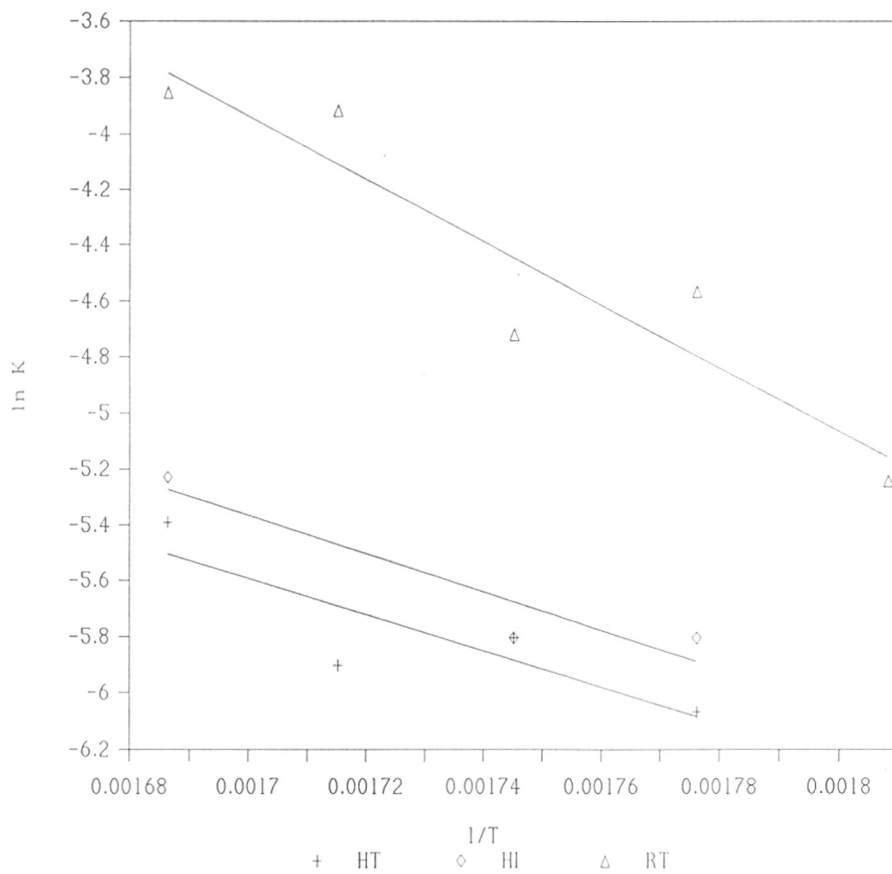


FIGURE 3.23 COMPARISON OF ARRHENIUS PLOTS OF SECOND STAGE UNCATALYSED REACTIONS OF HT, HI AND RT SYSTEMS

polyesterification between resorcinol diacetate and terephthalic acid is also intrinsically different from the HT and HI reactions in that the RDA is a liquid at room temperature. It is a very mobile liquid in the temperature range of the kinetic study. The enhanced rate points to an increase in the concentration of the carboxyl groups due to greater solubilisation of terephthalic acid by resorcinol diacetate relative to HQDA. The reacting molecules have higher mobility even at the start. Unlike the HT and HI series, the product is completely molten, as confirmed by microscopic observation at the reaction temperature. It is highly probable that reaction between resorcinol diacetate and insoluble terephthalic acid generates oligomers with carboxylic acid end groups which are soluble in RDA thereby increasing the concentration of carboxylic acid units in the reaction medium and resulting in enhanced rate.

The point at which break in the kinetic plots are observed in RT polyesterification are related to the increased concentration of carboxylic acid and hence are the reference points when the reaction acquires homogeneity vis-a-vis heterogeneity in HT, HI and oxybenzoate systems. The RT polyesterification starts as a slurry and gradually homogenises, a trend dramatically opposite to that noted for HT and HI systems. Such solubilisation of terephthalic acid has been noted in the melt copolyesterification of hydroquinone diacetate, 2-tert.butyl hydroquinone diacetate and terephthalic acid at 305° C³⁷. The system was initially heterogeneous at all mole ratios of hydroquinone diacetate : 2-tert.butyl hydroquinone diacetate, became homogeneous during the polyesterification due to solubilisation of terephthalic acid but shifted back to heterogeneity in the later stages due to phase separation of high melting oligomers.

In RT polyesterification system, RDA units drag in the TPA units into the reaction by solubilisation which increases their concentration and results in the observed increase in

rate of reaction and the compensation effect. The RT system differs from the hydroquinone diacetate, 2-tert.butyl hydroquinone diacetate and terephthalic acid system in that the polymer obtained at the end of the reaction is molten, and does not exhibit thermotropic character.

Zinc acetate, sodium acetate and dibutyltin oxide were tested for their catalysis and it was noticed that the differences between the catalysed and uncatalysed reactions were principally quantitative and not qualitative. Thus breaks in the second order kinetic plots and an induction are present in both these rate plots. However, breaks in the $1/(1-p)$ occur for lower values in uncatalysed reactions. Dibutyltin oxide was chosen as the catalyst^{23,24}. Also the nature of the plots were not altered by increasing the catalyst (dibutyltin oxide) concentration from 0.1 to 1.0 mole %, but the rates were marginally enhanced. The turnover number (number of reaction events in mol/sec/site) decreased with an increase in concentration of catalyst molecules. Thus, all the catalyst sites were not uniformly accessible for the second order reaction.

3.4 CHARACTERISATION

Infra-red spectra of HQDA and the copolyester HT are shown in **Figure 3.24**. These showed a band at 1740 cm^{-1} and at 1364 cm^{-1} corresponding to C=O stretching of aromatic ester and -CH₃ stretching of -COCH₃ respectively. In the copolyester [poly(1,4-phenylene oxy-1,4-carboxy phenylene)] an additional band is recorded at 1064 cm^{-1} which is due to p-disubstituted phenyl rings coupled with -OCO.

HT and HI polyesters were insoluble in all solvents. Oligomeric HT polyester is known to be soluble in the 1:1 V:V 4-chloro phenol : 1,1,2,2-tetrachloroethane mixed solvent system. The oligomeric polymers synthesised in this study were partially soluble in chloroform.

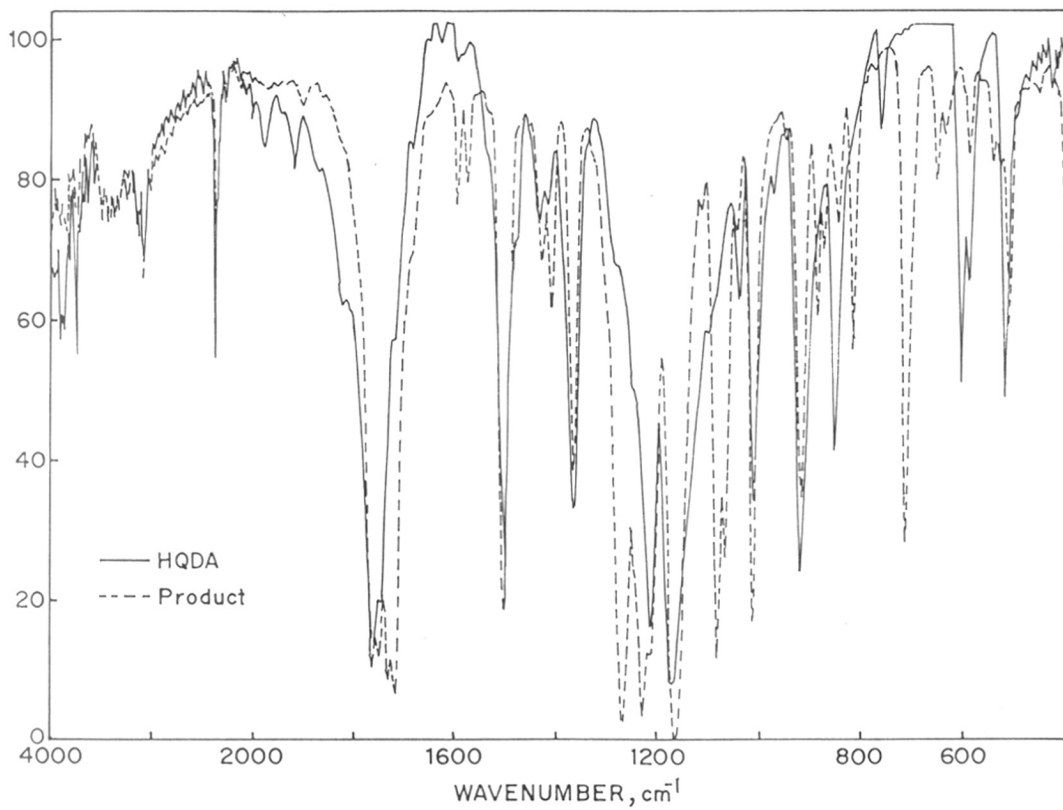


FIGURE 3.24 IR SPECTRUM OF HQDA (SOLID LINE) AND HT POLYESTER (DOTTED LINE)

This indicates a distribution of molecular weight where in the low molecular mass fraction is soluble in chloroform while the high molecular mass fraction is insoluble, nonmelting, hard solid. The DSC data corroborates this observation.

DSC traces of first heating cycle of HT polyester prepared by uncatalysed reaction are shown in **Figure 3.25** while **Figure 3.26** represents DSC thermograms of HI polyesters prepared by catalysed reaction. In addition to a broad endotherm with a peak around 385°C , a transition is noted between $200\text{-}300^{\circ}\text{C}$ in both HT and HI polyesters. The high temperature transition is independent of reaction temperature and owes its origin to a solid - solid transition and is followed by degradation. HT polyester is monoclinic. McIntyre³⁷ et Al reported the possibility of changes in the monoclinic structure in this temperature range for this polymer and supported it by X-ray diffraction data. Our X-ray results agree well with those reported by McIntyre. On opening the sample pans after the DSC scan, particles were found to be intact excepting for discolouration due to degradation.

In order to study the low temperature transitions in detail, HT and HI polymers prepared by both catalysed and uncatalysed reactions were extracted with chloroform. The DSC scan of chloroform soluble fraction from HT polyester synthesised at 270°C (sample - A) is shown in **Figure 3.27** reveals a transition at 193°C and a compound endotherm with a peak at 230°C corresponding to crystal - mesophase transition. This mesomorphic temperature range agrees well with that observed in the optical analysis under crossed polarised light. Samples of different degree of polymerisation were analysed by DSC. The area under the peaks due to mesomorphic transitions was found to decrease with increase in DP (**Figure 3.25**). Related DSC parameters are presented in **Table 3.9**. Chloroform insoluble fraction (sample - B) did not show any transition below 300°C (**Figure 3.27 (d)**). RT polyesters show a well defined first order transition in the range $290\text{-}300^{\circ}\text{C}$ (**Figure 3.28**) which corresponds to isotropisation as observed under optical microscopy. Linear rod shaped nature, which is a

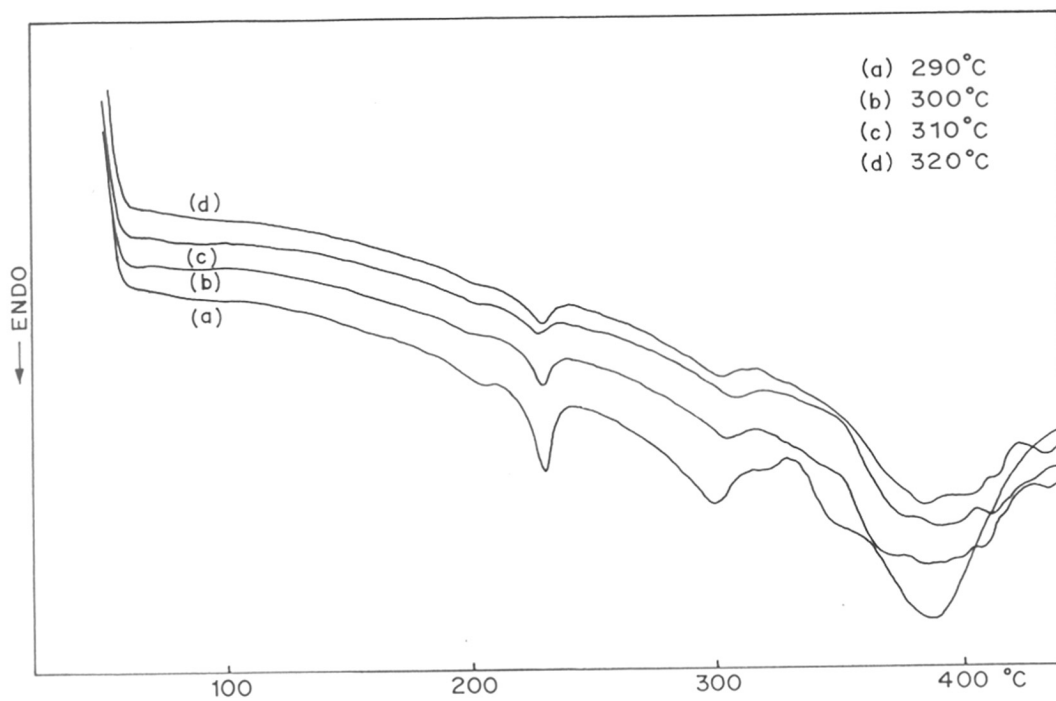


FIGURE 3.25 FIRST HEATING DSC TRACES OF UNCATALYSED REACTIONS OF HT POLYESTERS

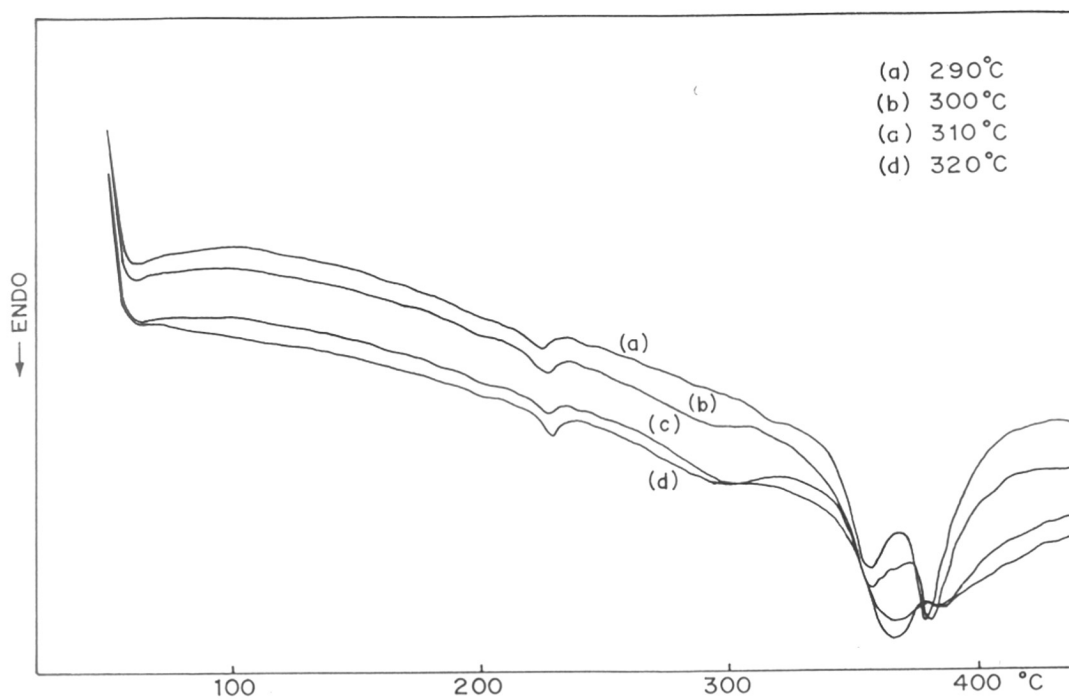


FIGURE 3.26 FIRST HEATING DSC TRACES OF CATALYSED REACTIONS OF HI POLYESTERS

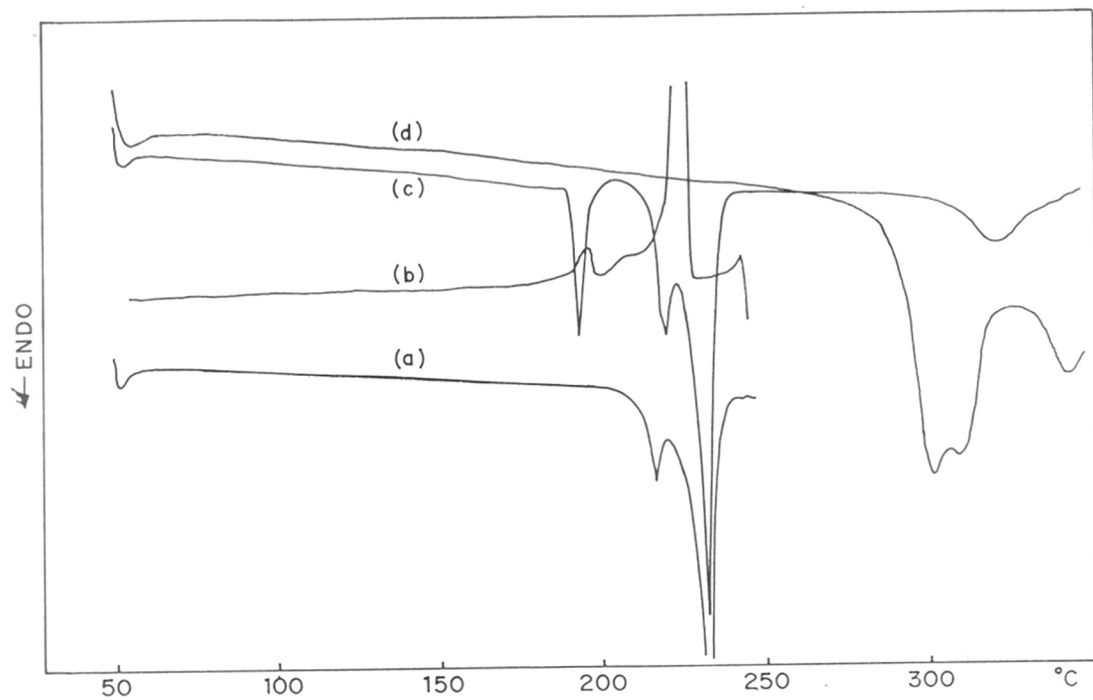


FIGURE 3.27 DSC TRACES OF SAMPLE - A (a) SECOND HEATING; (c) FIRST HEATING; (b) COOLING AND (d) FIRST HEATING DSC TRACE OF SAMPLE - B

TABLE - 3.9

DSC RESULTS OF MESOMORPHIC TRANSITIONS OF HT POLYESTERS PREPARED BY UNCATALYSED REACTION AT DIFFERING POLYMERISATION REACTION TEMPERATURES.

Polymn. Code	Reaction Temp./ °C	Mesomorphic Transitions			Heat of Fusion ΔH J/g		
		T ₁ °C	T ₂ °C	T ₃ °C	ΔH_1	ΔH_2	ΔH_3
1T	320	202	227.7	299.4	*	2.1	1.9
2T	310	200	226.1	306.0	*	1.2	1.5
3T	300	198	223.7	302.0	*	2.2	1.5
4T	290	202	229.0	297.5	0.5	4.7	7.8
5T	280	196	229.0	292.6	0.9	9.9	7.0
6T	270	201	231.0	279.0	5.4	35.7	11.7

* - This value is less than 0.5 J/g

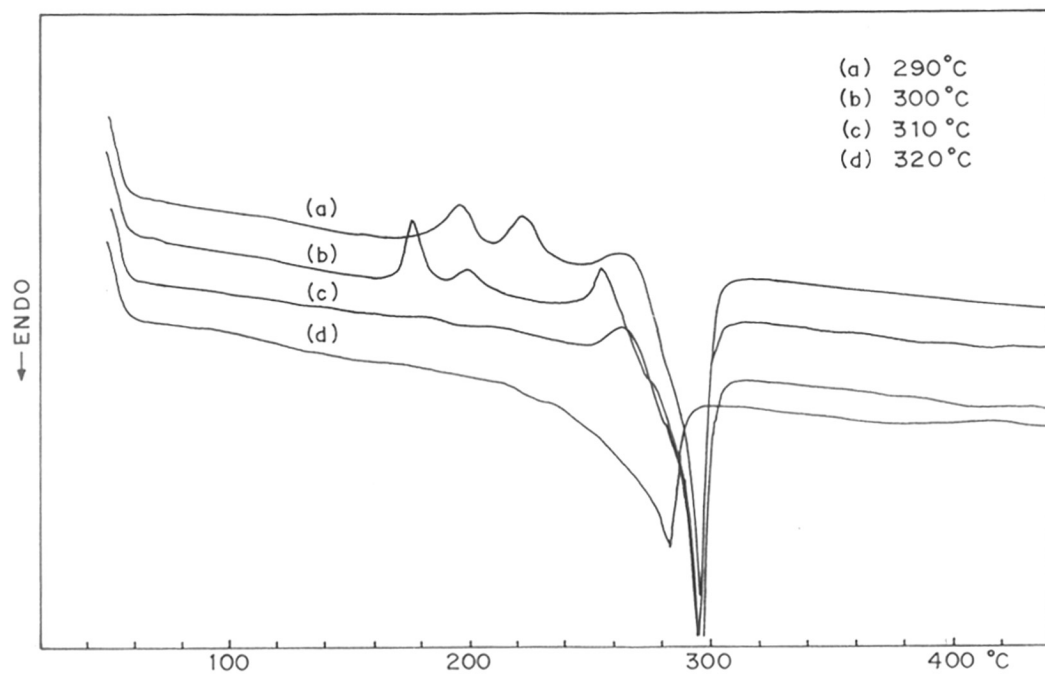
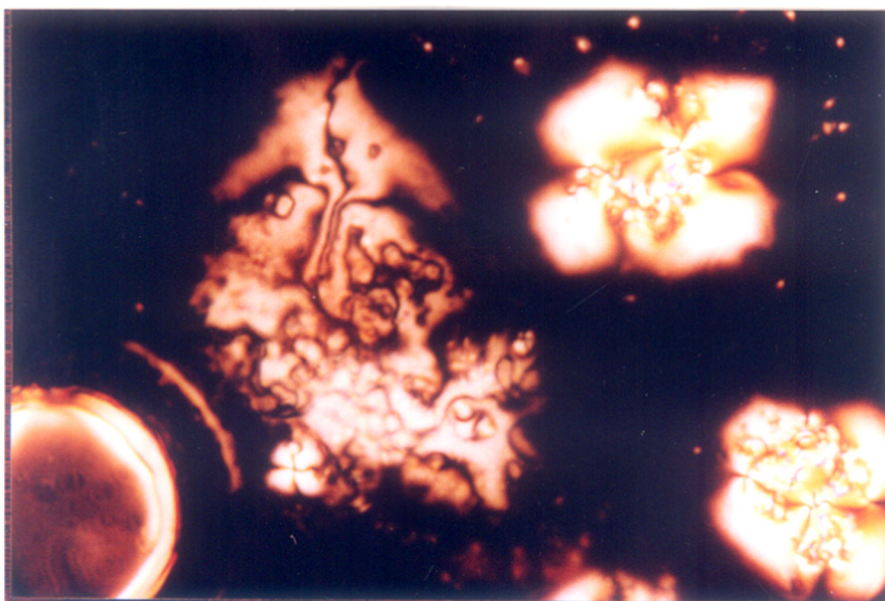


FIGURE 3.28 FIRST HEATING DSC TRACES OF UNCATALYSED REACTIONS OF RT POLYESTERS

prerequisite to formation of mesomorphic state, is not maintained in the RT polyester due to the alternate 1,3- and 1,4-linkages along the main chain. As a result, a single transition is observed in the DSC traces. The polyesters do not degrade till 450° C.

Optical analysis were carried out for few samples which showed a first order transition below 300° C. All HT and HI polyesters showed birefringence in the region 200 to 300° C. All these polyesters contained differing amounts of low molecular weight fraction soluble in chloroform, which depended on the synthesis temperature. Sample - A was analysed in detail to study the textures at different temperatures. The sample was heated at 5° C per minute. No change was observed till 172° C. At this temperature lot of movement was seen on the slide but no definite texture was recorded. Texture development started above 190° C. At 198° C some crystalline particles surrounded by bright spots were seen. The sample was held at this temperature for 30 minutes. Fan like structures started to appear. Temperature was then gradually increased. At 222° C (**Figure 3.29-(a)**) fans slowly change to beautiful threaded texture. This is also observable in **Figures 3.29-(b)** and **3.30-(a)** recorded at 225 and 229° C respectively. At 243° C the texture changes completely to schliren texture as seen in **Figure 3.30-(b)**. Flow and colours were observed till 265° C. It was obvious from the analysis that the textures were very sensitive to temperature and were very much dependent on the heating and cooling cycles. Instead of gradual heating, a fresh sample was heated to 234° C at the rate of 10° C per minute. **Figure 3.31-(a)** shows the texture of sample at this temperature. The sample was then cooled at 5° C per minute and the photograph was recorded at 224° C (**Figure 3.31-(b)**). On reheating from this temperature flow starts around 228° C and becomes profound at 230° C. Touching the slide maintained isothermally at 233° C with a cold pin leads to instant crystallisation, as seen in **Figure 3.32-(a)**. This is due to polycondensation on the

(a)



(b)

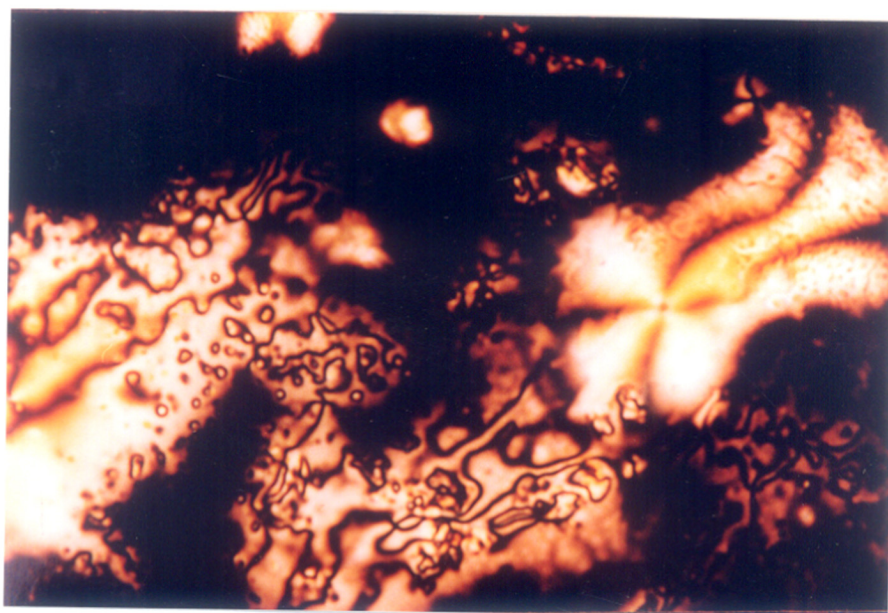
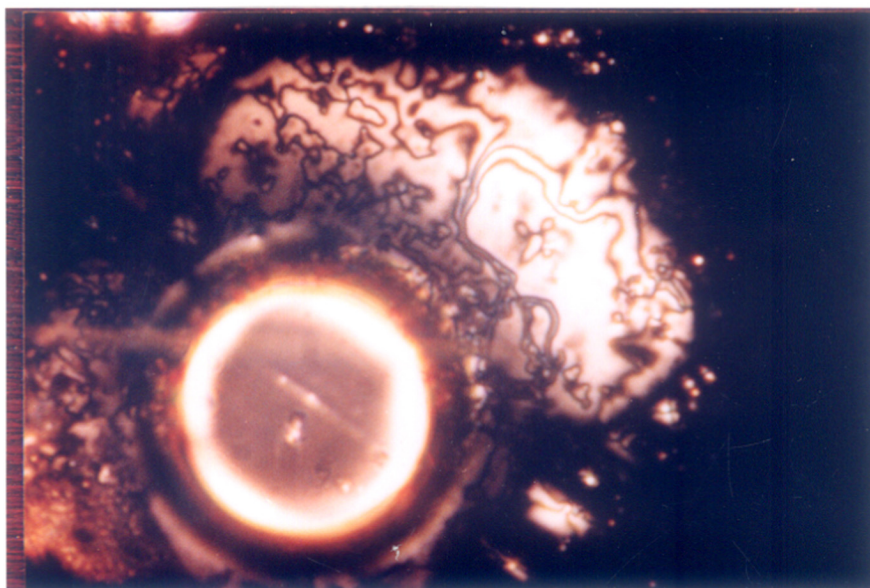


FIGURE 3.29 OPTICAL MICROGRAPHS OF SAMPLE - A, (a) AT 222° C AND (b) AT 225° C

(a)



(b)

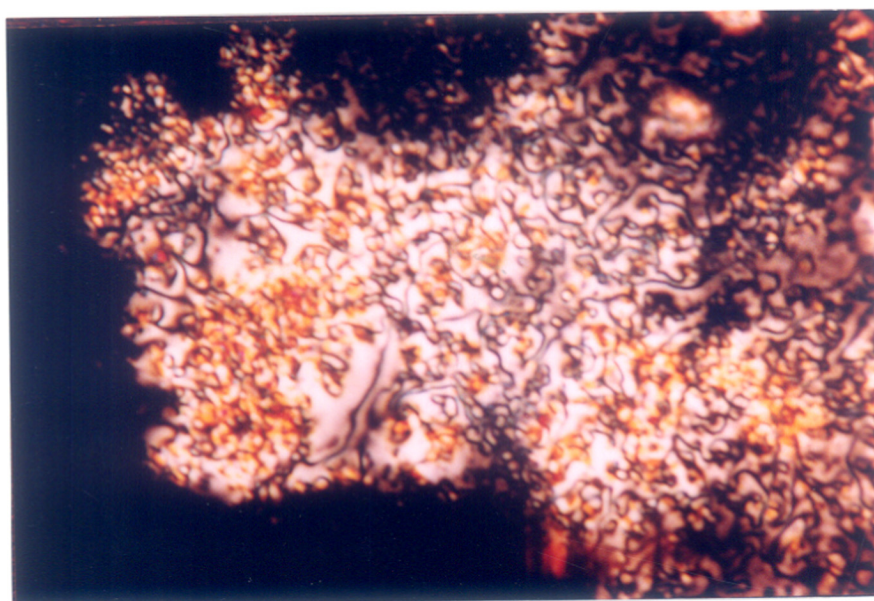
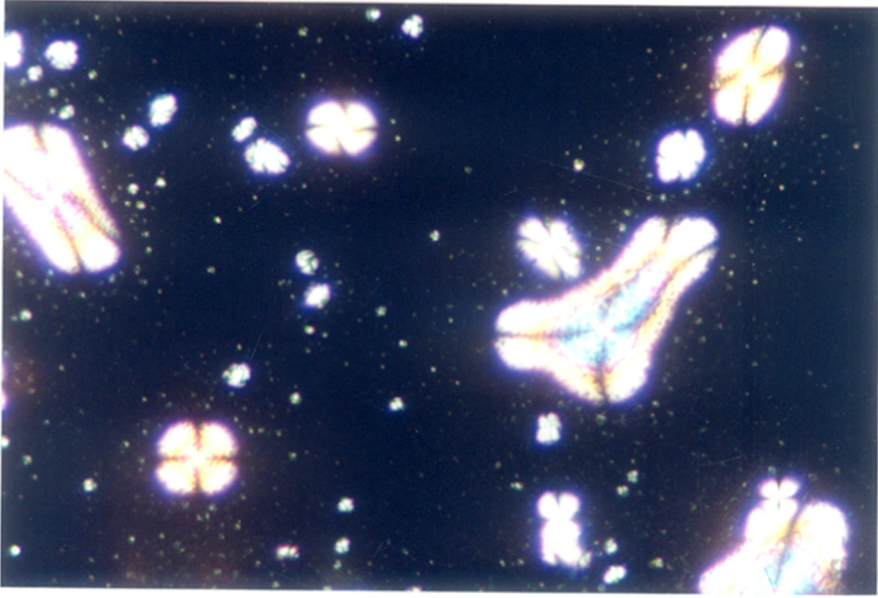


FIGURE 3.30 OPTICAL MICROGRAPHS OF SAMPLE - A (a) AT 229°C AND (b) AT 243°C

(a)



(b)

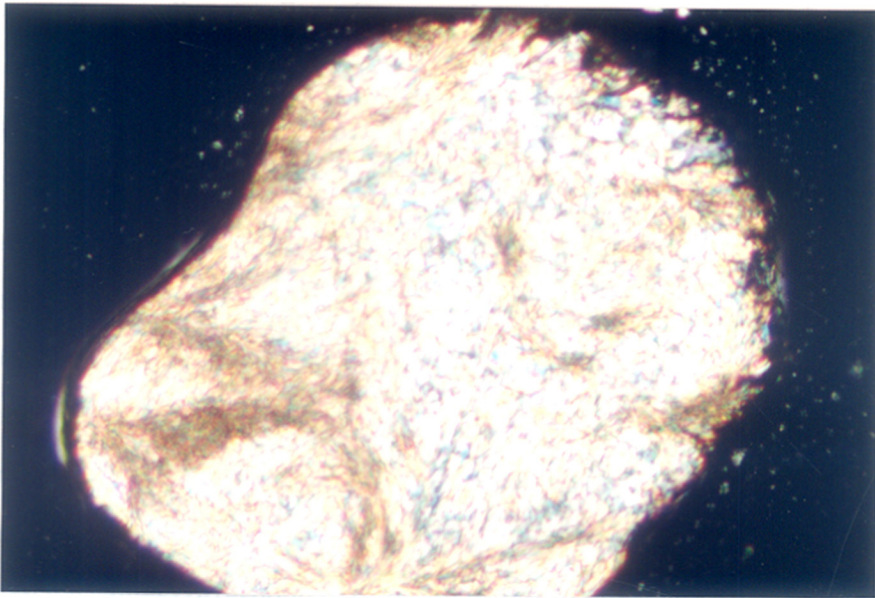
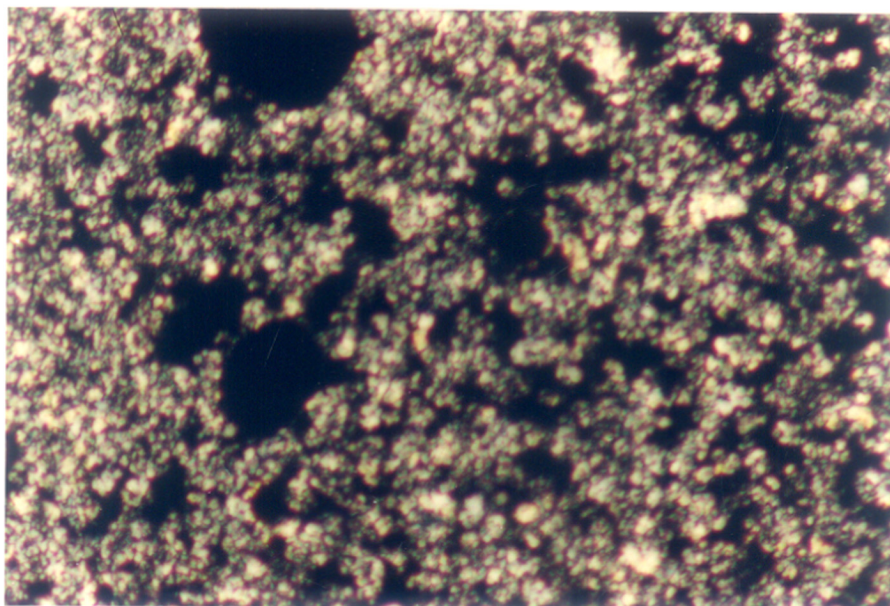


FIGURE 3.31 OPTICAL MICROGRAPHS OF SAMPLE - A (a) AT 234°C AND (b) AT 224°C

slide itself leading to further increase in the molecular weight. Removal of pin leads to instant melting. **Figure 3.32-(b)** shows the texture developed in the sample on heating directly to 230°C at the rate of 15°C per minute.

Room temperature X-ray of HT and HI polyesters show that these are highly crystalline (**Figures 3.33-(b), (c)**). This is due to linear, symmetric and regular backbone formed by 1,4-benzene repeating units. On similar lines the structure of RT should also be symmetric and regular and should be reflected in high percent crystallinity. In fact amorphous nature is indicated by diffraction data (**Figure 3.33-(a)**). This shows that directional effect of ester group along the polymer chain plays a major role in the packing and hence the crystallinity. Percent crystallinity values calculated from the area under the crystalline and amorphous peaks and d-spacing values calculated using Bragg's equation⁴⁴ are presented in **Table 3.10**. Sample - A was subjected to room temperature X-ray analysis (**Figure 3.34-(a)**). This Figure also shows the diffraction pattern of sample - B for comparison. The material is perfectly crystalline. Absence of amorphous halo confirms its nonpolymeric nature. This sample was further examined by high temperature X-ray diffraction. Results are presented in **Table 3.11**. Diffraction patterns were recorded on films. Sharp concentric rings in the diffraction pattern recorded at room temperature (**Figure 3.35-(a)**) suggest that the sample is highly crystalline. A very peculiar pattern is noted as the temperature is increased. Sharp rings characteristic of randomly oriented crystalline powder turn into arcs at 186°C (**Figure 3.35-(b)**), 198°C and 220°C (**Figures 3.36-(a) and (b)**). Generally, this kind of arching indicates alignment of structural elements. In the present case the temperature corresponds to the mesomorphic temperature range noted from optical and thermal analysis. Patterns of this type have been observed in oriented liquid crystalline polymers.^{45,46} A careful observation of **Table 3.11** shows that d-spacing values correspond to different orders of diffraction such as $n = 1$ to $n = 8$. If the innermost arc around 25.1° which corresponds to the length of the molecule (H-T-H

(a)



(b)

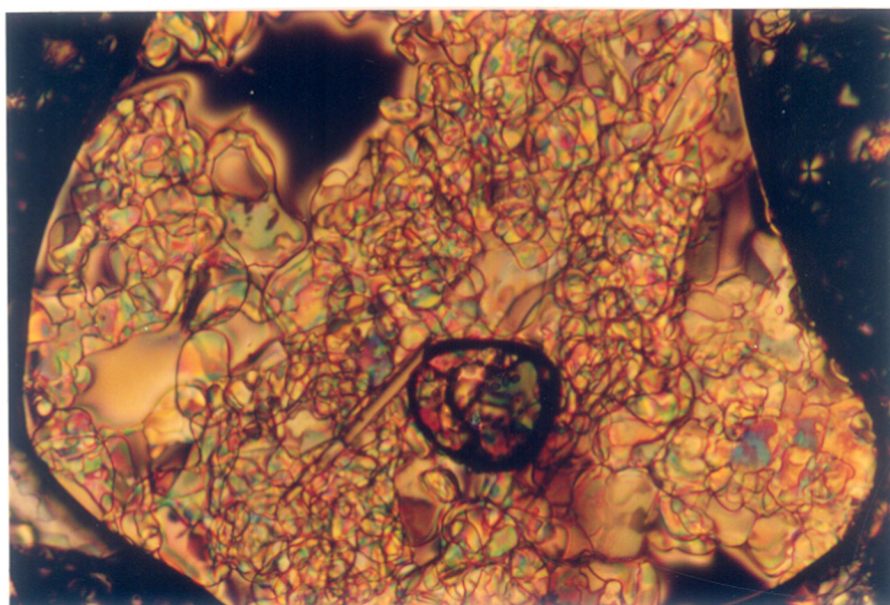


FIGURE 3.32 OPTICAL MICROGRAPHS OF SAMPLE - A (a) AT 233° C AND (b) AT 230° C

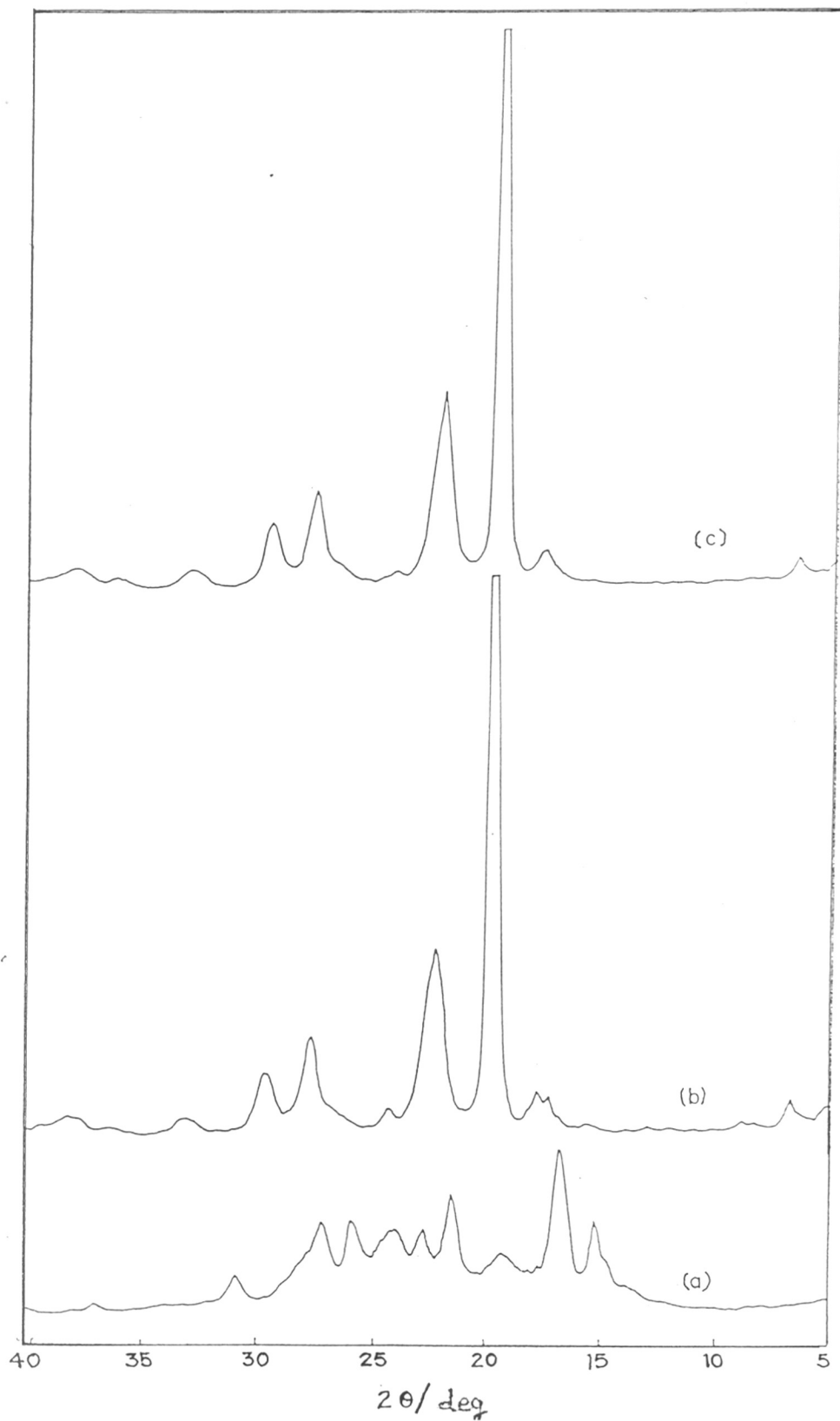


FIGURE 3.33 X-RAY DIFFRACTION PATTERN OF AS MADE POLYESTERS:(a) RT; (b) HT; (c) HI

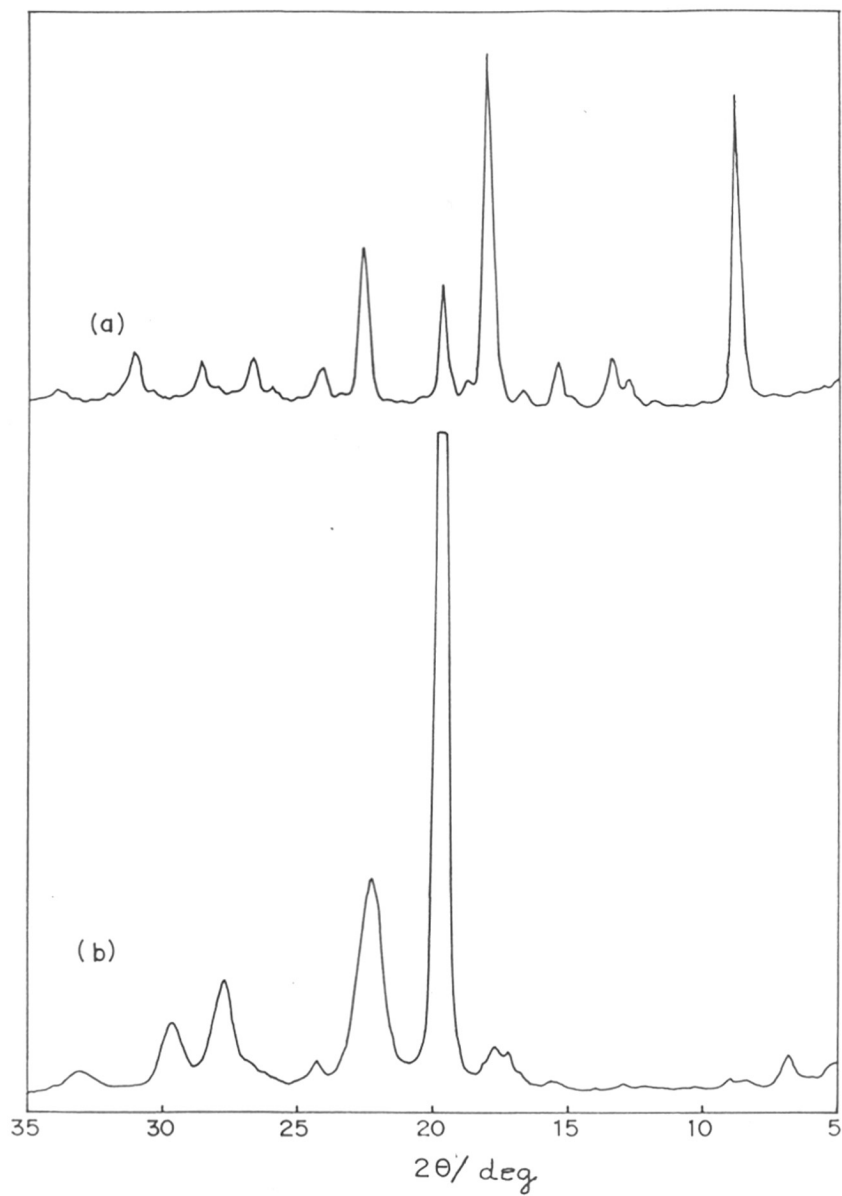
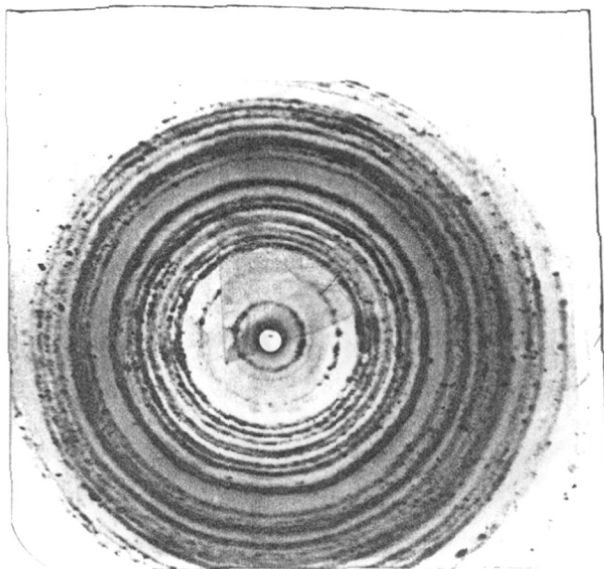


FIGURE 3.34 X-RAY DIFFRACTION PATTERN OF :(a) SAMPLE - A; (b) SAMPLE - B

(a)



(b)

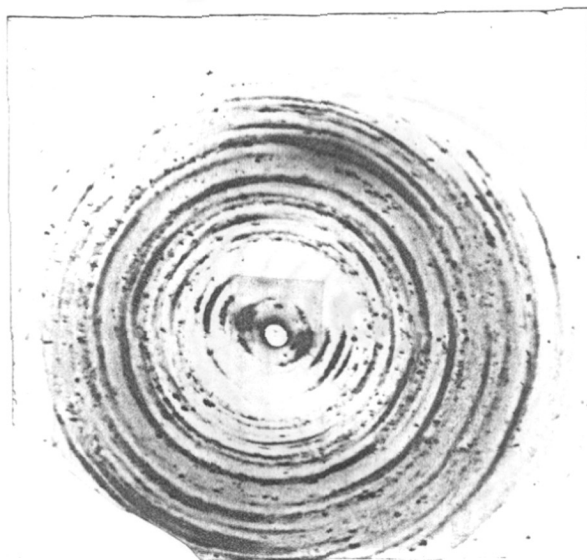
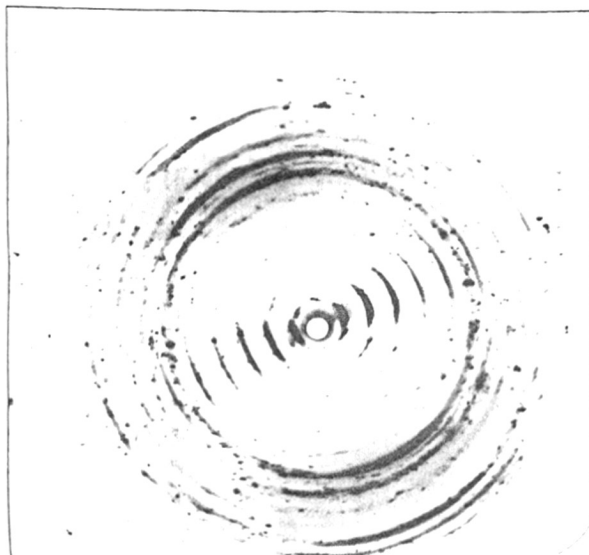


FIGURE 3.35 HIGH TEMPERATURE X-RAY DIFFRACTION FILM OF SAMPLE - A RECORDED AT : (a) ROOM TEMPERATURE; (b) 186°C

(a)

125



(b)

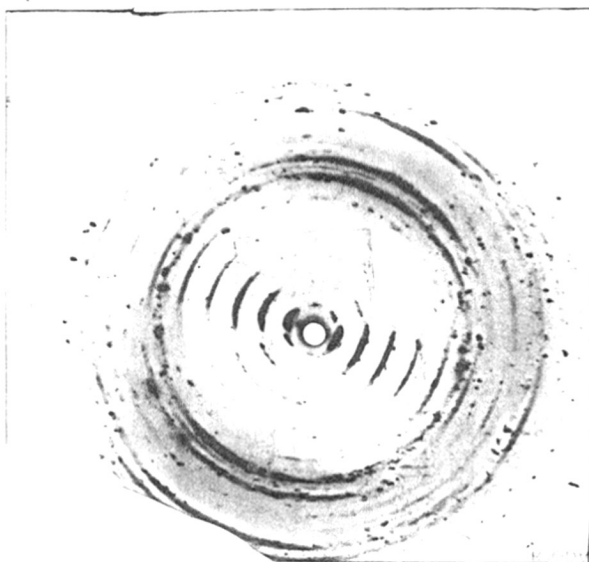


FIGURE 3.36 HIGH TEMPERATURE X-RAY DIFFRACTION FILM OF SAMPLE - A RECORDED AT : (a) 198°C; (b) 220°C

TABLE - 3.10
RESULTS OF ROOM TEMPERATURE X-RAY DIFFRACTION ANALYSIS

Polymer Compn.	% Crysta- llinity	Peak 2θ								'd' spacing $\overset{\circ}{\underset{\text{Å}}{A}}$							
		A	B	C	D	E	F	G	H	A	B	C	D	E	F	G	H
H/T 1/1	69.0	7.0	17.6	19.8	22.4	27.8	29.8	33.0	38.0	12.0	5.0	4.48	3.96	3.21	2.99	2.71	2.36
H/I 1/1	67.0	17.8	19.8	22.4	24.4	27.8	29.7	33.0	38.0	4.97	4.48	3.97	3.65	3.21	3.01	2.71	2.37
R/T 1/1	33.0	15.4	16.8	19.4	21.4	22.8	24.0	26.0	27.4	5.75	5.27	4.57	4.35	3.89	3.70	3.42	3.25

TABLE - 3.11
RESULTS OF HIGH TEMPERATURE X-RAY DIFFRACTION ANALYSIS.

	'd' spacing $\overset{\circ}{\underset{\text{Å}}{A}}$								Peak 2θ							
	A	B	C	D	E	F	G	H	A	B	C	D	E	F	G	H
Sample - A																
25°C	3.17	3.61	3.88	4.44	5.70	6.72	9.68	19.6	28.09	24.58	22.88	19.96	15.50	13.16	9.12	4.50
186°C	4.94	5.69	6.53	8.52	9.87	12.8	19.2	26.8	17.93	15.55	13.54	10.36	8.94	6.89	4.60	2.25
196°C	3.16	3.62	4.23	5.06	6.32	8.50	12.7	25.8	28.21	24.57	20.93	17.51	13.99	10.38	6.96	3.42
220°C	3.16	3.63	4.26	5.08	6.38	8.49	12.8	26.7	28.12	24.49	20.83	17.40	13.85	10.40	6.89	3.29
236°C	2.71	2.71	3.01	3.27	4.07	4.52	5.08	9.25	32.93	29.56	27.17	21.79	19.60	17.43	9.54	6.95
Sample - B																
25°C	3.19	3.53	3.91	4.46	5.14	12.8	19.1	----	27.86	25.20	22.74	6.88	19.86	17.22	6.88	4.61
186°C	3.28	3.57	4.00	4.52	5.14	12.9	20.3	----	27.16	24.90	22.20	19.59	17.23	6.79	4.35	----

with end groups), is considered as the principle order diffraction, then the other d-spacings are its multiples. Decrease in diffraction intensity for the higher orders also confirm this. The rings or arcs observed in the wide angle region at d-spacing of 4 \AA correspond to inter-chain spacing, while the small angle diffraction at d-spacing of 25 \AA reflects the layer spacing. Further increase in temperature to 236°C reveals the disappearance of arcs indicating randomisation of previously aligned structural elements (**Figures 3.37-(a)**). According to DSC analysis, the sample changes from mesomorphic to isotropic state in this region. As a result a diffuse hollow characteristic of liquids is expected in the diffraction pattern at this temperature, while presence of few rings suggest presence of crystalline particles. This observation also reflects the occurrence of postcondensation reaction during analysis, product of which melts at 340°C as seen in **Figure 3.27 (c)**. Similar reaction was also suspected during optical analysis. Diffraction pattern of sample - B was also taken at room temperature and at 186°C . **Figure 3.37-(b)** shows that it is crystalline and does not change at higher temperature.

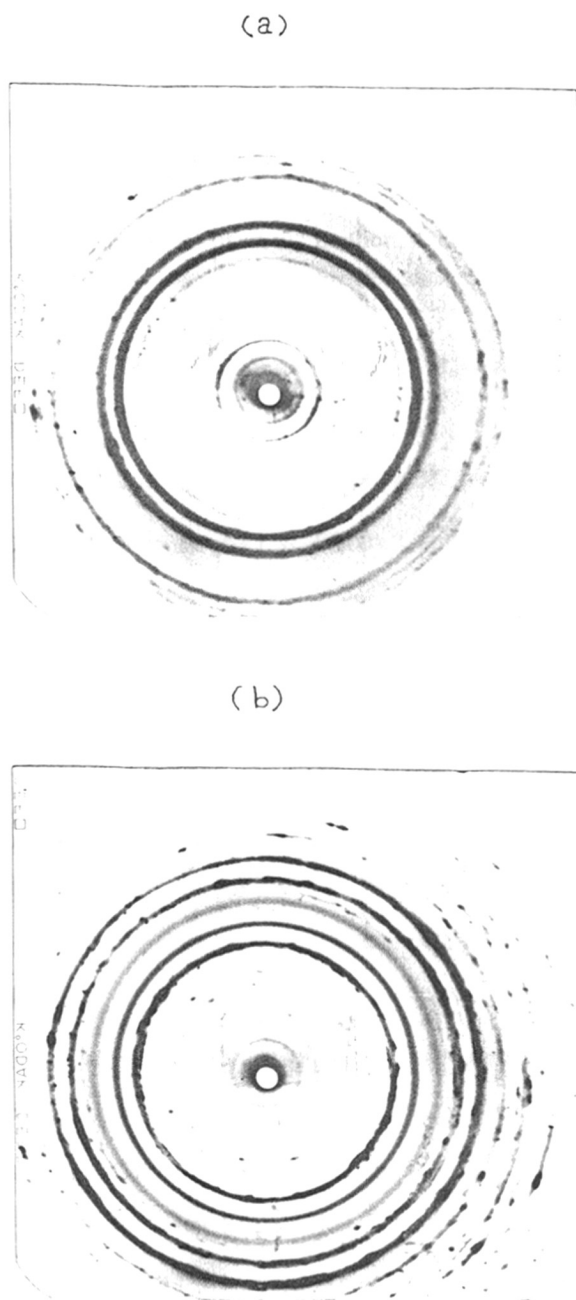


FIGURE 3.37 HIGH TEMPERATURE X-RAY DIFFRACTION FILM OF SAMPLE - A RECORDED AT (a) 236°C (b) SAMPLE - B RECORDED AT 186°C .

REFERENCES

1. G.W. Gray, "Polymer Liquid Crystals", (eds. A. Ciferri, W.R. Krigbaum, R.B. Meyer), Academic Press Inc. Ltd., London, p.5 (1982).
2. M.G. Dobb and J.E. McIntyre, *Adv. Polym. Sci.*, **60/61**, 61 (1984).
3. J. Economy, W. Volksen, C. Viney, R. Geiss, R. Siemens and T. Karis, *Macromolecules*, **21**, 2777 (1988).
4. H.R. Kricheldorf and G. Schwarz, *Polymer*, **31**, 481 (1990).
5. B.D. Dean, M. Matzner and J.M. Tibbitt, "Comprehensive polymer Science", Vol. **5** (eds. G.C. Eastmond, A. Ledwith, S. Russo and P. Sigwalt), Pergamon, Oxford (1989).
6. S.W. Kantor and F.F. Holub, (General Electric Co.), US Pat. 3160602 (1964).
7. S.P. Elliott, (E. I. DuPont de Nemours and Co.), US Pat. 4093595 (1978).
8. A.J. East, (Celanese Corp.), Eur. Pat. Appl. 88546 (1983).
9. R.W. Lenz, "Organic Chemistry of Synthetic High Polymers", Interscience, New York (1967).
10. L.B. Sokolov, "Synthesis of Polymers by Polycondensation", Isreal Program for Scientific Translations, Jerusalem (1968).
11. P.W. Morgan, "Condensation Polymers by Interfacial and Solution Method", John Wiley & Sons, Inc., New York (1965).
12. W.H. Carothers and F.J. Natta, *J. Am. Chem. Soc.*, **52**, 314 (1930).
13. P.J. Flory, *J. Am. Chem. Soc.*, **59**, 466 (1937).

14. P.J. Flory, "Principles of Polymer Chemistry", Cornell University Press, Ithaca, New York (1953).
15. R.T. Rolfe and Hinshelwood, *Trans. Faraday Soc.*, **30**, 935 (1934).
16. M.M. Davies, *Trans. Faraday Soc.*, **34**, 410 (1938).
17. V.V. Korshak and Z. Vinogradova, *Obshch Him.*, **22**, 1176 (1952).
18. V.V. Korshak, T.M. Frunze and I. Li, *Vysokomolekul. Soedin.*, **3**, 665 (1961).
19. M.M. Davies and D.R.J. Hill, *Trans. Faraday Soc.*, **49**, 395 (1953).
20. Tang Au Chin and Yao Kuo-Sui, *J. Polym. Sci.*, **35**, 219 (1959).
21. I. Vancso-Szmercsanyi and E. Makey-Bodi, *J. Polym. Sci., Part C* **16**, 3709 (1968).
22. I. Vulic and T. Schulpen, *J. Polym. Sci., Part A: Polym. Chem.*, **30**, 2725 (1992).
23. J. Mathew, R.V. Bahulekar, R.S. Ghadage, C.R. Rajan and S. Ponrathnam and S.D. Prasad, *Macromolecules*, **25**, 7338 (1992).
24. J. Mathew, R.S. Ghadage and S. Ponrathnam and S.D. Prasad, *Macromolecules*, **27**, 4021 (1994).
25. J. Koskikallio, "The Chemistry of the Carboxylic Acids and Esters", (eds. S. Patai), Interscience, New York (1969).
26. M. Levine and S.C. Temin, *J. Polym. Sci.*, **28**, 179 (1958).
27. J. Huang, J.P. Lablanc and H.K. Hall, *J. Polym. Sci., Part A: Polym. Chem.*, **30**, 345 (1992).
28. J.I. Jin, S. Antoun, C. Ober and R.W. Lenz, *Br. Polym. J.*, **12**(4), 132 (1980).
29. W.J.Jr. Jackson, Jr., *Mol. Cryst., Liq. Cryst.*, **23**, 169 (1989).
30. K.J. Laidler, "Theories of Chemical Reaction Rates", (eds. D.N. Hume, G. Stork, E.L. King, D.R. Herschbach, J.A. Pople), McGraw-Hill, Inc., New York, p.55 (1969).

31. J.R.Jr. Jackson, *Br. Polym. J.*, **12**, 154 (1980).
32. W.R. Krigbaum, R. Kotek, T. Ishikawa and H. Hakemi, *Eur. Polym. J.*, **20**, 225 (1984).
33. M.J.S. Dewar and R.M. Robert, *J. Am. Chem. Soc.*, **97**, 6658 (1975).
34. M.J.S. Dewar and R.S. Goldberg, *J. Org. Chem.*, **35**, 2711 (1970).
35. A. Adrien and E.P. Sergeant, "Ionisation Constants of Acids and Bases", *A Laboratory Manual*, Butler and Tanner Ltd., London, p.134 (1962).
36. W.M. AD Braam and B.J.R. Scholtens, *J. App. Polym. Sci.*, **50**, 2007 (1993).
37. Z.G. Li, J.E. McIntyre, J.G. Tomka and A.M. Voice, *Polymer*, **34**, 1946 (1993)
38. R. Cai and E.T. Samulski, *Macromolecules*, **27**, 135 (1994).
39. R. Cai and E.T. Samulski, *Macromolecules*, **25**, 563 (1992).
40. F. Navarro J.L. Serrano, *J. Polym. Sci., Part A, Polym. Chem.*, **30**, 1789 (1992).
41. J. Cao, G. Karayannidis, J.E. McIntyre and J.G. Tomka, *Polymer*, **34**, 1471 (1993).
42. Jung-II Jin, S.H. Lee and H.J. Park, *Polym. Prepr. 1987*, **28**, 122 (1970).
43. A. Clark, A., "The Theory of Adsorption and Catalysis", Academic Press, London, p.260 (1970).
44. L.E. Alexander, "X-ray diffraction methods in polymer science", Wiley Interscience, New York, p.36 (1969).
45. C. Noel, "Liquid Crystals and Ordered Fluids" [ed. A.C. Griffin and J.F. Johnson], Plenum Press, New York, **4**, p. 401 (1984).
46. C. Noel, "Recent Advances in Liquid Crystal Polymers" [ed. L. Chapoy,], Elsevier Applied Science Publishers Ltd, p. 155 (1985).

CHAPTER - 4

CHAPTER - 4

4.1 INTRODUCTION

Stiff chain polymers possessing the capability of forming a thermally stable mesophase have attracted considerable attention because of their potential application as high performance plastics.¹⁻³ It was theoretically predicted and experimentally proved that rigid rod like structure is a prerequisite for polymers to display thermotropy.⁴ Poly(4-phenylene terephthalate) was the most logical rigid rod polyester that could have generated an anisotropic liquid crystalline melt but glass transition (267°C) and melting temperature (467°C) are too high to be processable without degradation.⁵ As a result different structural modifications have evolved to control the melting temperature and thermotropy.⁶

Generation of nonlinear meta aromatic structural units by the incorporation of 1,3-benzene dicarboxylic acid, 1,3-benzene diol and 3-hydroxy benzoic acid (m-HBA), in conjunction with their linear counter-parts, is one of the ways of depressing melting temperature.⁷⁻¹⁰ However, the increase of nonlinear meta-phenylene defect beyond a certain critical value destroys liquid crystallinity of the melt. Extensive structure-property correlations with respect to the variance in the copolymer composition, sequence distribution of structural units in the polymer chain etc. have been undertaken¹¹⁻¹³ to control liquid crystallinity.

The polyesters prepared from these meta units and the common para units like terephthalic acid (TPA), hydroquinone (HQ) and 4-hydroxy benzoic acid (p-HBA) can be grouped depending on the number of meta phenylene units in the main chain as follows:

i) Three para units in the main chain (TPA, HQ, p-HBA); ii) Two para units and one meta unit; iii) One para unit and one meta unit; iv) One para unit and two meta units and v) Three meta units (IPA, RE, m-HBA).

Cottis et al¹⁴ and Jackson¹⁵ have studied the group (i) copolyesters and observed melting temperatures in excess of 600°C. The group (iv) and (v) copolyesters contain more than 50 mole % meta phenylene units and are unlikely to form liquid crystalline polymers. Therefore, most research has focused on the groups (ii) and (iii) and a large number of polyesters have been synthesised and studied to exploit liquid crystallinity.^{16,17} These results indicate that the critical percentage of m-phenylene units compatible with liquid crystallinity is around 60 mole %.

The reports by Rosenau-Eichin et al¹⁸ on the effect of meta phenylene units on liquid crystallinity of all aromatic polyesters indicate that the incorporation of the bent unit into polyester does lower the melting temperature but this $\gamma = 120^\circ$ defect considerably decreases the mesophase stability.

The polyesterification kinetics of these multicomponent systems have either remained largely unexplored or unrecorded in the open literature.¹⁹⁻²¹ Here we focus on the kinetics of melt acidolysis reactions between hydroquinone diacetate (HQDA), resorcinol diacetate (RDA), terephthalic acid (TPA), and isophthalic acid (IPA), forming two wholly aromatic copolyester systems such as HRT and HIT. The effect of monomer structure and composition on the reaction kinetics is investigated. The properties of the thermotropic copolyesters thus synthesised are also analysed.

The copolyesters were prepared in the melt by acidolysis reaction as described in the Section 2.3. RDA/IPA were used to introduce 60° kink in the linear chain formed by a combination of HQDA and TPA. The mole percent of RDA in HRT was varied from

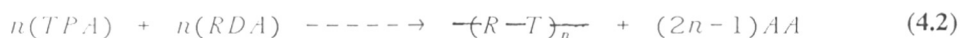
0% to 90% while that of IPA in HIT was changed from 0% to 50%. The ratio of structurally bent non-linear unit to the linear unit was used as a geometrical variable in the kinetic studies at different temperatures. The experimental kinetic data was generated by noting the volume of the bi-product acetic acid evolved with time at different isothermal temperatures.

Copolyesterification kinetics was investigated with the following objectives: (1) To study the effect of temperature; (2) To study the effect of comonomer composition; (3) To develop a kinetic model which will take into account the complexities introduced by a third comonomer in the reaction; (4) To compare with corresponding homopolyesterification kinetics presented in Chapter - 3.

A complex kinetic model is developed for two competing reactions. The fact that the reactions can be modelled with simple rate model is discussed based on reactivity ratios. Effect of reaction temperature and composition on the kinetics is explained from the rate law and Arrhenius plots. Complexity in the reaction is discussed by comparing it with the homopolyesterification reactions presented in Chapter - 3. Lastly, characterisation of copolyesters using thermal, optical and X-ray analysis are presented in Section 4.3.

4.2 HRT Copolyesterification

The HRT copolyester from hydroquinone diacetate (HQDA), resorcinol diacetate (RDA) and terephthalic acid (TPA) is formed from a series of two competing reactions as follows.



$$[A] = a_0 - x; [B] = b_0 - y; [C] = c_0 - z$$

where AA = acetic acid; [A] = concentration of TPA at time 't'; [B] = concentration of HQDA at time 't'; [C] = concentration of RDA at time 't' and a_0 , b_0 and c_0 denote the initial concentration of TPA, HQDA and RDA respectively. k_1 , k_2 , y , z denote the kinetic constants, moles of the monomers consumed respectively. x denotes the total moles of acetic acid (AA) produced through both reaction channels.

The rate of formation of acetic acid, which also equals the rate of decrease of concentration of TPA [A], is given by

$$-\frac{d[A]}{dt} = k_1[A][B] + k_2[A][C] \quad (4.3)$$

while for the other two comonomers we have

$$-\frac{d[B]}{dt} = k_1 [A] [B] \quad (4.4)$$

$$-\frac{d[C]}{dt} = k_2 [A] [C] \quad (4.5)$$

eliminating time by dividing equation (4.3) by (4.4) we get

$$\frac{d[A]}{d[B]} = \frac{k_2[C]}{k_1[B]} + 1 \quad (4.6)$$

from the stoichiometry of the reaction

$$[a_0] = [b_0] + [c_0] \quad (4.7)$$

from the above reaction scheme

$$[a_0] - x = [b_0] - y + [c_0] - z \quad (4.8)$$

which is nothing but

$$[A] = [B] + [C]$$

at time 't'

therefore,

$$[C] = [A] - [B] \quad (4.9)$$

Substituting this value of [C] in equation (4.6), we get

$$\frac{d[A]}{d[B]} = \frac{k_2}{k_1} \frac{[A] - [B]}{[B]} + 1 \quad (4.10)$$

$$\frac{d[A]}{d[B]} = k_r \frac{[A]}{[B]} + 1 - k_r \quad (4.11)$$

Where,

$$k_r = \frac{k_2}{k_1}$$

This equation reduces to the well known form

$$\frac{dy}{dx} + P(x)y = Q(x) \quad (4.12)$$

whose solution is represented by

$$ye^{\int p dx} = \int Qe^{\int p dx} + constant \quad (4.12a)$$

performing the above outlined manipulations we get

$$\int_{[B]}^{[B_0]} \frac{dB}{[B]^2 + f_2[B]^{1-k}} = \int_0^t k_1 t \quad (4.13)$$

This copolyesterification deals with the preparation of wholly aromatic rigid rod poly(1,4-oxy phenylene oxy-1,4- carboxy phenylene carboxy-1,3-oxy phenylene) by acidolysis between hydroquinone diacetate (HQDA), resorcinol diacetate (RDA) and terephthalic acid (TPA) (Figure 4.1). HQDA and RDA are molten while TPA is present as solid particles (30 um) at the temperature range over which kinetics were investigated. TPA could either react with HQDA to form rigid rod non-melting poly(1,4-oxy phenylene oxy-1,4-carboxy phenylene) or with RDA to form molten, isotropic poly(1,3-oxy phenylene oxy- 1,4-carboxy phenylene) at reaction temperature. Subsequent copolymerisation reaction will incorporate all the monomer units in the polyester chain. Thus, over the entire composition range, the reaction is initially a slurry consisting of TPA crystals in the molten HQDA and RDA. It changes gradually to either solid state polycondensation due to high melting intermediates at high mole fraction of HQDA or to a homogeneous molten intermediates at high mole fraction of RDA. This is true of the reactions in which concentration of RDA does not exceed 50%. In this composition range, the copolyester formed is a hard intractable solid at the end of the reaction. On the contrary, for the reactions wherein the ratio of HQDA:RDA is 40:60, 30:70, 20:80 and 10:90 the initially slurry reaction changes to homogeneous reaction in the melt. The product formed is in the molten state and is found to be soluble in 4-chloro phenol at 55°C. Experimental kinetic data was collected as represented in Table 4.1.

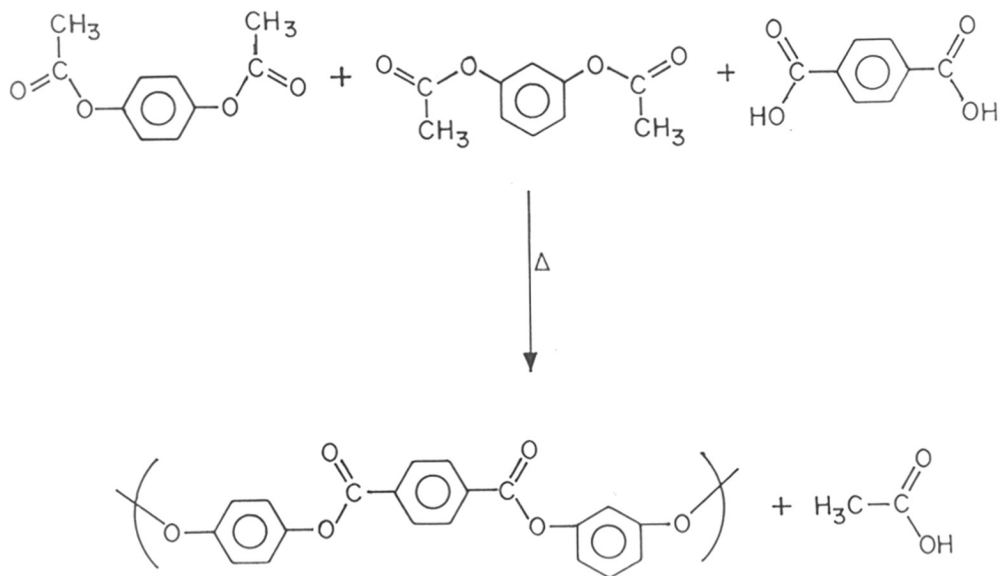


FIGURE 4.1 REACTION SCHEME FOR THE SYNTHESIS OF HRT COPOLYESTER

TABLE - 4.1

HIGH TEMPERATURE POLY-TRANSESTERIFICATION OF HYDROQUINONE DIACETATE [HQDA], RESORCINOL DIACETATE [RDA] AND TEREPHTHALIC ACID [TPA] WITHOUT CATALYST AT 320.0°C.

Reaction time	Volume of side product	Fractional conversion	Degree of polymerisation
[Minutes]	mL	[P]	{1/(1-P)}
1.3	0.1	0.0175	1.0178
2.6	0.3	0.0524	1.0554
3.0	0.4	0.0699	1.0752
3.3	0.5	0.0874	1.0958
3.7	0.6	0.1049	1.1172
4.2	0.7	0.1224	1.1394
4.8	0.8	0.1399	1.1626
5.3	0.9	0.1573	1.1867
5.7	1.0	0.1748	1.2119
6.0	1.1	0.1923	1.2381
6.8	1.3	0.2273	1.2941
7.8	1.5	0.2622	1.3555
8.8	1.7	0.2972	1.4229
10.0	2.0	0.3497	1.5376
11.1	2.2	0.3846	1.6250
11.7	2.3	0.4021	1.6725
12.5	2.5	0.4371	1.7764
13.0	2.6	0.4545	1.8333
14.1	2.8	0.4895	1.9589
15.0	3.0	0.5245	2.1029
15.7	3.1	0.5420	2.1832
16.2	3.2	0.5594	2.2698
16.7	3.3	0.5769	2.3636
18.2	3.5	0.6119	2.5766
18.7	3.6	0.6294	2.6981
19.3	3.7	0.6469	2.8317
20.1	3.8	0.6643	2.9792
24.4	4.2	0.7343	3.7632
25.5	4.3	0.7517	4.0282
28.7	4.5	0.7867	4.6885
30.3	4.6	0.8042	5.1071
36.3	4.7	0.8217	5.6078

It is seen from the kinetic treatment presented above that the introduction of a third comonomer leads to two competing reactions progressing simultaneously and liberating acetic acid. The copolymerisation kinetics and the copolymer properties will be governed by the rate of individual homopolymerisation reactions (4.1) and (4.2) since these would determine the compositions of the copolymers. In our earlier studies of kinetics of homopolyesterification we have observed that the reactivity ratio k_r (ratio of rate constant of RT and HT reaction at a fixed temperature) is ~ 2 (Table 4.2). Therefore, equation (4.13) is not applicable to the present copolymer reaction. Even if solution could be obtained it will be extremely complex.²² Therefore, we tried to fit copolyesterification reaction data of all the reactions into 1st, 2nd, 2.5th and 3rd order kinetic expressions. Figures 4.2 - 4.5 show rate law plots of HRT/50:50:100 corresponding to 1st, 2nd, 2.5th and 3rd order respectively. It was observed that the simple second order rate law was obeyed quite generally. Prior study also indicated that the second order kinetic laws are applicable to the homopolyesterification between hydroquinone diacetate and terephthalic acid (HT) series and resorcinol diacetate and terephthalic acid (RT) series (Sections 3.3.2 and 3.3.4). Therefore, the copolyesterification reaction was treated as if occurring via two simple second order reactions. The rate constants were determined from the plot of $1/(1-p)$ against time. (Table 4.3).

The second order rate law plots of HRT/80:20:100; HRT/20:80:100; HRT/75:25:100; HRT/60:40:100 and HRT/40:60:100 are shown in Figures 4.6-4.10. These figures reveal that second order kinetic behaviour is indeed true at all temperatures and over the entire composition range. The plots are characterised by presence of breaks and induction period, both of which are temperature dependent. Induction period decreases with increase in the reaction temperature and the breaks become sharper at higher temperature. Also, breaks occur progressively after longer reaction time with decrease in reaction temperature. In both regimes, separated by break, the kinetic order is the same. However, the change in

TABLE - 4.2

VARIATION OF REACTIVITY RATIO (k_D/k_O) WITH CONCENTRATION OF RDA

Concn. of RDA		k_D/k_O			
Mole%	320°C	310°C	300°C	290°C	
100	0.55	0.45	0.71	0.53	
90	0.34	0.44	0.39	1.20	
80	0.40	0.47	0.41	0.56	
70	0.37	0.47	0.45	0.54	
60	0.31	0.42	0.34	0.53	
50	0.39	0.36	0.61	0.53	
40	0.38	0.50	0.46	0.73	
30	0.40	0.55	0.70	0.68	
25	0.80	0.54	0.78	0.76	
20	0.57	0.70	0.86	0.98	
10	0.87	1.02	1.14	-	
0	1.41	1.99	1.71	1.75	

k_D = Dimerisation rate constant; k_O = Oligomerisation rate constant

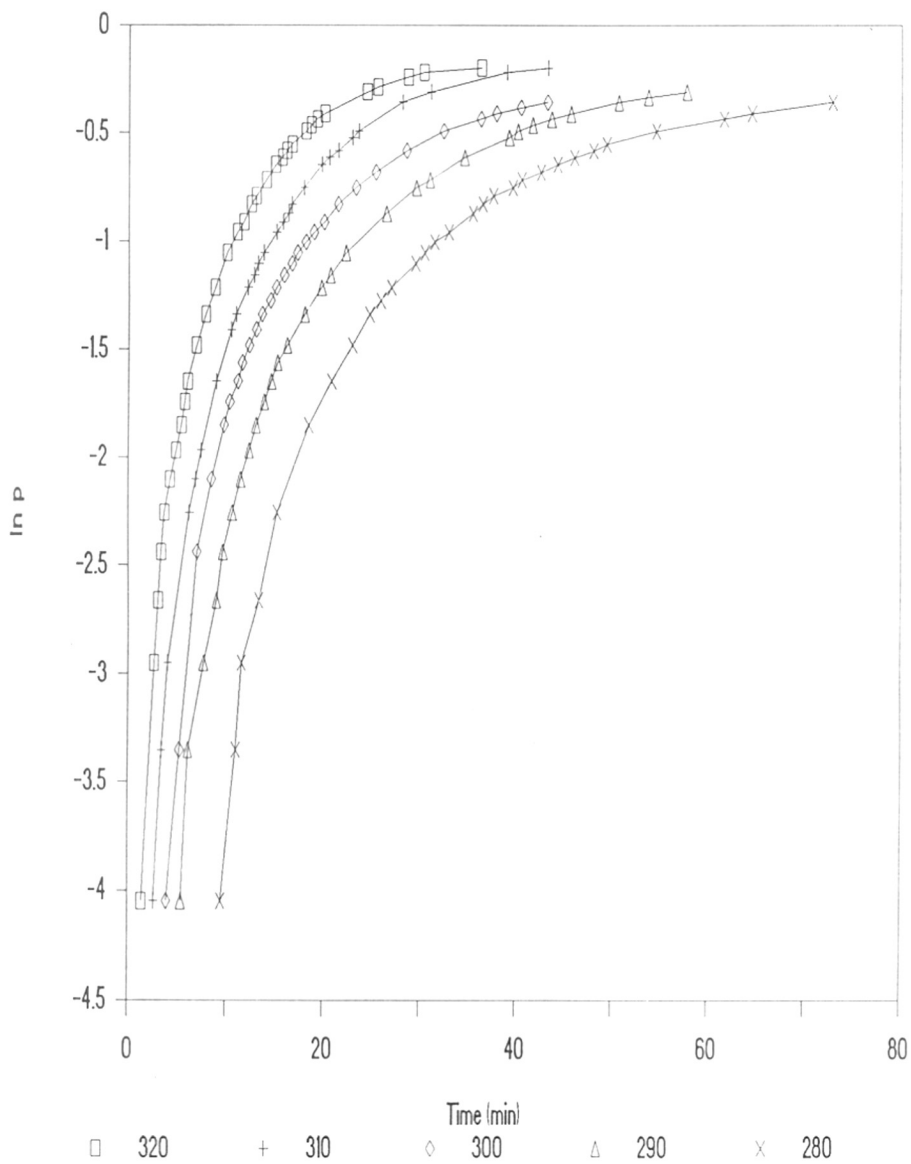


FIGURE 4.2 FIRST ORDER RATE LAW PLOT ILLUSTRATING THE EFFECT OF TEMPERATURE FOR HRT/50:50:100 REACTION

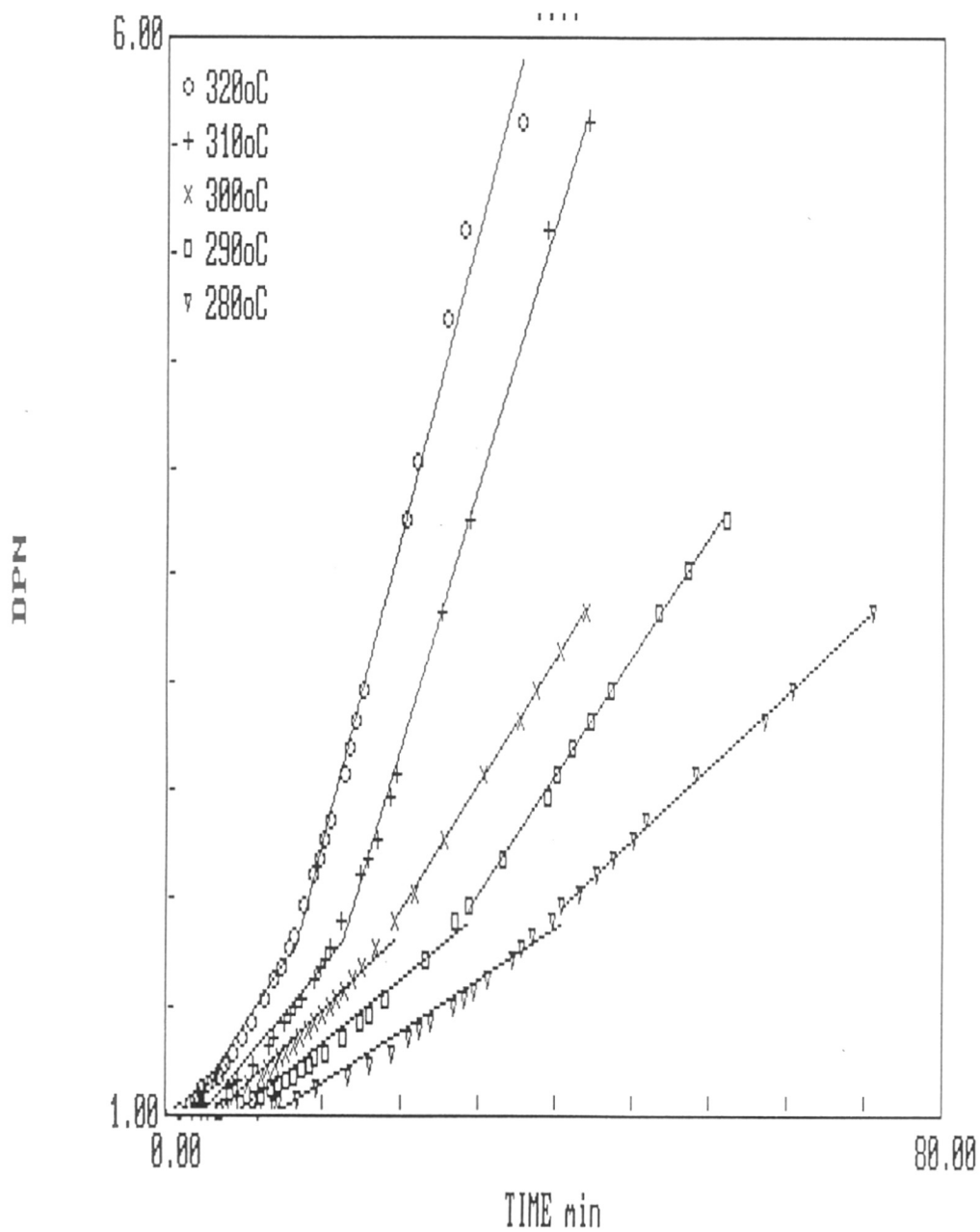


FIGURE 4.3 SECOND ORDER RATE LAW PLOT ILLUSTRATING THE EFFECT OF TEMPERATURE FOR HRT/50:50:100 REACTION

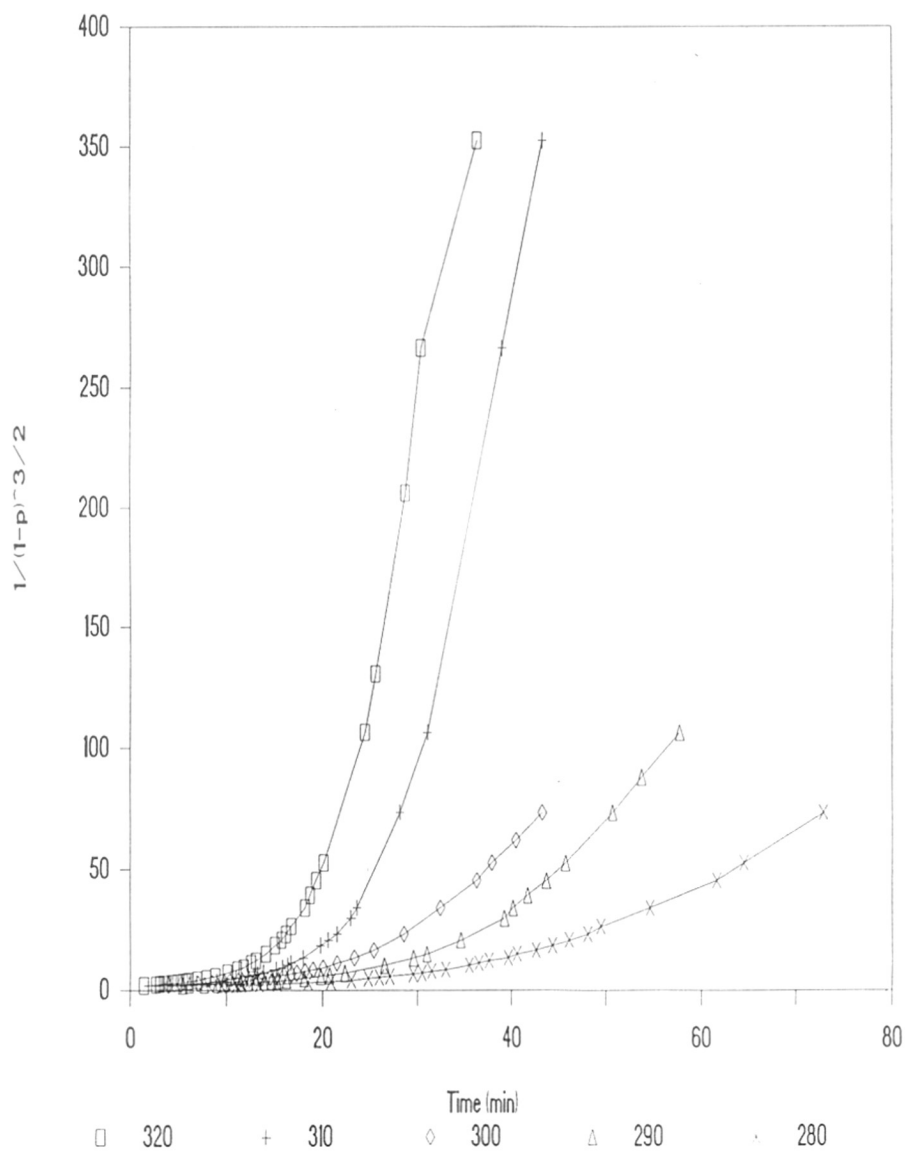


FIGURE 4.4 2.5TH ORDER RATE LAW PLOT ILLUSTRATING THE EFFECT OF TEMPERATURE FOR HRT/50:50:100 REACTION

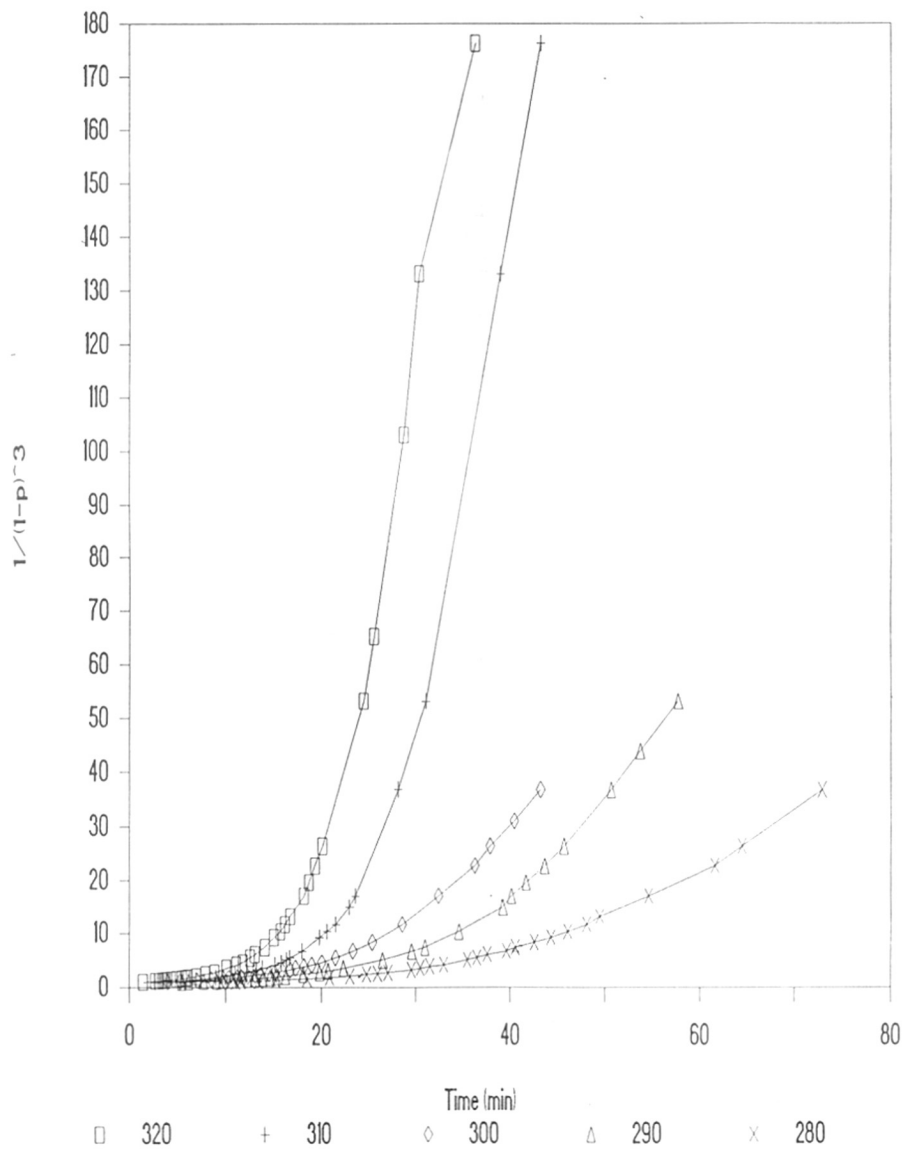


FIGURE 4.5 THIRD ORDER RATE LAW PLOT ILLUSTRATING THE EFFECT OF TEMPERATURE FOR HRT/50:50:100 REACTION

TABLE - 4.3

RESULTS OF KINETICS OF HRT COPOLYESTERIFICATION

Comp. H:R	Temp/°C	1/(1-p)	Indu- ction time minutes	k_D c^{-1}, t^{-1} *	k_O c^{-1}, t^{-1} *
100:0	320	2.5	4.3	0.00645	0.00456
	310	2.3	5.3	0.00543	0.00273
	300	2.2	6.7	0.00517	0.00302
	290	2.0	8.4	0.00405	0.00232
	280	1.8	14.7	0.00220	-
	270	1.3	18.2	0.00153	-
90:10	320	2.8	1.8	0.00870	0.01000
	310	2.9	4.8	0.00780	0.00760
	300	2.1	6.1	0.00480	0.00420
	290	-	-	-	-
80:20	320	4.3	2.1	0.00970	0.01700
	310	3.7	3.3	0.00910	0.01300
	300	2.9	4.7	0.00650	0.00750
	290	2.3	7.9	0.00430	0.00440
75:25	320	3.1	1.9	0.00880	0.01100
	310	4.3	3.7	0.00810	0.01500
	300	3.1	6.4	0.00580	0.00740
	290	2.1	7.2	0.00390	0.00510
70:30	320	5.6	1.5	0.01200	0.03000
	310	4.6	2.9	0.01000	0.01800
	300	3.7	5.0	0.00770	0.01100
	290	3.7	7.0	0.00590	0.00860
60:40	320	5.6	1.3	0.01100	0.02900
	310	4.3	2.9	0.00900	0.01800
	300	5.6	4.7	0.00870	0.01900
	290	2.6	5.5	0.00490	0.00670
	280	1.8	7.5	0.00320	-

Table continued on the next page ----->

•••• TABLE - 4.3 CONTINUED

Comp. H:R	Temp/°C	1/(1-p)	Indu- ction time minutes	k_D $c^{-1}.t^{-1}$ *	k_O $c^{-1}.t^{-1}$ *
55:45	320	5.1	1.3	0.01100	0.02900
	310	5.6	4.3	0.00780	0.02200
	300	4.0	5.2	0.00660	0.01200
	290	2.9	8.1	0.00440	0.00840
50:50	320	5.1	1.4	0.01260	0.03200
	310	5.6	2.5	0.00923	0.02550
	300	3.3	3.8	0.00753	0.01220
	290	3.7	5.1	0.00617	0.01150
	280	3.3	9.1	0.00498	0.00710
40:60	320	4.6	3.7	0.00690	0.02200
	310	5.1	3.9	0.00720	0.01700
	300	5.1	5.1	0.00590	0.01700
	290	3.5	10.3	0.00500	0.00950
30:70	320	5.1	1.9	0.01000	0.02700
	310	4.3	3.4	0.00760	0.01600
	300	4.6	5.6	0.00680	0.01500
	290	3.1	8.2	0.00400	0.00730
20:80	320	5.1	2.2	0.00930	0.02300
	310	4.0	4.3	0.00860	0.01800
	300	5.1	6.7	0.00660	0.01600
	290	3.1	8.4	0.00420	0.00750
10:90	320	4.3	5.1	0.00830	0.02400
	310	4.7	6.4	0.00848	0.01900
	300	4.7	8.0	0.00590	0.01500
	290	2.3	7.0	0.00410	0.00330

* k_D = rate constant of dimerisation reaction* k_O = rate constant of oligomerisation reaction

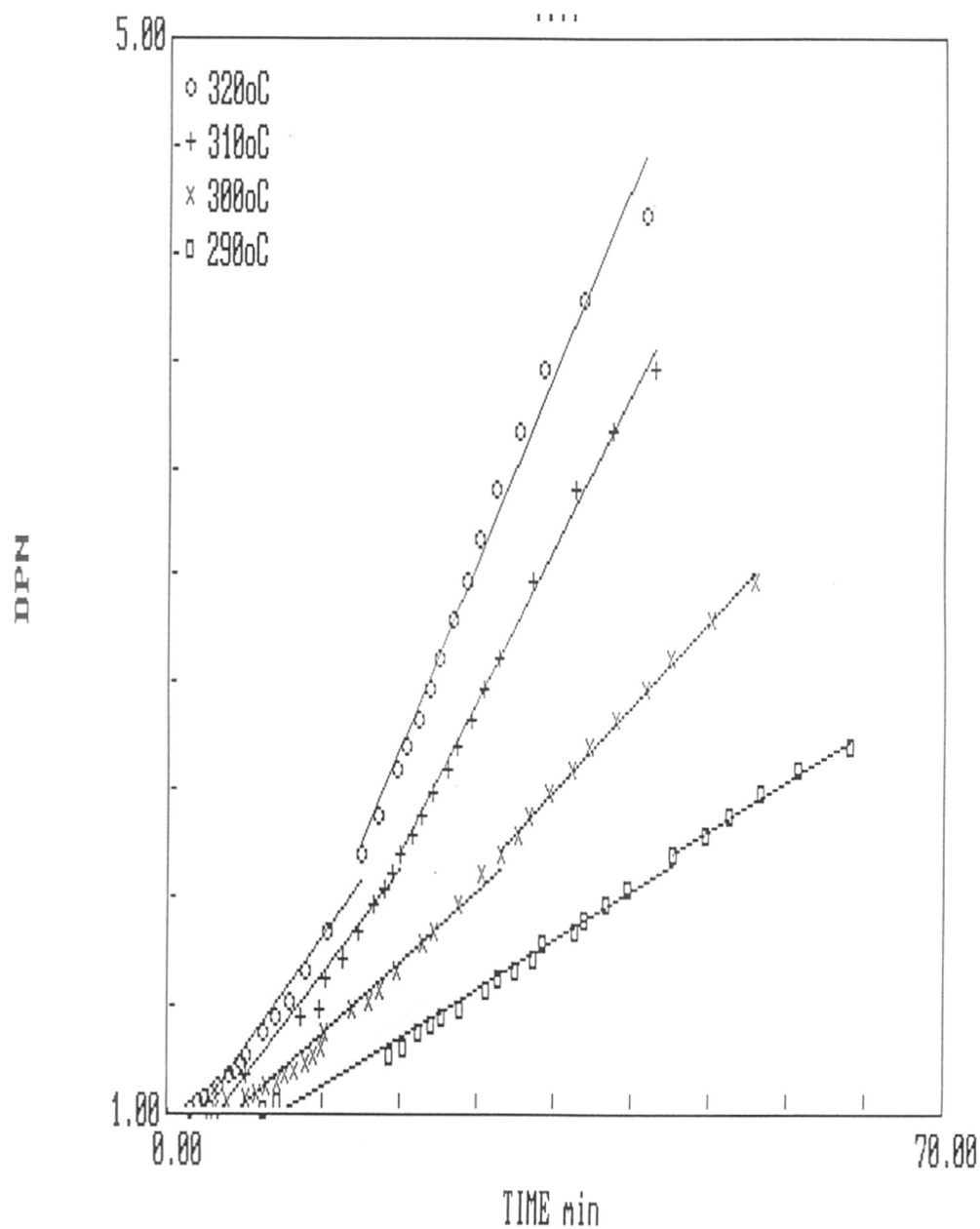


FIGURE 4.6 SECOND ORDER RATE LAW PLOT ILLUSTRATING THE EFFECT OF TEMPERATURE FOR HRT/80:20:100 REACTION

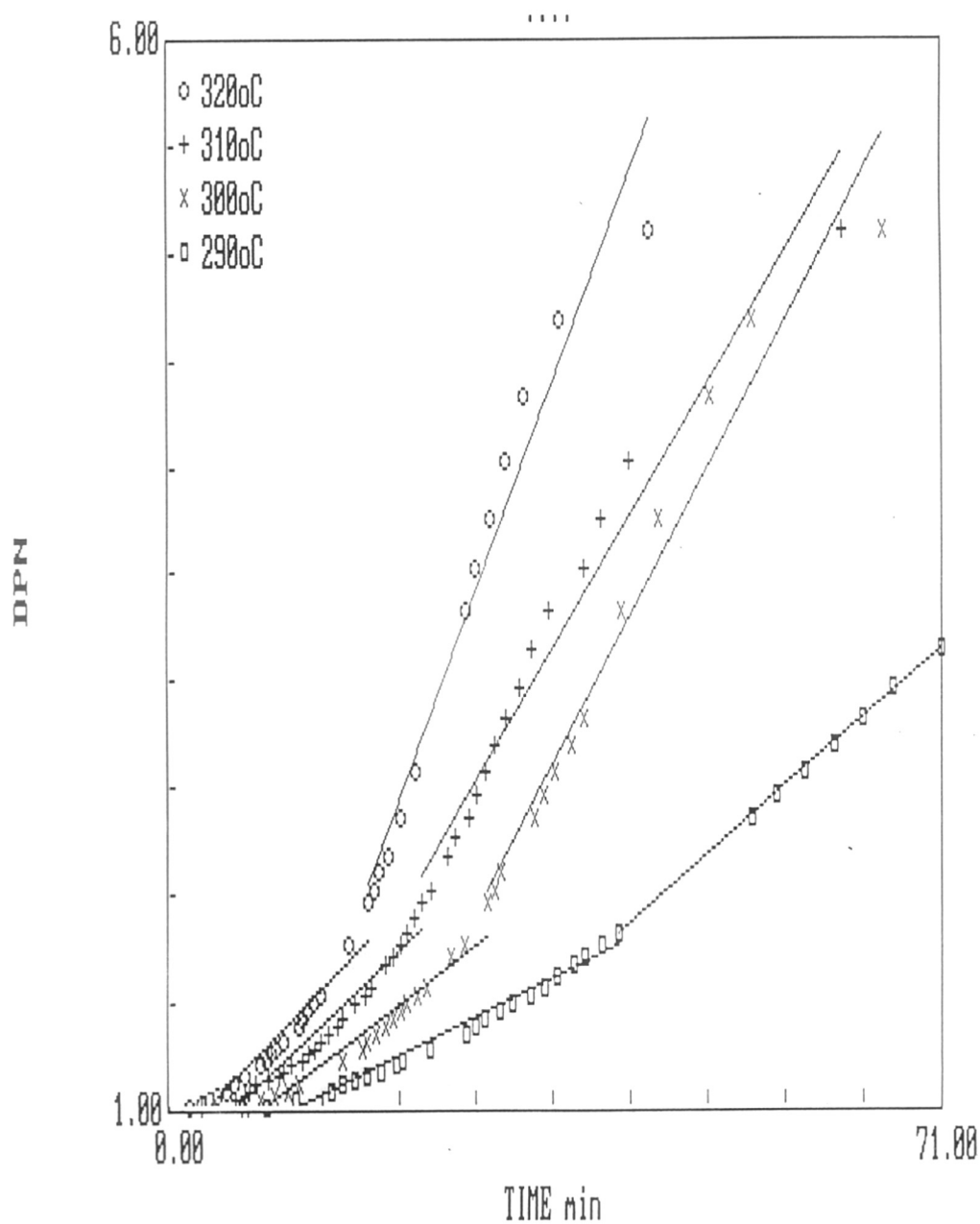


FIGURE 4.7 SECOND ORDER RATE LAW PLOT ILLUSTRATING THE EFFECT OF TEMPERATURE FOR HRT/20:80:100 REACTION

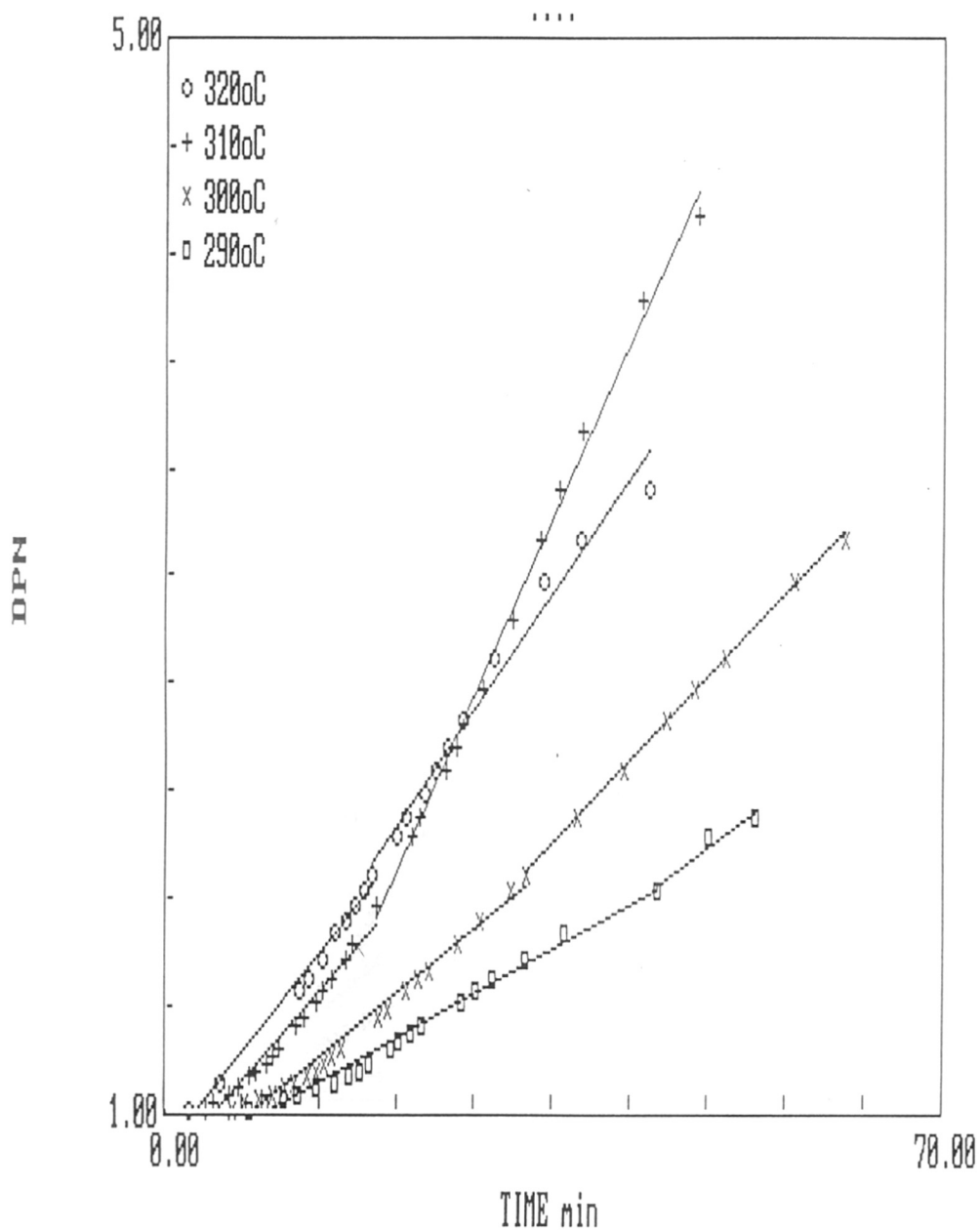


FIGURE 4.8 SECOND ORDER RATE LAW PLOT ILLUSTRATING THE EFFECT OF TEMPERATURE FOR HRT/75:25:100 REACTION

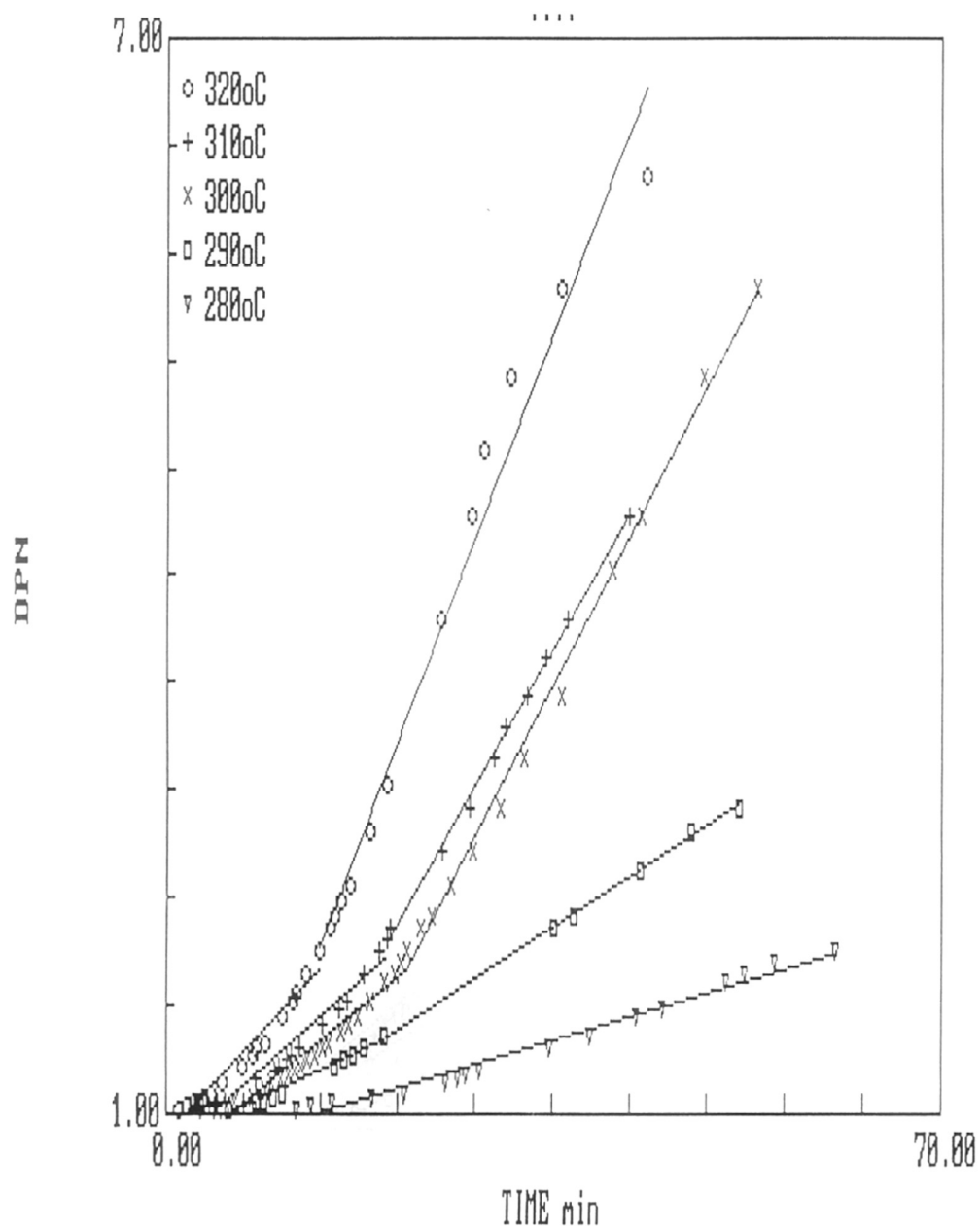


FIGURE 4.9 SECOND ORDER RATE LAW PLOT ILLUSTRATING THE EFFECT OF TEMPERATURE FOR HRT/60:40:100 REACTION

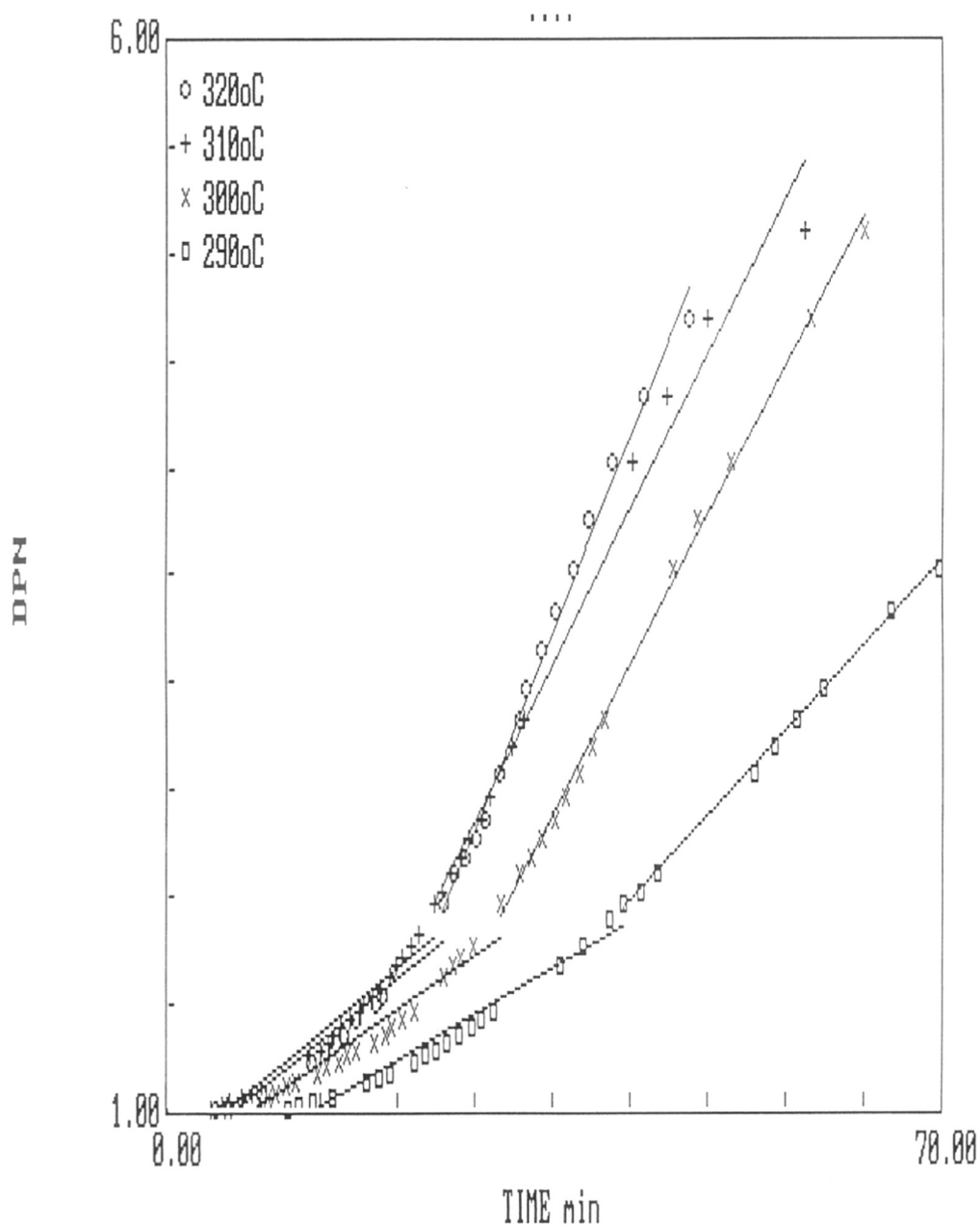


FIGURE 4.10 SECOND ORDER RATE LAW PLOT ILLUSTRATING THE EFFECT OF TEMPERATURE FOR HRT/40:60:100 REACTION

the slope of the graph after the break indicates the possibility of different rate behavior in the two regions. Separate kinetic parameters therefore are determined corresponding to both the regions.

The effect of temperature was studied from the Arrhenius plots, where in log rate constants were plotted against inverse temperature. **Figures 4.11 and 4.12** represent Arrhenius plot of HRT/50:50:100 first (before the break) and second (after the break) stage reaction respectively. The enthalpy of activation was calculated (**Table 4.4**) from the slope of the plot. The results in **Table 4.3** indicate that the oligomerisation (second stage) reaction rates are faster despite the high enthalpy of activation corresponding to this region. This is a consequence of simultaneous increase in the entropy of activation which leads to an overall decrease in the free energy of activation. Such entropy driven reactions are also reported by Devaux in the kinetic study of bisphenol-A polycarbonate-poly(butylene terephthalate) transesterification.²³ The rate increases gradually with increase in the concentration of RDA and vice-a-versa. In Section 3.3.2 it is seen that for HT/100:100 i.e. without the addition of RDA, rate of oligomerisation reaction is slower than the rate of dimerisation reaction due to diffusional constraints. Same was true for the copolyester containing 10 mole % of RDA. With further addition of RDA the trend started to reverse and at 80 and 90 mole% of RDA it resembles very much to RT system. **Figure 4.13** shows the effect of copolyesterification on reaction kinetics of HT and RT systems.

4.3 HIT Copolyesterification

The formation of HIT copolyester from hydroquinone diacetate (HQDA), isophthalic acid (IPA) and terephthalic acid (TPA) takes place by way of two competing reactions as follows:



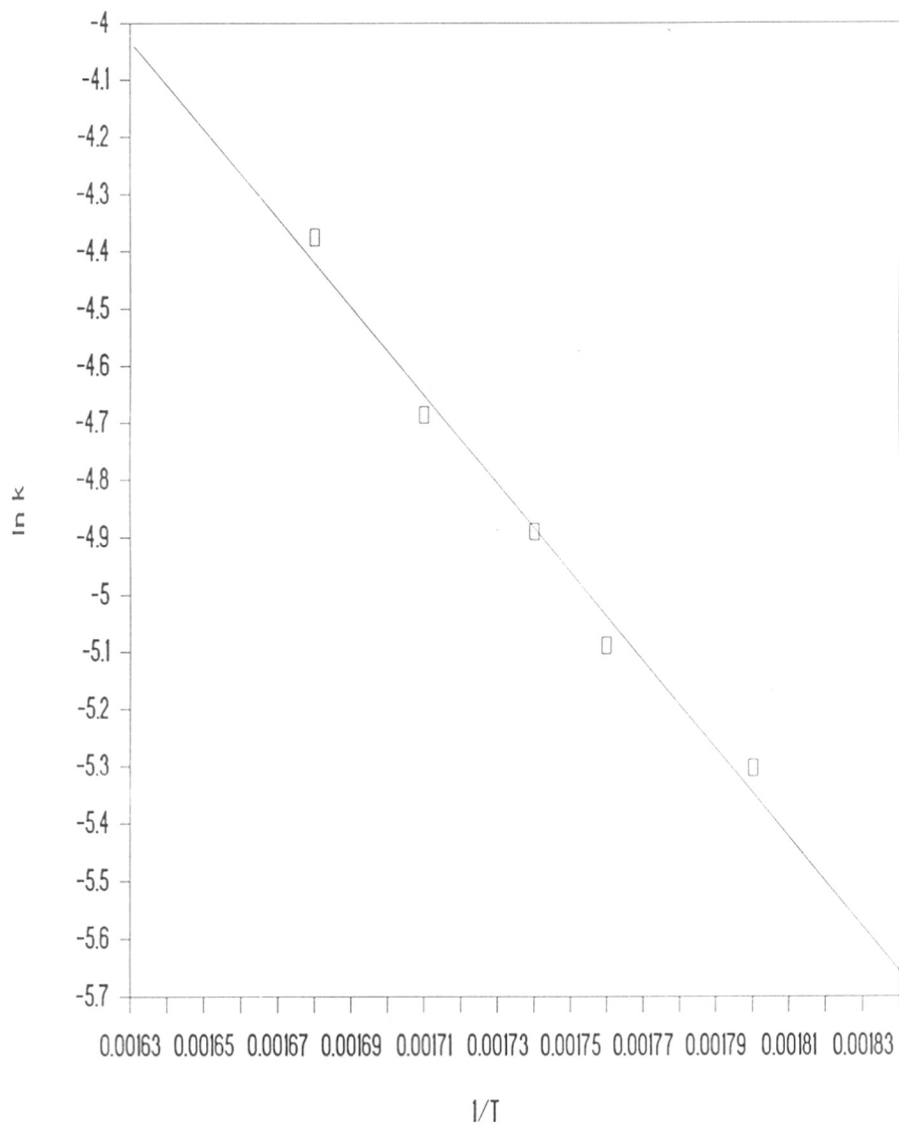


FIGURE 4.11 ARRHENIUS PLOT FOR HRT/50:50:100 REACTIONS PRIOR TO THE BREAK

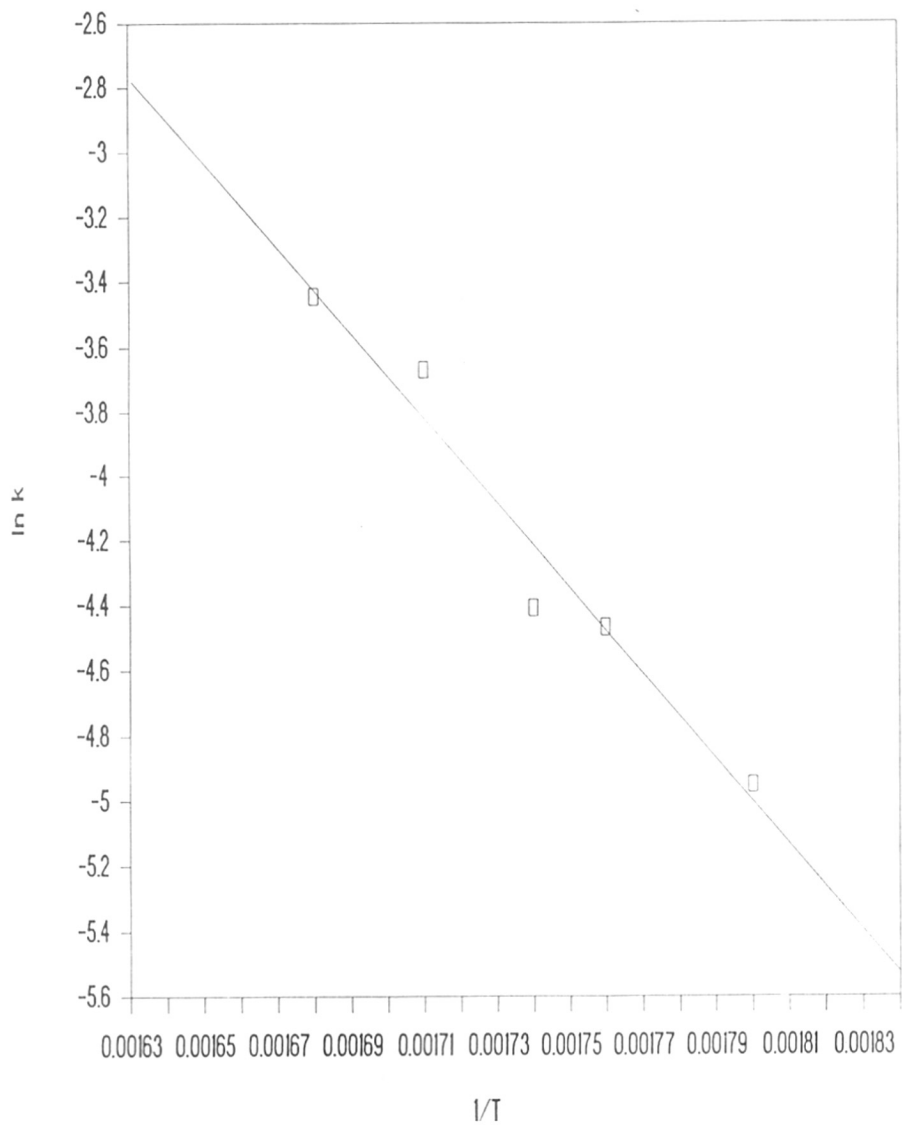


FIGURE 4.12 ARRHENIUS PLOT FOR HRT/50:50:100 REACTIONS AFTER THE BREAK

TABLE - 4.4

ACTIVATION ENERGIES (AE) FOR HRT COPOLYESTERIFICATION
PRIOR TO (AE_D) AND AFTER THE BREAK (AE_O)

H:R	AE _D	AE _O	ln A _D	ln A _O	ln A _O /A _D
10:90	16.18	51.68	08.83	39.89	4.51
20:80	18.95	24.65	11.34	17.03	1.50
30:70	20.50	28.73	12.66	20.52	16.2
40:60	7.39	17.83	1.25	11.20	8.96
50:50	15.46	26.28	8.58	18.65	2.17
55:45	21.22	31.81	13.32	23.25	1.74
60:40	21.20	36.92	10.29	27.50	2.67
70:30	17.47	31.57	22.99	20.52	0.89
80:20	19.98	33.55	12.25	24.21	1.97
90:10	19.82	28.91	11.97	19.73	1.65

A_D = Frequency Factor For Dimerisation Reaction

A_O = Frequency Factor For Oligomerisation Reaction

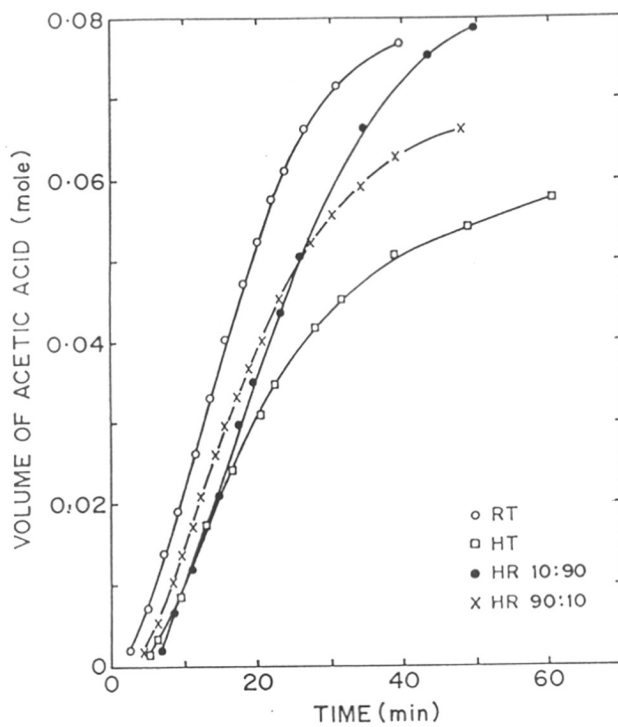
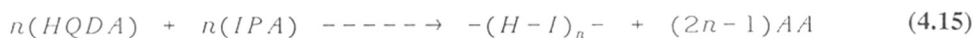


FIGURE 4.13 EFFECT OF COPOLYESTERIFICATION ON REACTION KINETICS



$$[\text{A}] = a_0 - x; [\text{B}] = b_0 - y; [\text{C}] = c_0 - z$$

where AA = acetic acid; [A] = concentration of HQDA at time 't'; [B] = concentration of TPA at time 't'; [C] = concentration of IPA at time 't' and a_0 , b_0 and c_0 denote the initial concentration of HQDA, TPA and IPA respectively. k_1 , k_2 , y , z denote the kinetic constants, moles of the monomers consumed respectively. x denotes the total moles of acetic acid (AA) produced through both reaction channels.

Kinetic treatment of the above reactions reduces to the same equation as was obtained for HRT system. (Equation 4.13) Therefore, for HIT system we get

$$\int_{[B]}^{[B_0]} \frac{dB}{[B]^2 + f_2[B]^{1-k_r}} = \int_0^t k_1 dt$$

Where,

$$f_2 = (a_0 - b_0) (b_0)^{(-k_r)} \quad (4.16)$$

From the study of homopolyesterification kinetics of HT and HI it was observed that the reactivity ratio $k_r \sim 1$ and hence $k_1 = k_2$ (Table 4.2). Then,

$$f_2 = \frac{(a_0 - b_0)}{b_0} = \frac{a_0}{b_0} - 1 \quad (4.17)$$

therefore, the denominator of equation (4.13) becomes

$$[B]^2 + \left(\frac{a_0}{b_0} - 1 \right) [B]^2 \quad (4.18)$$

$$[B]^2 \left(1 + \frac{\alpha_0}{b_0} - 1 \right) \quad (4.19)$$

$$\frac{\alpha_0}{b_0} [B]^2 \quad (4.20)$$

Substituting above value in the denominator of equation (4.13), it changes to the following

$$\int_{[B]}^{[B_0]} \frac{1}{\frac{\alpha_0}{b_0} [B]^2} d[B] \quad (4.21)$$

$$= \frac{\alpha_0}{b_0} \int_{[B]}^{[B_0]} \frac{1}{[B]^2} d[B] \quad (4.22)$$

$$= \frac{b_0}{\alpha_0} \int_{[B_0]}^{[B]} \frac{1}{[B]^2} d[B] \quad (4.23)$$

$$-\frac{b_0}{\alpha_0} \frac{1}{[B]} = k_1 t \quad (4.24)$$

$$-\frac{b_0}{\alpha_0} \frac{1}{(b_0 - \gamma)} = k_1 t \quad (4.25)$$

$$-\frac{b_0}{\alpha_0} \frac{1}{b_0 \left(1 - \frac{\gamma}{b_0} \right)} = k_1 t + \text{const.} \quad (4.26)$$

$$- \frac{1}{\alpha_0 \left(1 - \frac{\gamma}{b_0}\right)} = k_1 t + \text{const} \quad (4.27)$$

$$- \frac{1}{1 - \frac{\gamma}{b_0}} = \alpha_0 k_1 t + \text{const} \quad (4.28)$$

$$\frac{1}{1 - \rho} = \alpha_0 k_1 t + \text{const} \quad (4.29)$$

The above equation is nothing but simple second order rate equation. This proves that the three component system comprising of H, T and I can be defined kinetically by conventional second order rate laws.

This copolyesterification system deals with the preparation of wholly aromatic rigid rod poly(1,4-carboxy phenylene carboxy-1,4-oxy phenylene oxy-1,3-carboxy phenylene) by acidolysis between hydroquinone diacetate (HQDA), isophthalic acid (IPA) and terephthalic acid (TPA) (**Figure 4.14**). HQDA is molten while TPA and IPA are present as solid particles (30um) at the temperature range over which kinetics were investigated. HQDA could either react with TPA to form rigid rod non-melting poly(1,4-oxy phenylene oxy-1,4-carboxy phenylene) or with IPA to form again non-melting poly(1,4-oxy phenylene oxy-1,3-carboxy phenylene) at reaction temperature. Subsequent copolymerisation reaction will incorporate all the monomer units in the copolyester chain. Thus, over the entire composition range, the reaction is initially a slurry consisting of TPA and IPA crystals in the molten HQDA. It changes to solid state polycondensation due to high melting intermediates. This is true of all the reactions even in the polyester containing highest concentration (50 mole %) of bent monomer

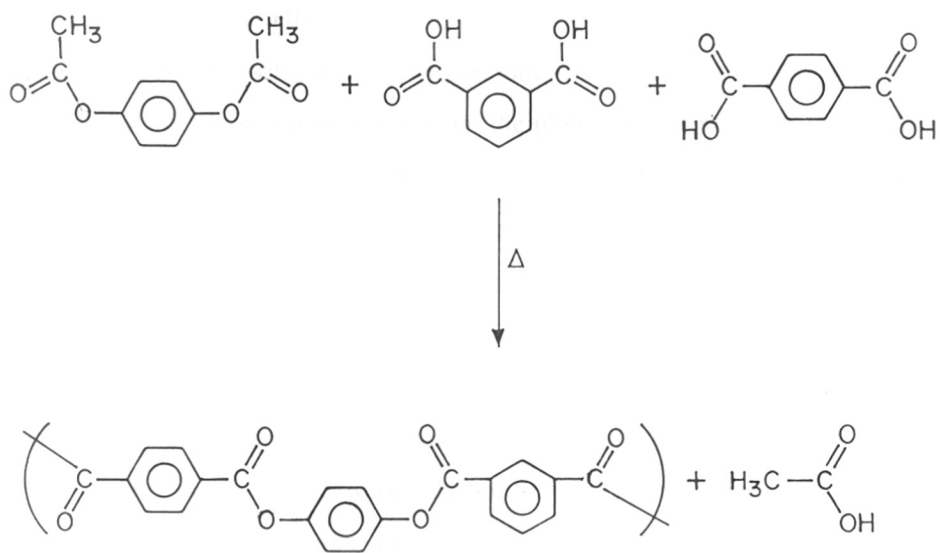


FIGURE 4.14 REACTION SCHEME FOR THE SYNTHESIS OF HIT COPOLYESTER

IPA. In all these reactions, the product is a hard intractable solid insoluble in all common solvents at the end of the reaction. Experimental kinetic data of volume of acetic acid recorded with time for HIT/100:50:50 reaction is presented in **Table 4.5**.

The kinetic treatment implies that copolyesterification reaction can be treated as progressing through two parallel second order reactions. Second order plots showing the effect of temperature on HIT/100:50:50; HIT/100:45:55 and HIT/100:10:90 reactions are shown in **Figures 4.15 - 4.17** respectively. The rate constants are calculated (**Table 4.6**) from the slope of these plots. It is observed from the plots that second order kinetic behavior is followed quite generally at all reaction temperatures over the entire composition range. It is also obvious from these figures that these reactions do not reach very high conversion under normal pressure. This is because both the diacid monomers under consideration are high melting and intractable. Also, sublimation and thermal degradation problems limit the reaction temperature to below 320° C. System is heterogeneous even after dimerisation. As a result concentration of reactive acid functional groups is not enough for further reaction. This problem is more pronounced at lower reaction temperatures. Since the extent of reaction is low compared to the other three component system (HRT) the breaks are not seen in the plots. But it can be predicted from the reaction medium that the rates will decrease if the reaction proceeds after dimerisation as was the case in HT and HI homopolyesterification. The rate law plots are characterised by the presence of induction period which increases with decrease in temperature.

Variation of rate constant with temperature was studied from the Arrhenius plots (**Figure 4.18**). Energy of activation was calculated (**Table 4.7**) from the slope of these plots. Rate constants vary with temperature but are independent of concentration of monomers. The effect of copolyesterification on the kinetics of HT and HI systems is shown in **Figure 4.19**.

TABLE - 4.5

HIGH TEMPERATURE POLY-TRANSESTERIFICATION OF HYDROQUINONE DIACETATE [HQDA], ISOPHTHALIC ACID [IPA] AND TEREPHTHALIC ACID [TPA] WITHOUT CATALYST AT 320.0°C.

Reaction time	Volume of side product	Fractional conversion	Degree of polymerisation
[Minutes]	mL	[P]	{1/(1-P)}
3.1	0.1	0.0175	1.0178
4.5	0.2	0.035	1.0362
5.6	0.3	0.0524	1.0554
6.5	0.4	0.0699	1.0752
7.6	0.5	0.0874	1.0958
9.9	0.8	0.1399	1.1626
11.6	1.0	0.1748	1.2119
12.3	1.1	0.1923	1.2381
13.3	1.2	0.2098	1.2655
14.1	1.3	0.2273	1.2941
15.0	1.4	0.2448	1.3241
15.9	1.5	0.2622	1.3555
16.9	1.6	0.2797	1.3884
17.8	1.7	0.2972	1.4229
18.5	1.8	0.3147	1.4592
19.6	1.9	0.3322	1.4974
20.9	2.0	0.3497	1.5376
21.8	2.1	0.3671	1.5801
23.5	2.2	0.3846	1.6250
24.2	2.3	0.4021	1.6725
25.8	2.4	0.4196	1.7229
27.3	2.5	0.4371	1.7764
29.3	2.6	0.4545	1.8333
31.2	2.7	0.4720	1.8940
33.7	2.8	0.4895	1.9589

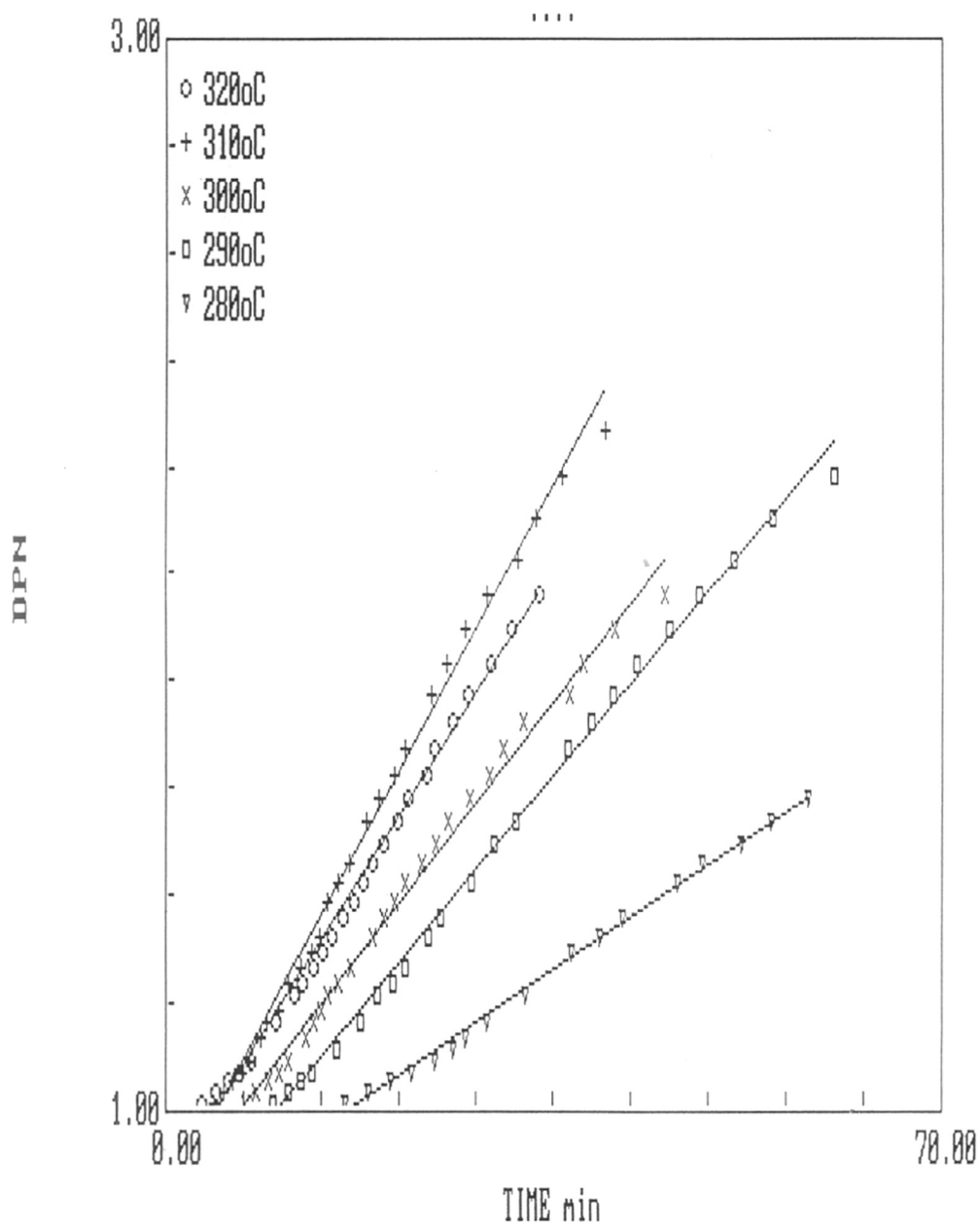


FIGURE 4.15 SECOND ORDER RATE LAW PLOT ILLUSTRATING THE EFFECT OF TEMPERATURE FOR HIT/100:50:50 REACTION

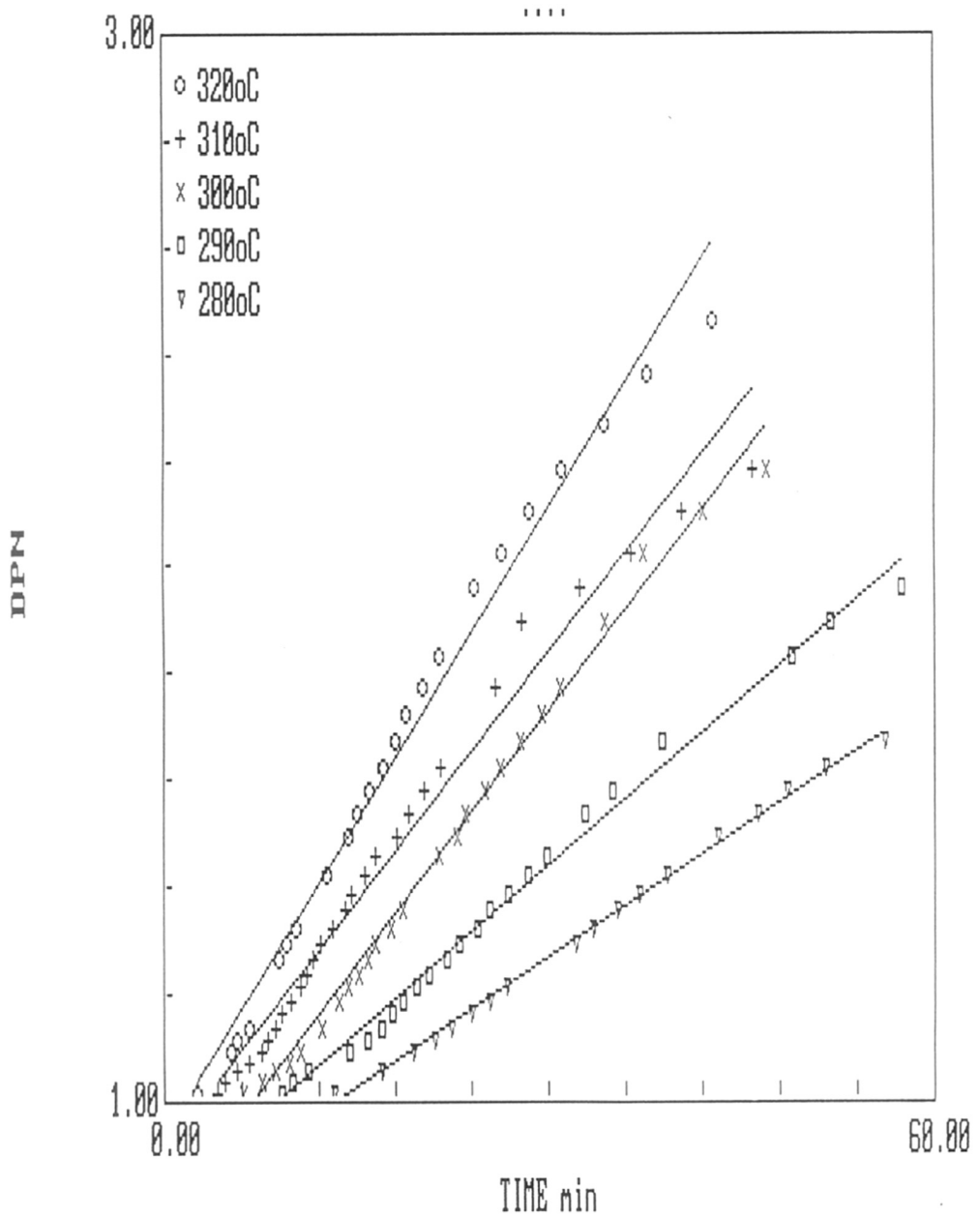


FIGURE 4.16 SECOND ORDER RATE LAW PLOT ILLUSTRATING THE EFFECT OF TEMPERATURE FOR HIT/100:45:55 REACTION

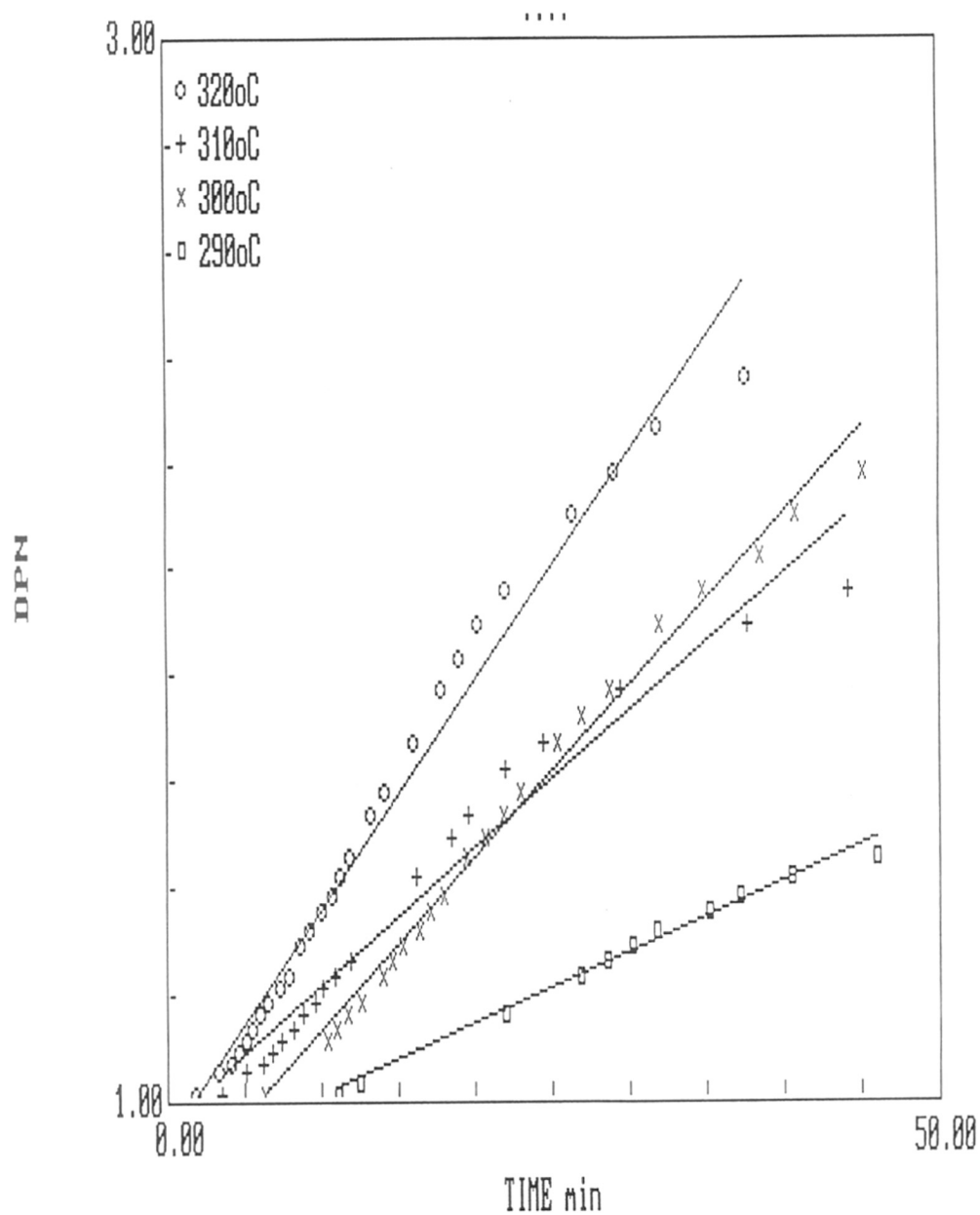


FIGURE 4.17 SECOND ORDER RATE LAW PLOT ILLUSTRATING THE EFFECT OF TEMPERATURE FOR HIT/100:10:90 REACTION

TABLE 4.6
RESULTS OF KINETICS OF HIT COPOLYESTERIFICATION

Composition	Temp/°C	1/(1-p)	Induction time	k
I:T			minutes	c ⁻¹ .t ⁻¹
50:50	320	1.9	2.7	0.00548
	310	2.2	4.2	0.00636
	300	1.9	7.0	0.00445
	290	2.1	9.2	0.00411
	280	1.5	14.3	0.00235
45:55	320	2.4	2.4	0.00650
	310	2.1	4.1	0.00515
	300	2.1	6.2	0.00526
	290	1.9	8.3	0.00348
	280	1.6	12.0	0.00270
40:60	320	2.1	1.9	0.00461
	310	1.9	4.0	0.00421
	300	1.7	6.5	0.00296
	290	1.5	8.6	0.00258
35:65	320	1.4	3.0	0.00315
	310	1.5	4.7	0.00276
	300	2.1	6.0	0.00458
	290	1.5	8.6	0.00246
30:70	320	1.6	2.7	0.00436
	310	1.6	4.7	0.00291
	300	1.5	6.9	0.00268
25:75	320	1.8	3.4	0.00421
	310	1.2	5.4	0.00531
	300	1.2	6.0	0.00510
	290	1.7	9.3	0.00311
20:80	320	1.9	2.0	0.00535
	310	2.1	3.4	0.00588
	300	2.1	5.2	0.00520
	290	1.9	6.9	0.00400
10:90	320	2.3	2.0	0.00715
	310	1.9	3.5	0.00431
	300	2.1	6.2	0.00538
	290	1.4	9.5	0.00223

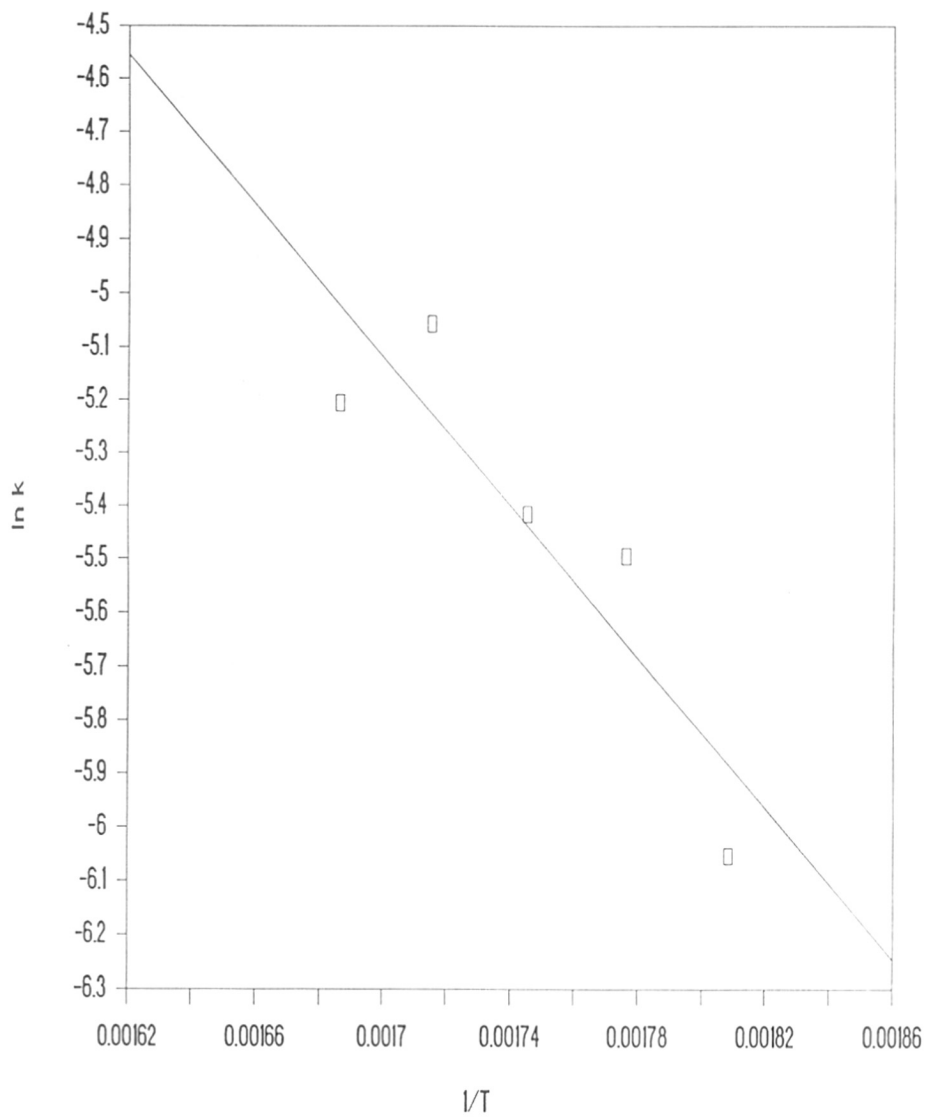


FIGURE 4.18 ARRHENIUS PLOT FOR HIT/100:50:50 REACTIONS.

TABLE - 4.7
ACTIVATION ENERGIES (AE) FOR HIT COPOLYESTERIFICATION

I:T	AE kCal/mole	ln A
50:50	14.10	6.86
45:55	14.64	7.30
40:60	15.44	7.64
35:65	10.86	5.29
30:70	16.23	8.14
25:75	5.93	0.32
20:80	6.85	0.61
10:90	23.01	14.30

A = Frequency Factor

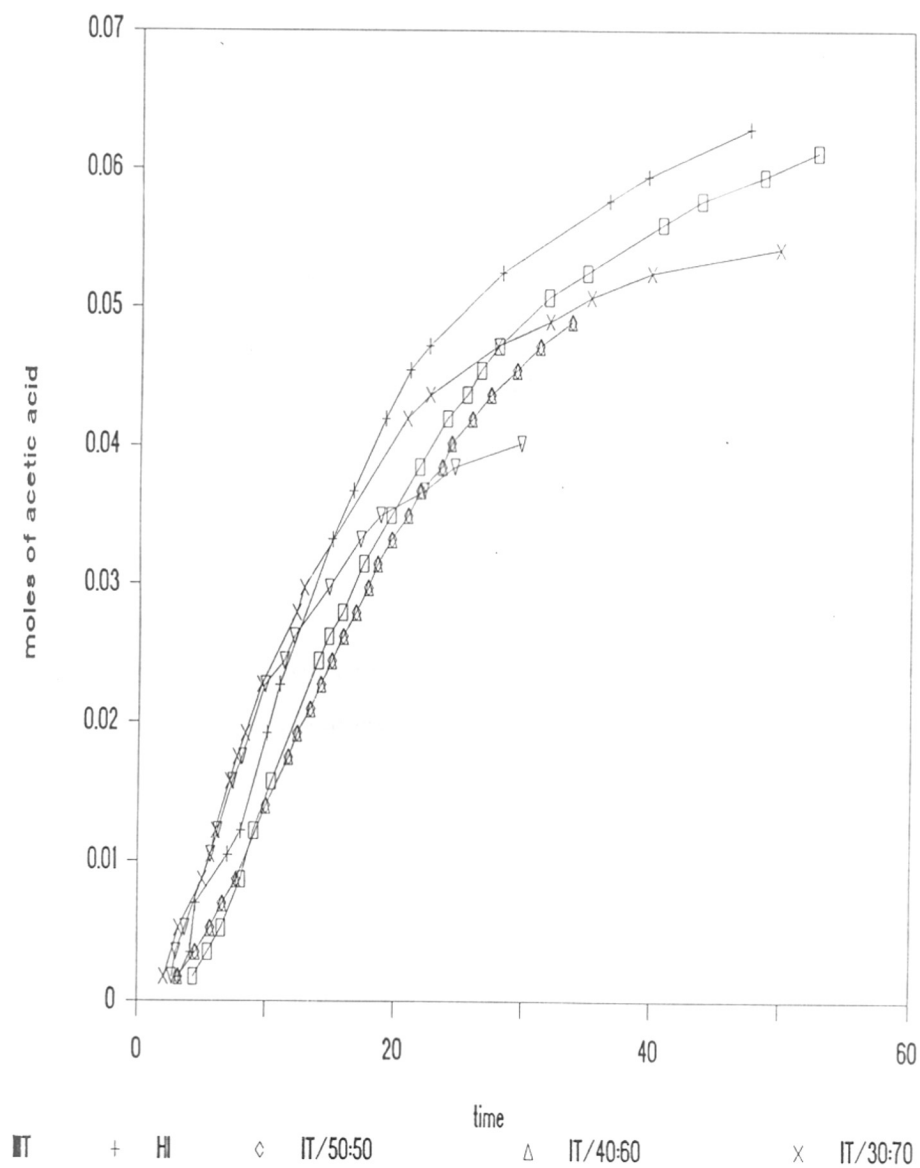


FIGURE 4.19 EFFECT OF COPOLYESTERIFICATION ON REACTION KINETICS

4.4 CHARACTERISATION

The product formed at the end of the reaction was crushed and purified from starting monomers for further characterisation. 5-10 mg of each sample was run on DSC and first heating scans were recorded from 50 to 450° C at the rate of 20° C per minute.

The melting endotherms in **Figure 4.20** show the effect of reaction temperature on thermal behaviour of HRT/50:50:100 copolyesters. First order transition is noted in the range of 350 to 370° C during first heating cycle. As the synthesis temperature is increased the degree of polymerisation (DP) also increased and therefore melting peak maxima increases from 350 to 370° C. Peak width decreased with increase in the reaction temperature suggesting narrow crystal size distribution at higher temperature. Polyesters were found to degrade above 450° C. This polyester shows only a glass transition at 155° C in the second heating scan.

First heating cycles of HRT polyesters synthesised at 320° C but varying in composition are shown in **Figures 4.21-4.23**. It is obvious from these DSC traces that their thermal behavior is very sensitive to the copolyester composition. All polyesters in **Figure 4.21** show a broad hump and a cold crystallisation peak around 150° C in addition to multiple endotherms in the region of 200-300° C. The product, a molten mass, was poured out from the reactor after the reaction which may prevent equilibrium crystallisation. As a result a cold crystallisation peak appears in the first heating cycle. The nature of this peak is dependent on scanning rate. The presence of multiple peaks indicate the possibility of morphological reorganisation of lower melting, less perfect crystallites to better organised structures at higher temperatures. It was observed that if the scanning rate is decreased to 5° C per minute, a well developed T_g around 150° C and a single endotherm around 259° C appears in the second heating scan of all polyesters. At decreased rates of cooling the molecules get sufficient time to undergo equilibrium crystallisation. This is also the reason for higher heat of crystallisation

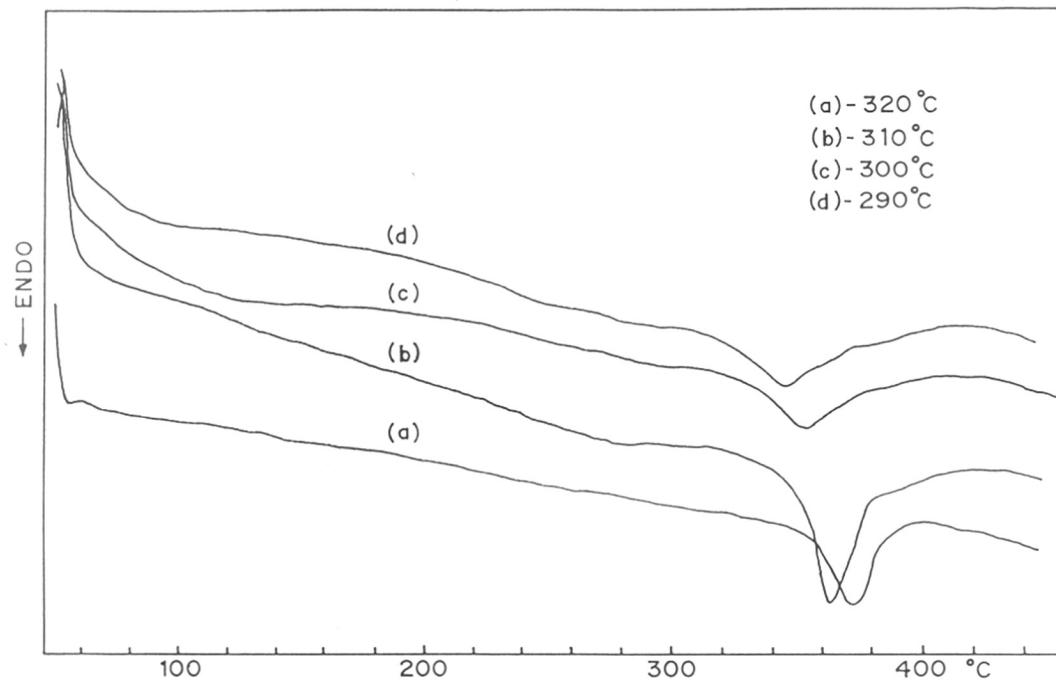


FIGURE 4.20 FIRST HEATING DSC TRACES ILLUSTRATING THE EFFECT OF REACTION TEMPERATURE ON HRT/50:50:100 COPOLYESTER

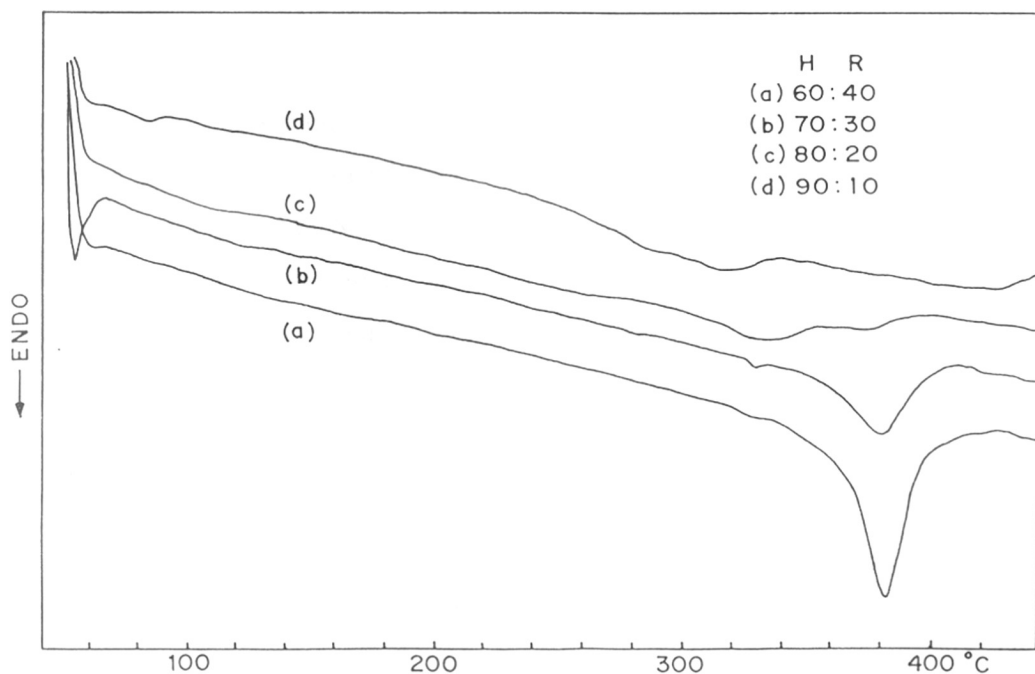


FIGURE 4.21 FIRST HEATING DSC TRACES ILLUSTRATING THE EFFECT OF COMPOSITION ON THE HRT COPOLYESTERS SYNTHESISED AT 320°C

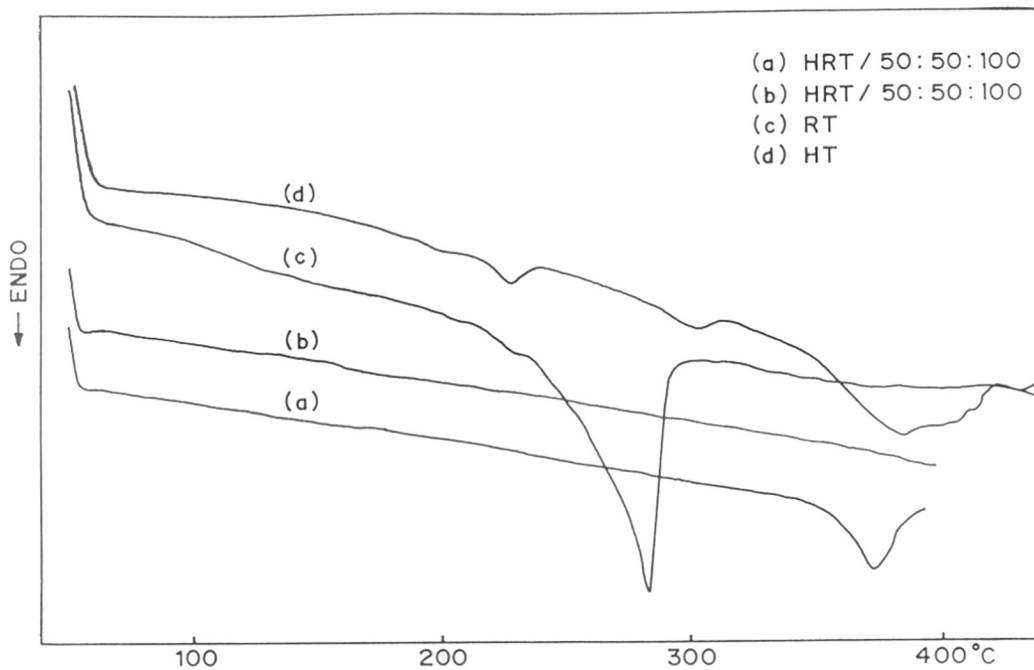


FIGURE 4.22 COMPARISON OF DSC TRACES OF (a)-HT; (b)-RT AND HRT/50:50:100 [(c)-FIRST HEATING; (d)-SECOND HEATING] POLYESTERS SYNTHESISED AT 320°C

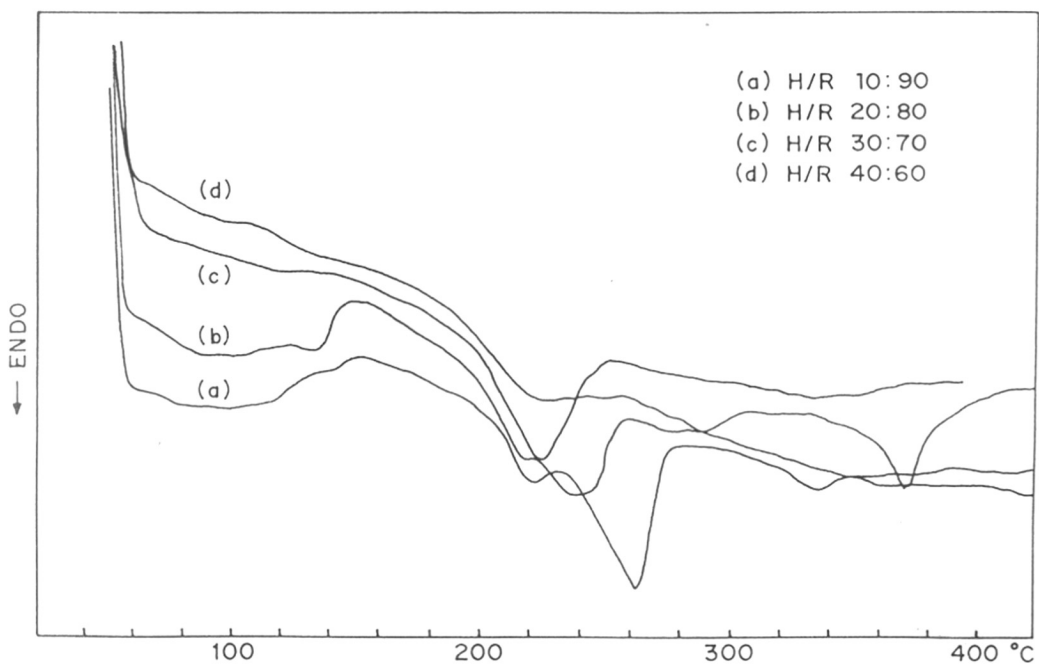


FIGURE 4.23 FIRST HEATING DSC TRACES ILLUSTRATING THE EFFECT OF COMPOSITION ON THE HRT COPOLYESTERS SYNTHESISED AT 320°C

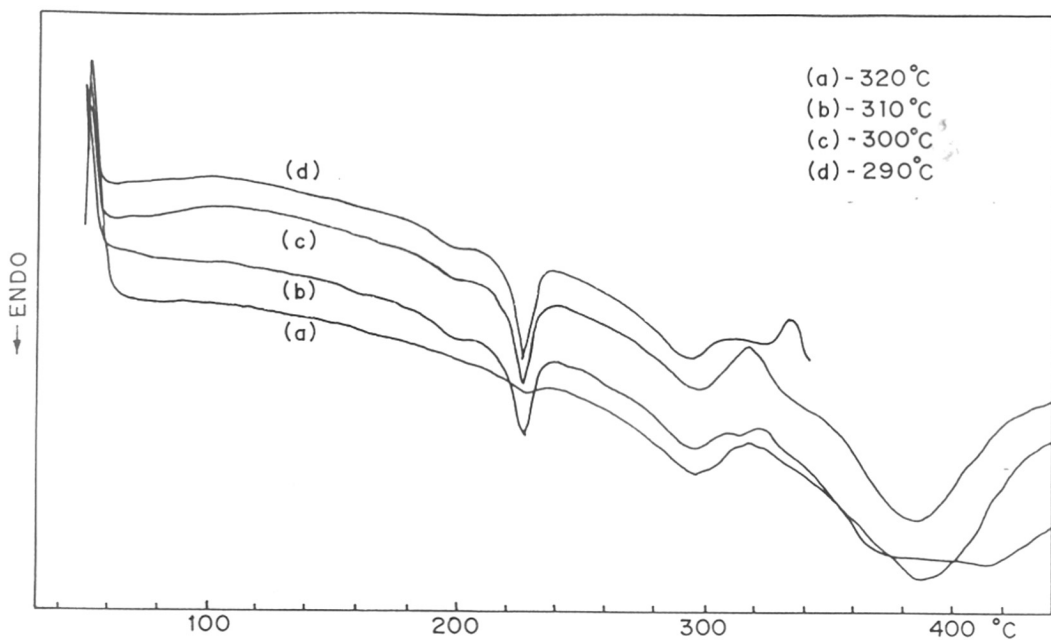


FIGURE 4.24 FIRST HEATING DSC TRACES ILLUSTRATING THE EFFECT OF REACTION TEMPERATURE ON HIT/100:50:50 COPOLYESTER

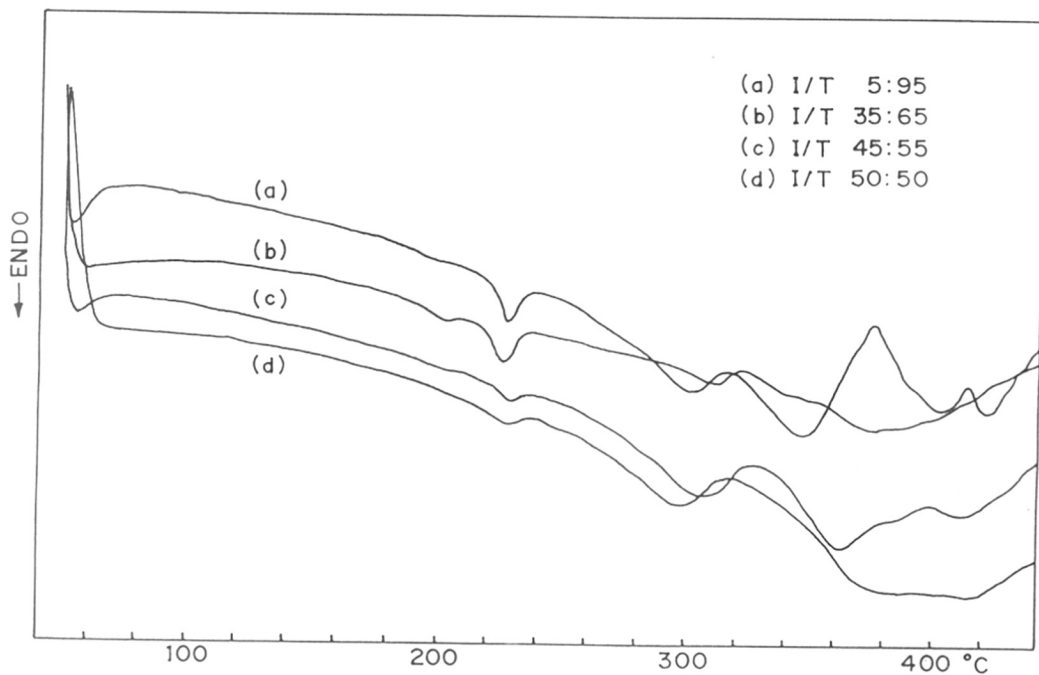


FIGURE 4.25 FIRST HEATING DSC TRACES ILLUSTRATING THE EFFECT OF COMPOSITION ON HIT COPOLYESTERS SYNTHESISED AT 320°C

of composition on the thermal treatment of the polyesters synthesised at 320° C is presented in **Figure 4.25**. First order transitions below 300° C are noted in the cooling and second heating scans as well. These mesophasic transitions were further confirmed from optical analysis using polarising microscope from the birefringence under crossed polariser and were assigned to the chloroform soluble oligomeric fraction of copolyesters. Similar observations were recorded in HT and HI systems as mentioned in Section 3.3.2 and Section 3.3.3 respectively.

In general, polyesters synthesised at different temperature show a cold crystallisation peak, T_g , exotherms and endotherms; whose occurrence, position and energies of transition are dependent on copolymer composition. The effect of comonomer composition on the melting temperature is seen clearly from the phase diagrams in which mole% of monomer is plotted against T_m . The composition curve goes through a minimum for RDA around 60-70 mole% at all the four temperatures. (**Figure 4.26 and 4.27**.)

In optical observations under crossed polarisers no birefringence was observed. RDA copolyesters are known to be shear sensitive. Therefore, the polyesters were studied under the effect of shear and time. It is reported that the copolyester TPA/4-HBA/RDA loses liquid crystallinity¹⁴ when the concentration of TPA/RDA units exceed 33%. It is also reported by Lenz et.al.¹² that the chloro hydroquinone-terephthalic acid copolyesters retain liquid crystallinity till 60 mole% resorcinol. However, no textures could be observed for the HRT polyesters in the present study. It is found¹⁷ that 4-HBA/HQDA/IPA polyesters are liquid crystalline if HQDA/IPA units are less than 67 mole%. HIT copolyesters in the present study showed fan shaped and schlieren texture corresponding to smectic and nematic phases in the oligomeric product. High temperature transition could not be studied on the polarising microscope.

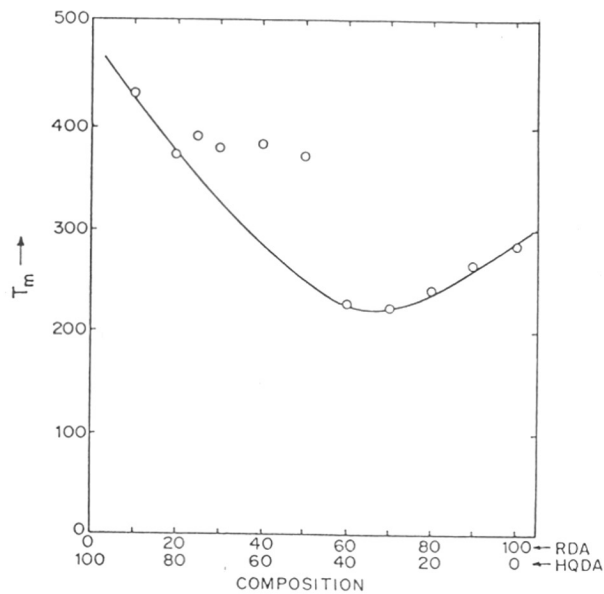


FIGURE 4.26 A PLOT OF COMPOSITION VERSUS MELTING TEMPERATURE OF HRT COPOLYESTERS SYNTHESISED AT 320°C

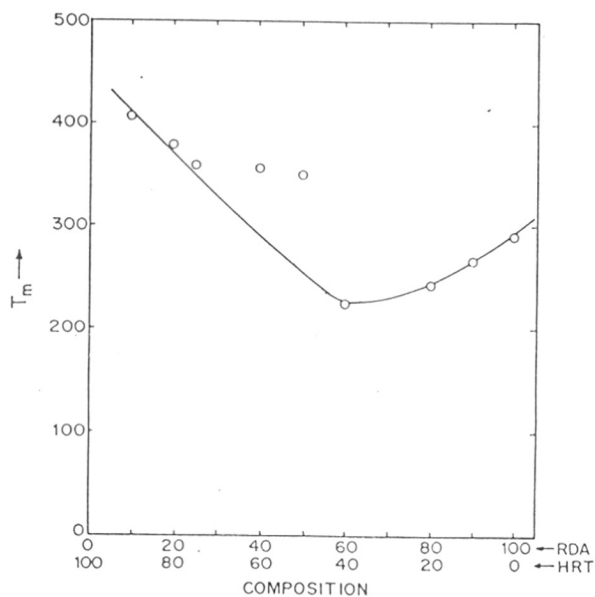


FIGURE 4.27 A PLOT OF COMPOSITION VERSUS MELTING TEMPERATURE OF HRT COPOLYESTERS SYNTHESISED AT 300°C

Figure 4.28 shows powder X-ray diffractograms of as synthesised HRT polyesters recorded at room temperature. Values of d-spacing and percent crystallinity calculated from the area under the peak are tabulated in **Table 4.8**. HT homopolyester is highly crystalline owing to its linear rigid rod structure. Incorporation of kinking monomer in the form of RDA reduces the packing ability and hence the copolymers crystallise with difficulty. **Figure 4.29** shows that the copolyesters of other three component system (HIT) containing an acidic kink are highly crystalline.

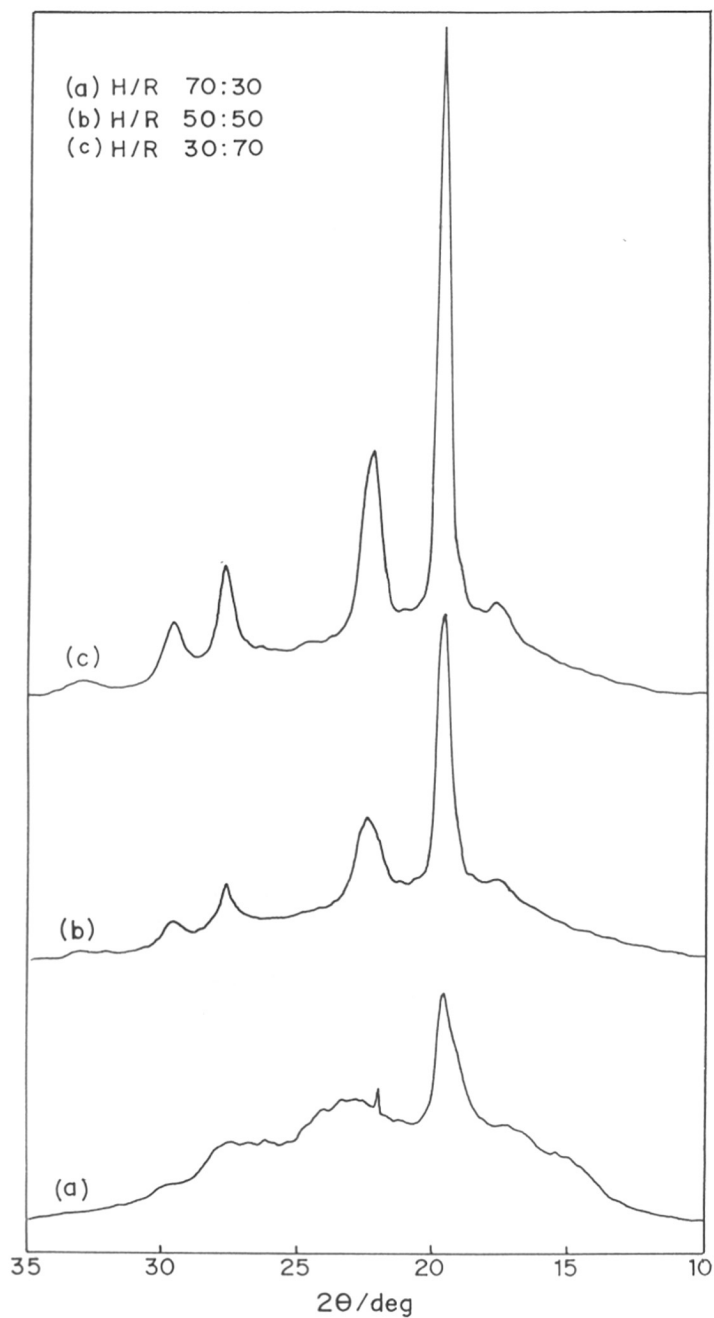


FIGURE 4.28 X-RAY DIFFRACTION PATTERN OF AS MADE HRT POLYESTERS:(a) HRT/70:30:100; (b) HRT/50:50:100; (c) HRT/30:70:100

TABLE - 4.8
RESULTS OF ROOM TEMPERATURE X-RAY DIFFRACTION ANALYSIS

Polymer Composn.	% Crysta- llinity	Peak 2θ											'd' spacing $\overset{\circ}{\underset{\text{Å}}{A}}$				
H:R:T SYSTEM																	
100:0:100	69.0	7.0	17.6	19.8	22.4	27.8	29.7	33.0	38.0	4.97	4.48	3.97	3.65	3.21	3.01	2.71	2.37
90:10:100	56.95	17.2	19.6	22.2	27.6	29.6	33.1	38.2	5.15	4.52	3.99	----	3.22	3.01	2.70	2.35	----
75:25:100	42.50	17.6	20.0	22.5	28.0	29.8	33.0	----	5.04	4.44	3.95	----	3.18	2.99	2.71	----	----
70:30:100	34.04	17.8	19.6	22.2	27.8	29.6	33.0	----	4.52	----	3.96	----	3.22	3.01	----	----	----
50:50:100	24.87	----	19.6	22.4	27.6	29.6	----	----	----	----	----	----	----	----	----	----	----
30:70:100	16.50	17.4	19.6	23.4	27.4	29.8	----	----	5.75	5.09	4.52	3.79	3.25	2.99	----	----	----
10:90:100	20.20	15.4	16.8	19.4	21.9	24.2	26.2	27.5	31.2	5.75	5.28	4.57	4.06	3.67	3.40	3.24	2.80
0:100:100	33.00	15.4	16.8	19.4	21.4	22.8	26.0	27.4	5.75	5.27	4.57	4.35	3.89	3.70	3.42	3.25	----
H:I:T SYSTEM																	
100:50:50	70.45	6.85	16.8	19.8	22.2	27.8	29.0	33.2	37.8	12.9	5.27	4.48	4.00	3.20	2.99	2.69	2.38
100:80:20	68.11	17.8	19.8	22.2	27.8	29.6	33.0	----	----	4.98	4.48	3.99	3.21	3.01	2.71	----	----

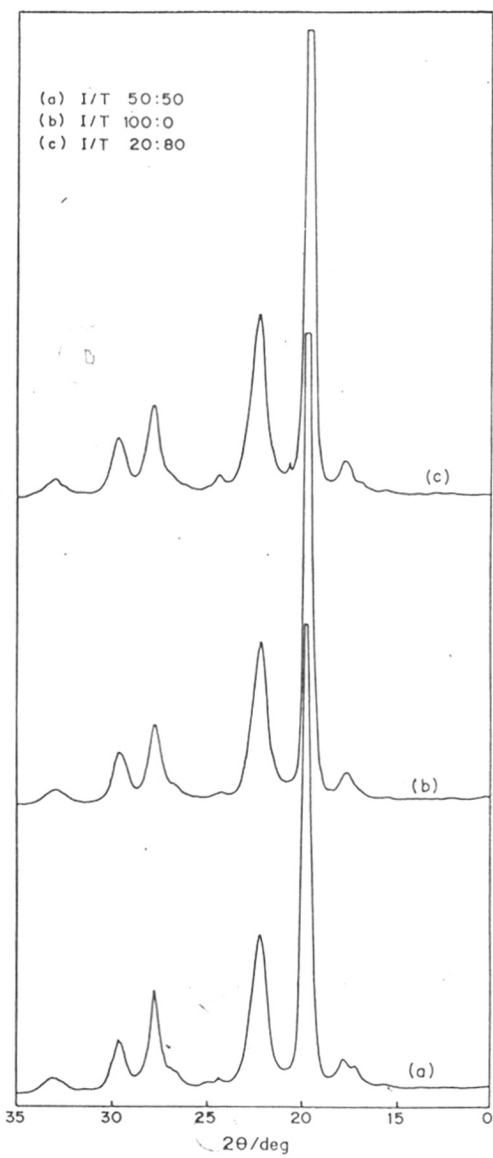


FIGURE 4.29 COMPARISON OF X-RAY DIFFRACTION PATTERNS OF AS MADE HIT POLYESTERS WITH HI POLYESTER

REFERENCES:

1. J. Economy, and K. Goranov, *Adv. Polym. Sci.*, **117**, 222 (1994).
2. M.C. Gabriele, *Plastics Tech.*, **36**, 92 (1990).
3. M.C. Gabriele, *Plastics Tech.*, **40**, 104 (1994).
4. G.W. Gray, 'Polymer Liquid Crystals', (eds. A. Ciferri, W.R. Krigbaum, R.B. Meyer,), Academic Press Inc. Ltd., London, p.5 (1982).
5. V. Frosini, G. Levita, J. Landis and A. Woodward, *J. Polym. Sci., Polym. Phys. Ed.*, **15**, 239 (1977).
6. R. Cai, and E.T. Samulski, *Macromolecules*, **25**, 563 (1992).
7. Z.G. Li, J.E. McIntyre, J.G. Tomka, and A.M. Voice, *Polymer*, **34**, 1946 (1993).
8. J. Cao, G. Karayannidis, J.E. McIntyre, and J.G. Tomka, *Polymer*, **34**, 1471 (1993).
9. R. Cai, and E.T. Samulski, *Macromolecules*, **27**, 135 (1994).
10. Jung- II Jin, S.H. Lee, and H.J. Park, *Polym. Prepr.*, **28**, 122 (1987).
11. M.J.S. Dewar, and R.S. Goldberg, *J. Org. Chem.*, **35**, 2711 (1970).
12. B.W. Jo, R.W. Lenz and Jung-II Jin, *Makromol.Chem., Rapid Commun.*, **3**, 23 (1982).
13. J.Asrar, H. Toriumi, J. Watanabe, W. Krigbaum and A. Ciferri, *J. Polym. Sci., Polym. Physc. Ed.*, **21**, 1119 (1983).
14. S. Cottis, J. Economy and B. Nowak., (Carborundum) US. Patent, 3,637,695 (1972).
15. J.R. Jackson, Jr., *Br. Polym. J.*, **12**, 154 (1980).

16. A. Erdemir, D. Johnson, J. Tomka, *Polymer*, **27**, 441 (1986).
17. R.W. Lenz, J-I. Jin, *Macromolecules*, **14**, 1405 (1981).
18. R. Rosenau- Eichin, M. Ballauff and J. Grebowicz, *Polymer*, **29**, 518 (1988).
19. I. Vulic, and T.J. Schulpen, *Polym. Sci., Part A: Polym. Chem.*, **30**, 2725 (1992).
20. J. Mathew, R.V. Bahulekar, R.S. Ghadage, C.R. Rajan, and S. Ponrathnam and S.D. Prasad, *Macromolecules*, **25**, 7338 (1992).
21. J. Mathew, R.S. Ghadage, S. Ponrathnam and S.D. Prasad, *Macromolecules*, **27**, 4021 (1994).
22. J.I. Steinfeld, "Chemical Kinetics and Dynamics" Prentice - Hall, Inc., New Jersey, p.32 (1989).
23. J. Devaux, *J. Polym. Sci., Polym. Phys. Ed.*, **20**, 1901 (1982).

CONCLUSION

CHAPTER - 5

High temperature acidolysis type transesterification reactions were studied using hydroquinone diacetate - terephthalic acid (HT), hydroquinone diacetate - isophthalic acid (HI), and resorcinol diacetate - terephthalic acid (RT) as model systems. In the first two the reactions start as a slurry and progressively tend to solid state reactions. In the RT system, the initially slurry reaction homogenises with conversion. Breaks were noticeable in the rate of reaction in all systems. In all three systems both regimes separated by the break are describable most exactly by simple second order rate law.

Specific reaction rates are in the range 10^{-2} - 10^{-3} $\text{conc}^{-1}\text{time}^{-1}$. Rate in RT system is an order of magnitude higher than the other two. Activation energies for the reactions lie in the range 15-20 kCal/mole. Compensation effect observed in RT system indicates that it is an entropy driven reaction.

Characterisation of polyesters was carried out using various methods of thermal and optical analysis. A low molecular liquid crystalline fraction of both HT and HI systems, isolated from chloroform is liquid crystalline. This fraction shows textures corresponding to both smectic and nematic mesophases under crossed polarisers. These mesophasic transitions agree well with those recorded by DSC. HT and HI polyesters are linear and uniformly packed crystalline materials. The high temperature X-ray pattern of low molecular mass fraction is characterised by the presence of a series of arcs corresponding to different orders of diffraction. RT polyesters are amorphous, low melting and isotropic.

Rate constants and other kinetic parameters obtained by studying melt polyesterification kinetics of HT, HI and RT system can be effectively used in studying hydroquinone diacetate - isophthalic acid - terephthalic acid (HIT) and hydroquinone diacetate - resorcinol diacetate - terephthalic acid (HRT) system.

The kinetics of HRT system was found to be comparable to that of PET-OB where similar competing reactions occur. A complex kinetic model is not necessary to understand the kinetics of HRT system. It can be concluded from the analysis that the copolyesterification of three component system follows simple second order kinetic laws. Breaks are observed in the rate law plot consequent to the increased reactivity of initially intractable TPA monomer with the progress of the reaction. Reaction rate increases in the second stage (after the break) gradually with increase in the concentration of RDA. The rate constants of HRT system are higher than that of HT system. The degree of polymerisation also increases on copolymerisation. It is known that if the rate equation is correct the rate constant should be constant. It should depend on temperature but be independent of concentration of the reactants. This is confirmed from the fact that second order rate law is obeyed over the entire composition range and the drastic change in the rate constants was observed only for the extreme composition where in RDA is 10 mole %. Important feature of HRT system is that some kind of compensation effect is responsible for the progress of reactions in the second stage. It can be concluded that the overall copolymerisation kinetics is influenced by the reaction between RDA and TPA than the reaction between HQDA and TPA.

A geometrical effect, that is, a straight 180° vs a bent 120° structural variation, caused by the introduction of 1,3-benzene diacetate (RDA) can clearly be seen from the thermal and the X-ray diffraction behaviour of the copolyesters. The melting temperature of otherwise intractable hydroquinone terephthalate polyester can be very effectively reduced by using the diol kink in the form of resorcinol monomer.

All aromatic main chain homopolyester hydroquinone terephthalate (HT) can also be modified by introducing acidic kink in the backbone in the form of nonlinear isophthalic acid as a comonomer. Reaction kinetics of homo and copolyesterification however follows the same pattern. Thus copolyesterification of HIT is a second order bimolecular condensation

reaction having rate constants in the range $10^{-2} - 10^{-3} \text{ conc}^{-1}\text{time}^{-1}$ and activation energies of the order of 15-20 kCal/mole. Reactions are characterised by an induction period and the degree of polymerisation achieved is restricted by complexity of reaction. HIT copolyesterification reactions followed simple kinetics with no breaks in the rate law plots. A random copolyester of HIT as against HRT polyester can be obtained because the rates of homopolyesterification reactions of HT and HI are comparable. Consequently, no glass transition is noted for HIT polyesters during DSC analysis.

Copolyesters are hard solids insoluble in all common and drastic solvents. It can be concluded from the X-ray diffraction analysis that HIT polyesters are crystalline which indicate better packing ability of the kinking isophthalate unit relative to the other kinking unit based on resorcinol.

Thermal analysis indicates the presence of low molecular mass liquid crystalline fraction in HIT system. This fraction is soluble in chloroform and shows mesomorphic transitions below 300°C . Both fan shaped and schlieren textures were observed under cross polarised light at temperatures corresponding to the mesomorphic transitions. Fluidity at these temperatures is indicative of its low molecular mass.

The study of isophthalic acid based liquid crystal polyesters by Cai and Samulski indicate that in certain circumstances, a high percentage of nonlinear monomer can be incorporated into liquid crystal polymers. The poly(p-phenylene terephthalate co p-phenylene isophthalate) with as much as 85 mole% of 4-phenylene isophthalate exhibits a melting temperature of 355°C and a mesophase range of 30°C . The copolyesters with lower percentage of isophthalate exhibit wider mesophase range. They opined a great uncertainty over the polymerisation: whether it is random or favours blocky structure. In fact it is observed from

detailed kinetic study of HT, HI and HIT system that the rates of HT and HI are comparable and therefore it is more likely that the copolyester HIT will have a randomised sequence of the two acidic (isophthalic and terephthalic) units along the chain.

From the analysis of both HIT and HRT copolyesters it can be concluded that resorcinol is the more effective kinking monomer than isophthalic acid and thus makes the linear homopolyester of HT relatively tractable.

PUBLICATIONS

1. Structure Development in Powder Processing of Polyphenylene Sulphide; J.P. Jog, A. Lodha, and V.M. Nadkarni, *Advances in Polymer Technology*, **11**, 41-52 (1992)
2. A process for the preparation of non - melting liquid crystalline polymers, A. Kotha, A. Lodha, J. Mathew, R.S. Ghadage, C.R. Rajan and S. Ponrathnam, *Indian Patent* (908/DEL/93)
3. A process for the preparation of thermotropic liquid crystalline polymers, A. Lodha, J. Mathew, R.S. Ghadage, C.R. Rajan and S. Ponrathnam, *Indian Patent* (Filed)
4. Copolyesters of poly(ethylene terephthalate), hydroquinone diacetate and terephthalic acid : A Simple Rate Model for Catalysed Synthesis in Melt, J. Mathew, R.S. Ghadage, S.D. Prasad, A. Lodha and S. Ponrathnam, (Communicated) 'Macromolecules'
5. Polycondensation Reaction Kinetics of Wholly Aromatic Polyesters, A. Lodha, R.S. Ghadage and S. Ponrathnam, (Accepted) 'Polymer'
6. Detailed Kinetics of Liquid Crystalline Copolyester Synthesis. Copolyesterification between poly(ethylene terephthalate), terephthalic acid and hydroquinone diacetate, R.S. Ghadage, A. Lodha, J. Mathew, S.D. Prasad and S. Ponrathnam (Accepted) 'Macromolecular Symposia'

TH-1054